Ground-Water Flow in the Surficial Aquifer System and Potential Movement of Contaminants from Selected Waste-Disposal Sites at Cecil Field Naval Air Station, Jacksonville, Florida

By Keith J. Halford

U.S. GEOLOGICAL SURVEY

Water-Resources Investigations Report 97–4278

Prepared in cooperation with the

Southern Division Naval Facilities Engineering Command, U.S. Navy

Tallahassee, Florida
1998

U.S. DEPARTMENT OF THE INTERIOR
BRUCE BABBITT, Secretary

U.S. GEOLOGICAL SURVEY
Thomas J. Casadevall, Acting Director

The use of firm, trade, and brand names in this report is for identification purposes only and does not constitute endorsement by the U.S. Geological Survey.

For addtional information write to:

District Chief
U.S. Geological Survey, WRD
Suite 3015
227 North Bronough Street
Tallahassee, FL 32301

Copies of this report can be purchased from:

U.S. Geological Survey
Branch of Information Services
Box 25286
Denver, CO 80225-0286

CONTENTS

FIGURES

TABLES

CONVERSION FACTORS, VERTICAL DATUM, ABBREVIATIONS AND ACRONYMS

Multiply	By	To obtain
	Length	
foot (ft)	0.3048	meter
foot per mile (ft/mi)	0.1894	meter per kilometer
	Area	
square foot (ft^2)	0.0929	square meter
square mile (mi^2)	2.590	square kilometer
	Flow	
cubic foot per day (ft^3/d)	0.02832	cubic meter per day
gallon per minute (gal/min)	0.06309	liter per second
inch per year (in/yr)	25.4	millimeter per year
	Hydraulic Conductivity	
foot per day (ft/d)	0.3048	meter per day
	****Transmissivity***	
foot squared per day (ft^2/d)	0.0929	meter squared per day

Temperature in degrees Fahrenheit (°F) may be converted to degrees Celsius (°C) as follows:
°C=(°F-32)/1.8

Sea level: In this report, "sea level" refers to the National Geodetic Vertical Datum of 1929 (NGVD of 1929)--a geodetic datum derived from a general adjustment of the first-order level nets of both the United States and Canada, formerly called Sea Level Datum of 1929.

***Transmissivity:** The standard unit for transmissivity is cubic foot per day per square foot times foot of aquifer thickness [(ft^3/d)/ft^2]ft. In this report, the mathematically reduced form, foot squared per day (ft^2/d), is used for convenience.

Acronyms and additional abbreviations used in report:

DEM	Digital Elevation Model
DI	Deep infiltration
ET	Evapotranspiration
MODFLOW	Modular Finite-Difference Model
NAS	Naval Air Station
RMS	Root-mean-square
SR	State Road
T*	Time base
T_c	Critical times
USGS	U.S. Geological Survey

Ground-Water Flow in the Surficial Aquifer System and Potential Movement of Contaminants from Selected Waste-Disposal Sites at Cecil Field Naval Air Station, Jacksonville, Florida

By Keith J. Halford

Abstract

As part of the Installation Restoration Program, Cecil Field Naval Air Station, Jacksonville, Florida, is considering remedial-action alternatives to control the possible movement of contaminants from sites that may discharge to the surface. This requires a quantifiable understanding of ground-water flow through the surficial aquifer system and how the system will respond to any future stresses.

The geologic units of interest in the study area consist of sediments of Holocene to Miocene age that extend from land surface to the base of the Hawthorn Group. The hydrogeology within the study area was determined from gamma-ray and geologists' logs.

Ground-water flow through the surficial aquifer system was simulated with a seven-layer, finite-difference model that extended vertically from the water table to the top of the Upper Floridan aquifer. Results from the calibrated model were based on a long-term recharge rate of 6 inches per year, which fell in the range of 4 to 10 inches per year, estimated using stream hydrograph separation methods. More than 80 percent of ground-water flow circulates within the surficial-sand aquifer, which indicates that most contaminant movement also can be expected to move through the surficial-sand aquifer alone. The surficial-sand aquifer is the uppermost unit of the surficial aquifer system.

Particle-tracking results showed that the distances of most flow paths were 1,500 feet or less from a given site to its discharge point. For an assumed effective porosity of 20 percent, typical traveltimes are 40 years or less. At all of the sites investigated, particles released 10 feet below the water table had shorter traveltimes than those released 40 feet below the water table. Traveltimes from contaminated sites to their point of discharge ranged from 2 to 300 years. The contributing areas of the domestic supply wells are not very extensive. The shortest traveltimes for particles to reach the domestic supply wells from their respective contributing areas ranged from 70 to 200 years.

INTRODUCTION

Inorganic and organic priority contaminants defined by the U.S. Environmental Protection Agency (USEPA, 1988) have been detected in surface water, sediment, and ground-water samples collected near abandoned waste-disposal sites at Cecil Field Naval Air Station (NAS), Jacksonville, Florida (fig. 1). Concern exists that such contaminants may move with the underlying ground water into nearby creeks where contaminants could be readily transported to other parts of the air station or downstream to neighboring properties. As part of the Installation Restoration Program, Cecil Field NAS is considering remedial-action alternatives to control the movement of contaminants from those sites that may otherwise discharge to the surface.

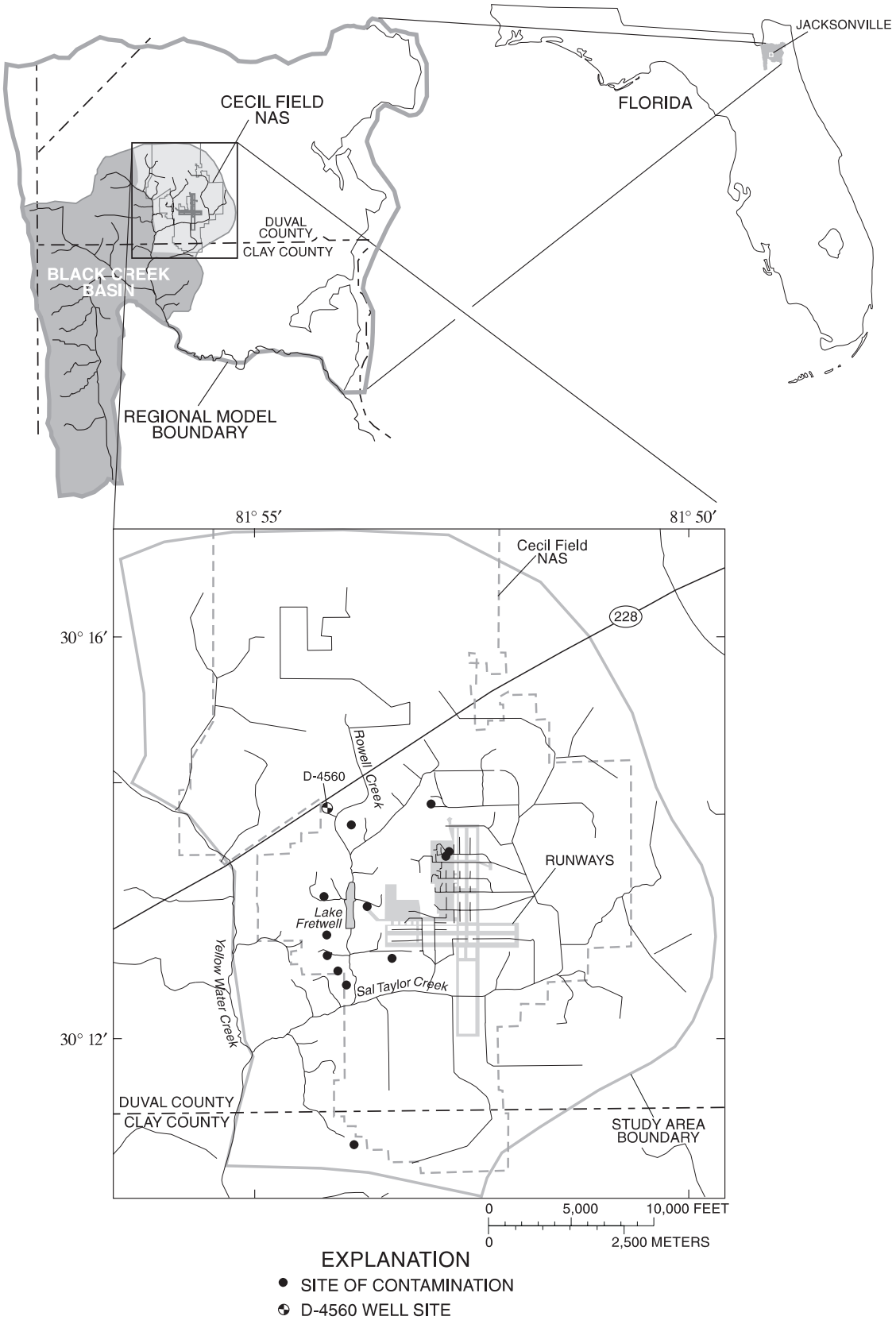

Figure 1. Location of the study area, sites of contamination, and well D-4560.

This requires a quantifiable understanding of how the ground-water flow system responds to current conditions and to any future stresses imposed on the system. Numerical simulation provides the most tractable way of achieving this level of understanding.

Cecil Field NAS, located in west Duval County, Florida (fig. 1), serves the U.S. Navy as a master jet base. From the early 1950's to the early 1980's, a large variety of solid and liquid waste materials generated by Cecil Field NAS was disposed in unlined pits, landfills, or in open areas of the air station. Twelve sites (fig. 1) were identified in 1986 for further investigation and potential remediation (U.S. Department of the Navy, 1992a). In some cases, wastes were placed in direct contact with the ground water in the surficial-sand aquifer at the time of disposal. Suspected wastes include fuels and oils, solvents, paints, pesticides, detonated ordnance, ash, and debris. Analyses of ground-water, sediment, and surface-water samples collected by previous investigators near many of these sites have yielded detectable concentrations of extractable organic compounds and heavy metals.

The dissolved constituents of jet fuel, lubricants, and solvents (benzene, dichlorobenzene, toluene, acetone, napthalene, and trichloroethene) are the primary contaminants that may be transported by ground water at Cecil Field NAS. The movement of these dissolved constituents is similar to the advective flow of the ground water, as the solubility of these contaminants is usually low and the concentrations are not great enough to significantly alter the density of the ground water. These dissolved constituents sorb to the porous media of the aquifers and confining units, which retards the rate of travel, but does not affect the direction of travel.

Purpose and Scope

This report presents the results of a study to analyze ground-water flow in the surficial aquifer system in a 36-mi^2 area that includes most of the Cecil Field NAS (fig. 1). The report includes ground-water-level and surface-water-discharge data, a description of the hydrogeologic framework, and an estimate of the water budget and base flow in the study area. Simulation results are presented from a calibrated, three-dimensional finite-difference, ground-water flow model of the 36-mi^2 area. A regional and cross-sectional model are presented to support the lateral boundaries of the study area and the approach used for model calibration, respectively. Estimates of ground-water movement from existing and potential sites of contamination to their discharge points by way of particle tracking (Pollock, 1989) are presented.

Description of the Study Area

The study area is in the northeastern corner of the Black Creek Basin (fig. 1) and is drained by Yellow Water, Sal Taylor, and Rowell Creeks (fig. 1). A section of Rowell Creek was impounded to create Lake Fretwell. Most soils in the basin are comprised of fine sands. There is little topographic relief; slopes generally are 0 to 2 percent. Depth to the water table generally ranges from 0 to 5 ft below land surface (Stem and others, 1978). Most of the area is forested by pine trees.

The climate of Duval County is humid, subtropical. Average precipitation over the study area is about 54 in/yr with more than half falling from June to September (Owenby and Ezell, 1992). The long-term potential evaporation rate from the study area has been estimated to be 48 in/yr (Farnsworth and others, 1982, map 3). The average yearly temperature is 79 °F (Owenby and Ezell, 1992).

The geology and hydrology of the study area and surroundings have been described in numerous reports as summarized in Spechler (1994), but most describe features at a county-wide scale and focus primarily on the Upper Floridan aquifer. Causey and Phelps (1978) described the extent and availability of water from the surficial-aquifer system in Duval County.

Acknowledgments

The author extends his appreciation to Cliff Casey, Southern Division Naval Facilities Engineering Command, and Maria Pinenburg and Drew Lonergan, ABB Environmental Services, for assistance provided during this study.

GEOHYDROLOGY

The geologic units of interest in the study area include sediments of Holocene to Miocene age that extend from land surface to the base of the Hawthorn Group (fig. 2). Previous investigators have defined this sequence as two regional hydrogeologic units: the surficial aquifer system and the intermediate confining unit (Spechler, 1994). In this report, this sequence has been

Series	Formation	Lithology	Spechler (1994)	This report	
			Hydrogeologic unit		Model layer
Holocene to Upper Miocene	Undifferentiated surficial deposits	Silty-sand and clay lenses	Surficial aquifer system	Surficial-sand aquifer	1, 2, 3
		Clay and shell beds		Blue-marl confining unit	4
		Limestone and sand		Upper-rock aquifer	5
Miocene	Hawthorn Group	Clay and interbedded phosphatic sands	Intermediate confining unit	Gray-marl confining unit	--
		Limestone and sand		Lower-rock aquifer	6
		Clay, interbedded phosphatic sands, limestone, and dolomite		Lower confining unit	--
Eocene	Ocala Limestone	Marine limestone	Upper Floridan aquifer	Upper Floridan aquifer	7

(Modified from Spechler, 1994)

Figure 2. Generalized geologic and hydrogeologic units and aquifers beneath Cecil Field Naval Air Station.

further subdivided into six local hydrogeologic units, because this study is primarily concerned with ground-water movement near the surface.

The surficial aquifer system was subdivided into three hydrogeologic units: the surficial-sand aquifer, the blue-marl confining unit, and the upper-rock aquifer (fig. 2). The surficial-sand aquifer consists of silty sand with interbedded clay lenses that are about 1 ft thick. The first 10 to 20 ft of the blue-marl confining unit is usually a blue-green clay which grades to a mixture of sand, shell, and clay at the top of the upper-rock aquifer. The upper-rock aquifer is a layered composite of limestone and sand.

The intermediate confining unit defined by Spechler (1994) was subdivided into three hydrogeologic units: the gray-marl confining unit, the lower-rock aquifer, and the lower confining unit (fig. 2). The gray-marl confining unit consists of a gray clay interspersed with phosphatic sand stringers. The composition of the lower-rock aquifer is similar to that of the upper-rock aquifer. The lower confining unit is about 200 ft thick in the vicinity of Cecil Field NAS and consists of marine clays and discontinuous limestone stringers.

The hydrogeologic structure within the study area was defined by depth and thickness data from gamma-ray logs and geologists' logs. Typical gamma ray and geologist's logs are shown in figure 3 for

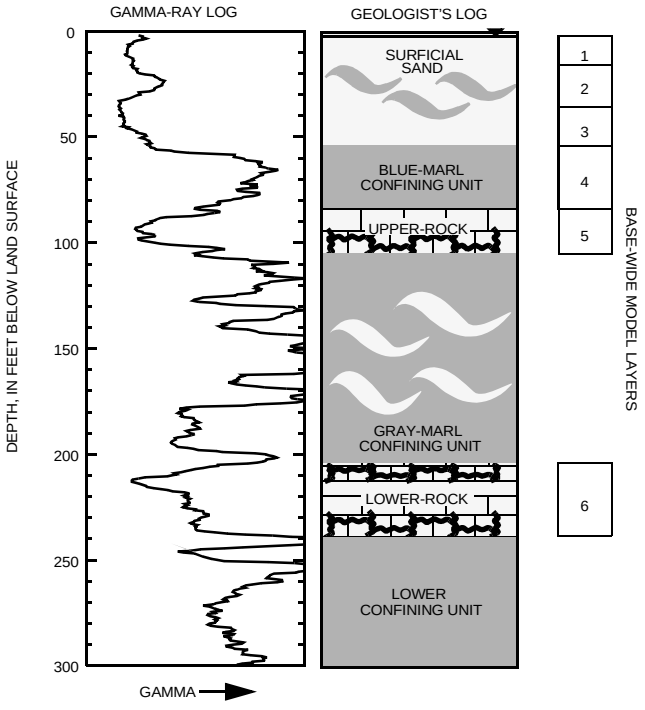

Figure 3. Gamma-ray log and geologist's log of well D-4560, a typical hydrogeologic column of the first 300 feet below Cecil Field Naval Air Station, and model-layer correlations for this study.

well D-4560. The gamma-ray log responds to the natural radioactivity of the formation which generally increases with increasing clay content. Phosphatic sands are an exception and are usually much more radioactive than clays. Within the surficial aquifer system, the hydrogeologic units are clearly defined by the gamma-ray log. This definition becomes less clear for the deeper units in the intermediate confining unit because the gamma-ray log is responding to phosphatic sands in addition to clayey materials.

Additional logs from beyond the study area were used to define the base of the surficial-sand aquifer and the thicknesses of the other hydrogeologic units (fig. 4). These additional logs ensured that the hydrogeologic framework estimated for the study area would be consistent with the regional framework. The configuration of the base of the surficial-sand aquifer is irregular (fig. 5), but generally dips to the south and east in the study area. Regionally, the base of the surficial-sand aquifer dips to the east at a slope ranging from 5 to 20 ft/mi (Leve, 1966).

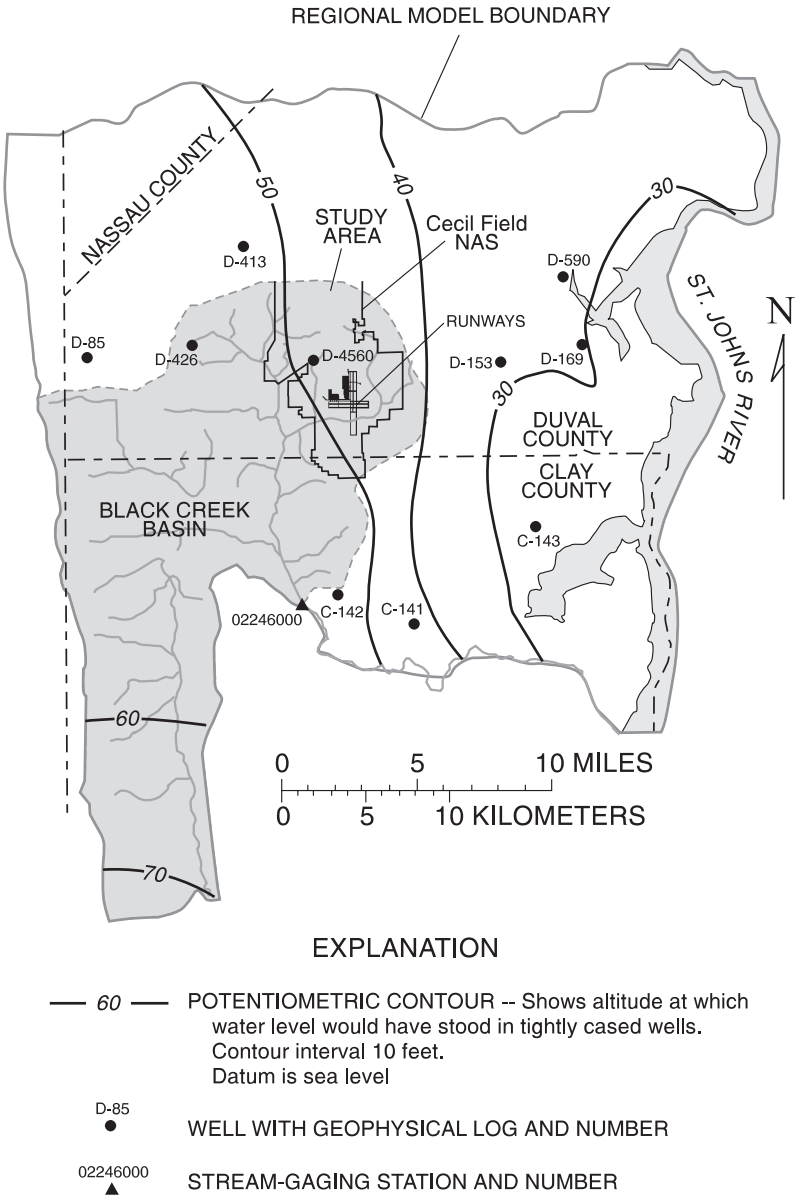

Figure 4. Location of selected wells used to define the hydrogeologic framework and the potentiometric surface of the Upper Floridan aquifer, May 1993, in the study area, Black Creek Basin, regional model areas, and the location of stream-gaging station Black Creek near Middleburg (02246000).

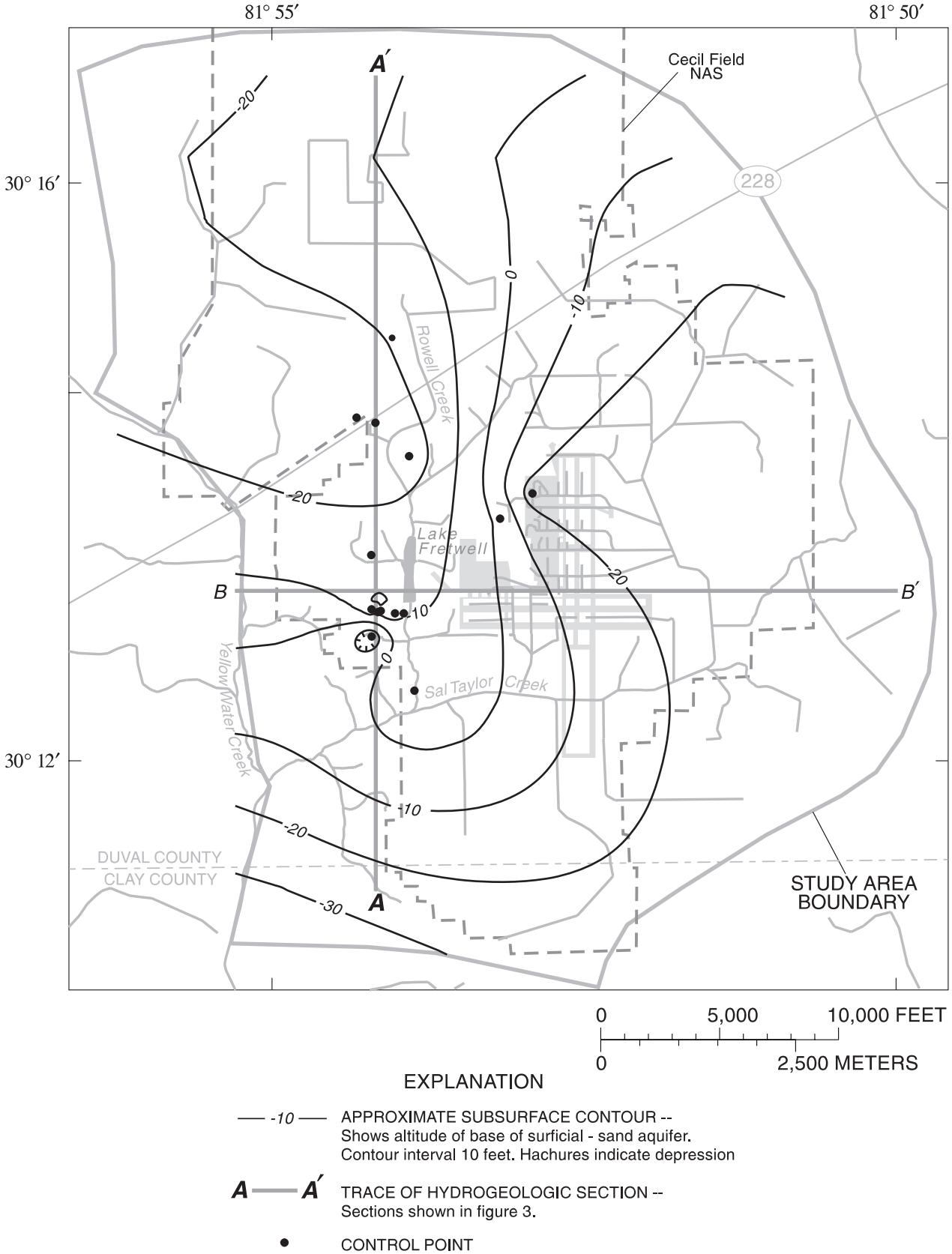

Figure 5. Altitude of base of the surficial-sand aquifer in the study area.

The thickness of the surficial-sand aquifer was estimated by subtracting the elevation at the base of the surficial-sand aquifer from the elevation at land surface (fig. 6). Thicknesses of the five remaining hydrogeologic units (figs. 7-11) were estimated by interpolation between logs located both within the study area and from beyond the study area (fig. 4). The blue-marl confining unit (fig. 7) is thickest near Lake Fretwell and is thinnest northeast of the runways. The thickness of the upper-rock aquifer ranges from less than 15 to more than 25 ft (fig. 8) and averages about 20 ft. The gray-marl confining unit is thickest north of State Road (SR) 228 (fig. 9) and generally thins toward the southeast. The thickness of the lower-rock aquifer ranges from about 30 ft north of SR 228 to more than 70 ft in the southern part of the study area (fig. 10). The lower confining unit ranges from about 170 ft to more than 220 ft (fig. 11) and averages about 200 ft over the study area. Total thickness was used because the ground-water pathlines are of interest. If the unit thicknesses represented on figures 5 through 11 are composited, generalized hydrogeologic sections could be cut from the total volume. Two such sections are shown in figure 12 that illustrate the variations in thickness and altitude of the five uppermost hydrogeologic units.

WATER BUDGET AND RECHARGE ESTIMATES

A long-term water budget of the surficial aquifer system can be described by the following equation:

$$P - ET - Q - DI = \Delta S \cong 0, \qquad (1)$$

where

P is precipitation, in inches per year;

ET is evapotranspiration, in inches per year;

Q is stream discharge, in inches per year, which is composed of surface runoff, Q_S, and base flow, Q_B;

DI is deep infiltration to the Upper Floridan, in inches per year; and

ΔS is change in storage, in inches per year, which is assumed to be negligible over the long term.

Where these various budget components enter and exit the system is depicted in figure 13. Precipitation (54 in/yr) and stream discharge at Black Creek near Middleburg (02246000) (fig. 4), 15 in/yr, were measured. Deep infiltration (1 in/yr) was estimated previously (Krause and Randolph, 1989). Evapotranspiration (38 in/yr) is precipitation minus stream discharge and deep infiltration. All terms represent averages over periods of 30 years or more.

Pumpage was not considered in the water budget because Cecil Field NAS is supplied only by wells screened in the Upper Floridan aquifer (U.S. Department of the Navy, 1992a). Several domestic wells existing adjacent to Cecil Field NAS (fig. 14) are probably screened in the upper-rock aquifer (U.S. Department of the Navy, 1992a). If all of the 17 domestic wells shown in figure 14 continually withdraw 13,000 gal/d, then the total discharge amounts to 0.008 in/yr across the study area.

Recharge, N, is the subcomponent of the water budget that drives ground-water flow through the surficial aquifer system. Both the surficial-sand and upper-rock aquifers respond to recharge events which correspond with periods of intense rainfall. Part of the rainfall is rejected as recharge and contributes to stream discharge as surface runoff, Q_S (fig. 13). These storm events appear as abrupt increases in stream discharge (fig. 15).

The long-term recharge rate can be defined as: $N = P - ET - Q_S$ or $N = Q - Q_S + DI$. Direct estimates of N are complicated by the uncertainties associated with evaluating surface runoff (Q_S), evapotranspiration (ET), and deep infiltration (DI).

Periodic recharge to ground water can be estimated by hydrograph separation. Many methods have been documented and most assume that stream discharge has two components, surface runoff and base flow (Meyboom, 1961; Rutledge, 1993; Domenico and Schwartz, 1990). Base flow is the component of stream discharge contributed by ground-water discharge and can serve as an estimate of recharge, assuming that surface-water basin boundaries generally correspond with ground-water divides and that measured stream discharge is uncontrolled by upstream diversion or regulation.

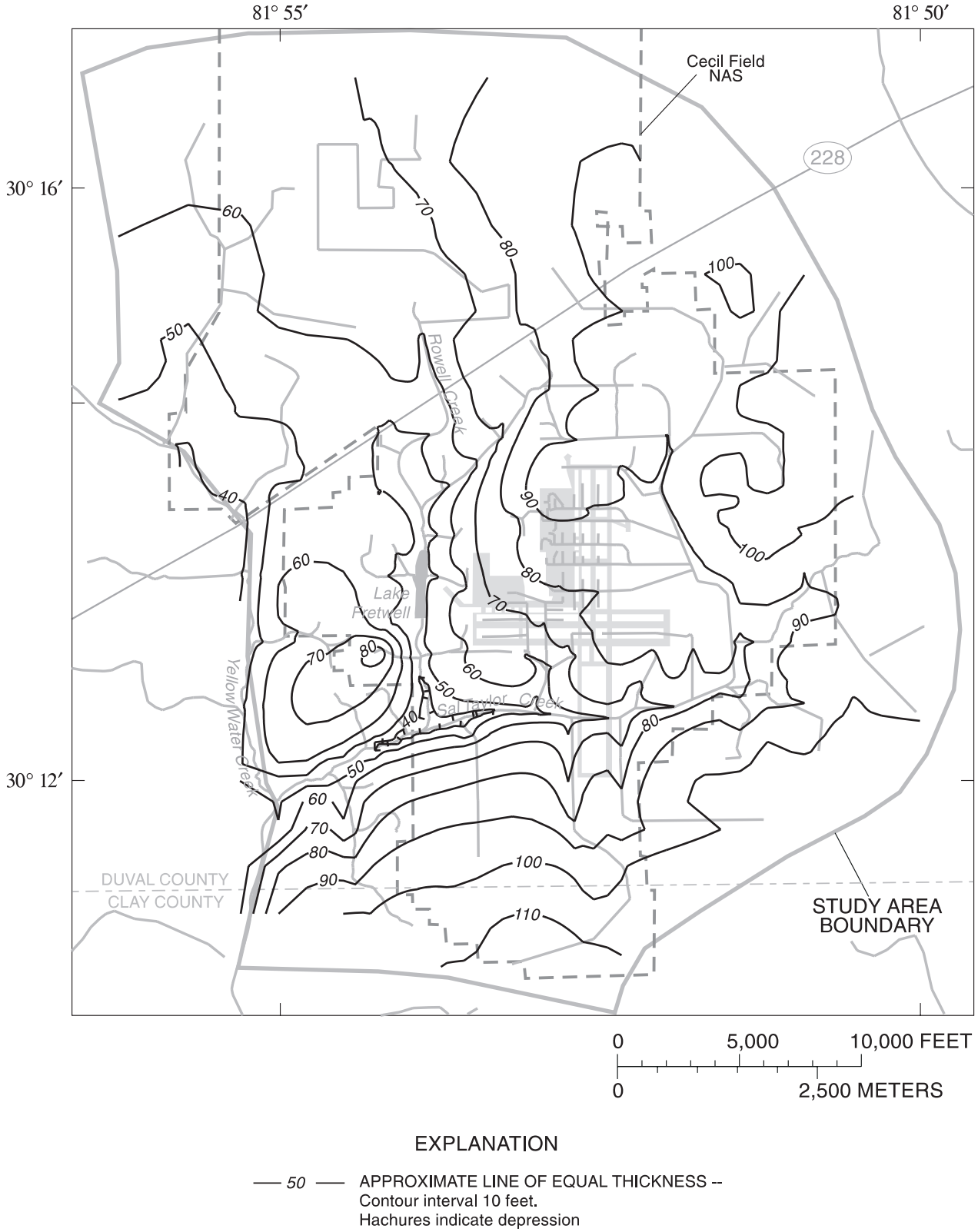

Figure 6. Thickness of the surficial-sand aquifer.

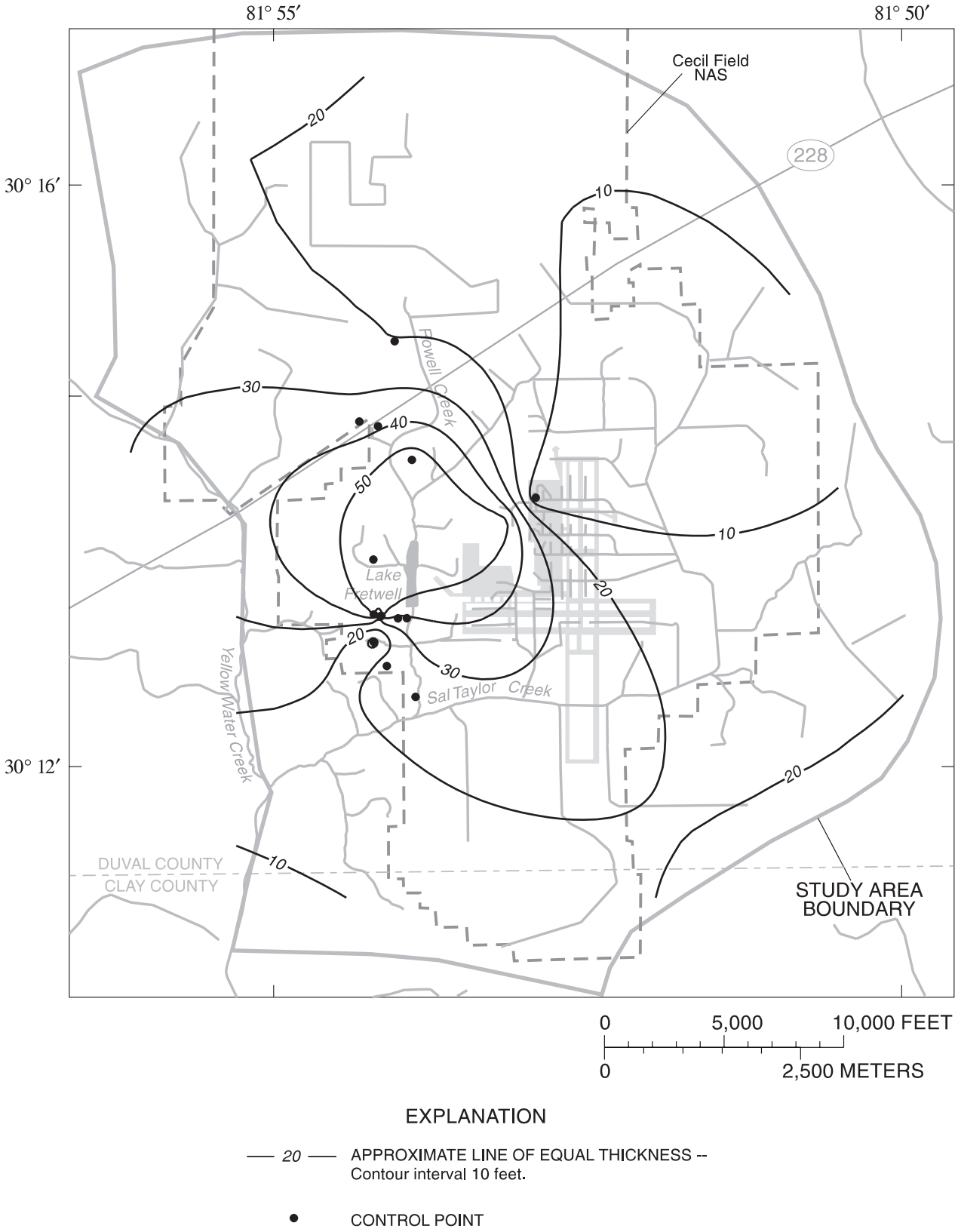

Figure 7. Thickness of the blue-marl confining unit.

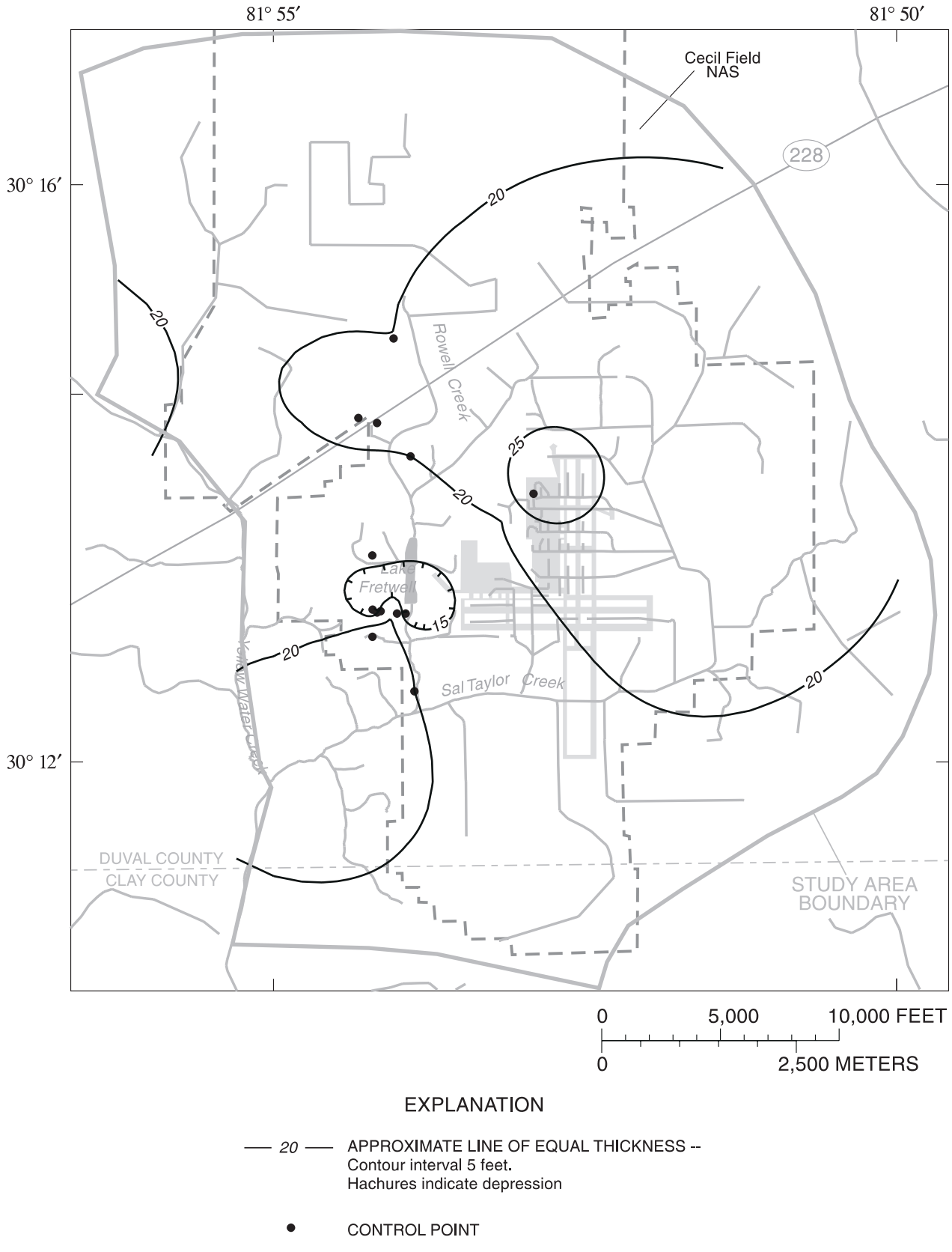

Figure 8. Thickness of the upper-rock aquifer.

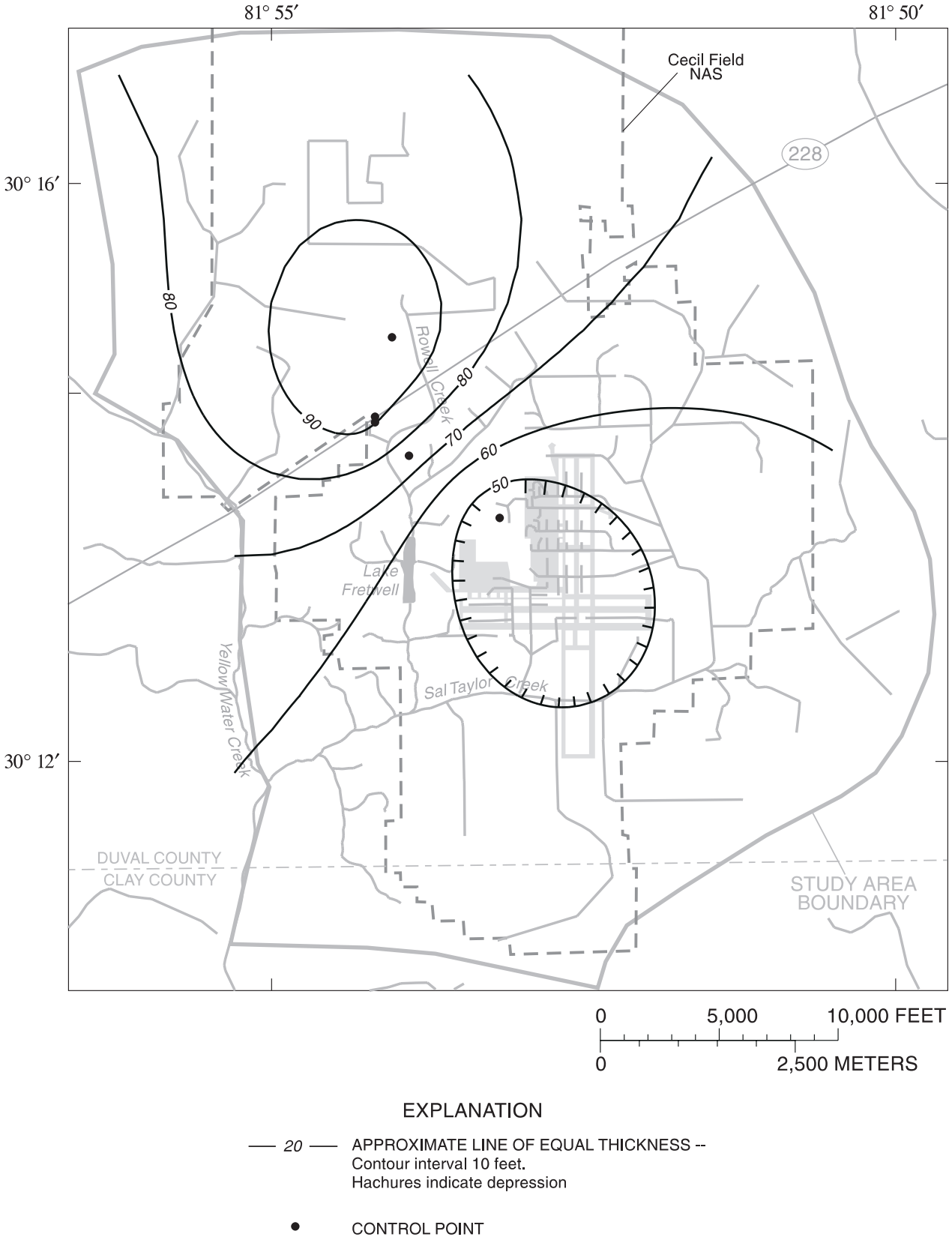

Figure 9. Thickness of the gray-marl confining unit.

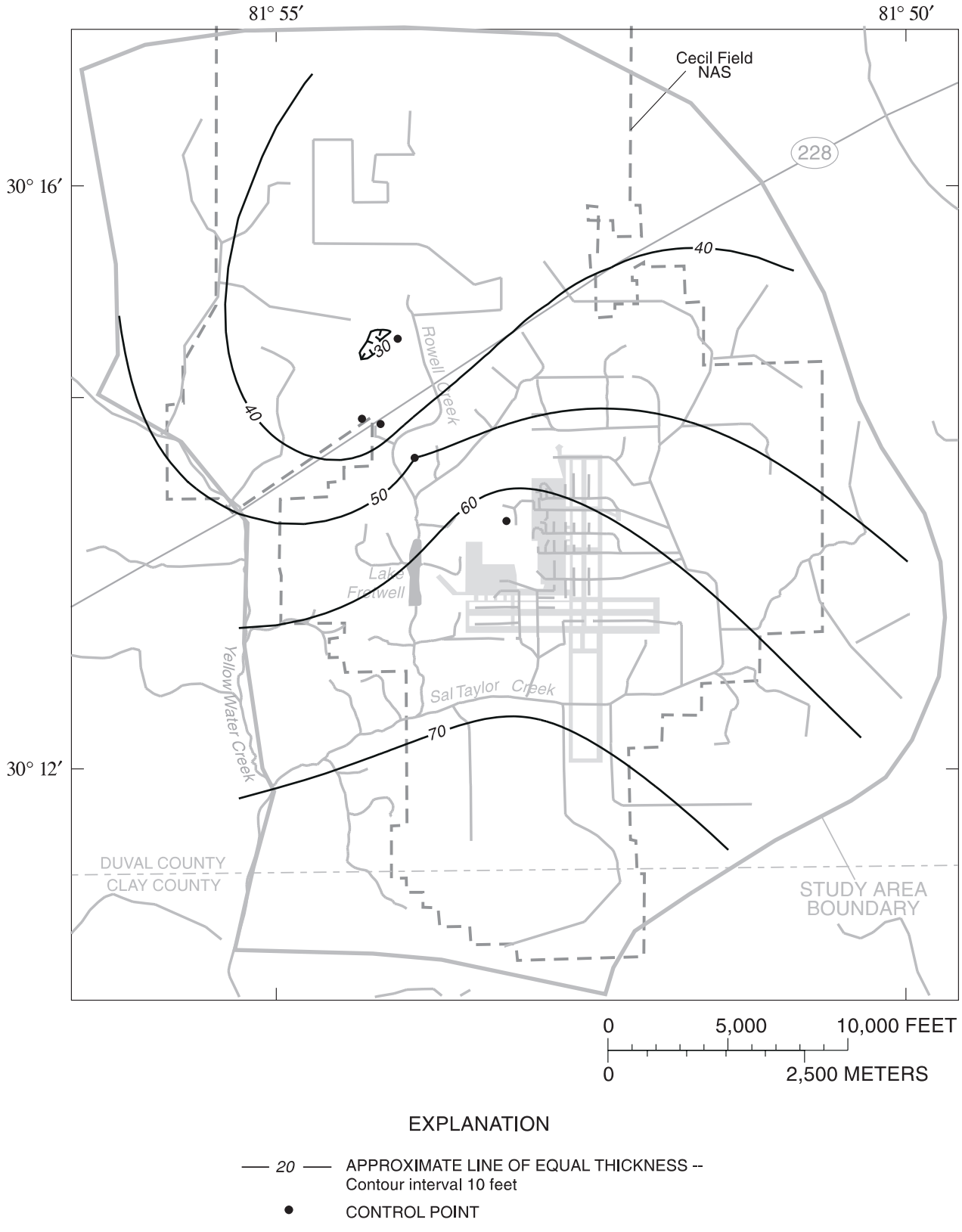

Figure 10. Thickness of the lower-rock aquifer.

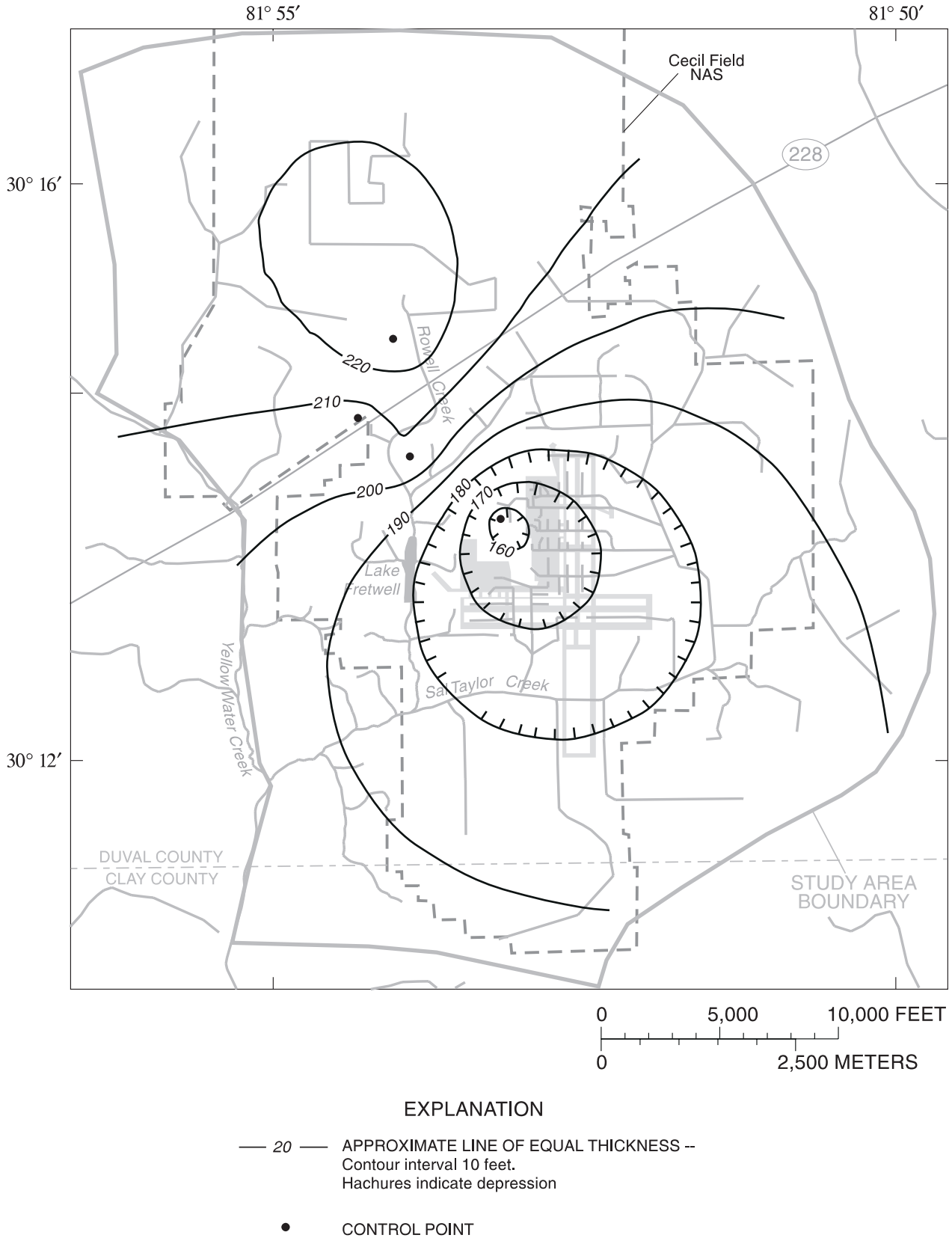

Figure 11. Thickness of the lower confining unit.

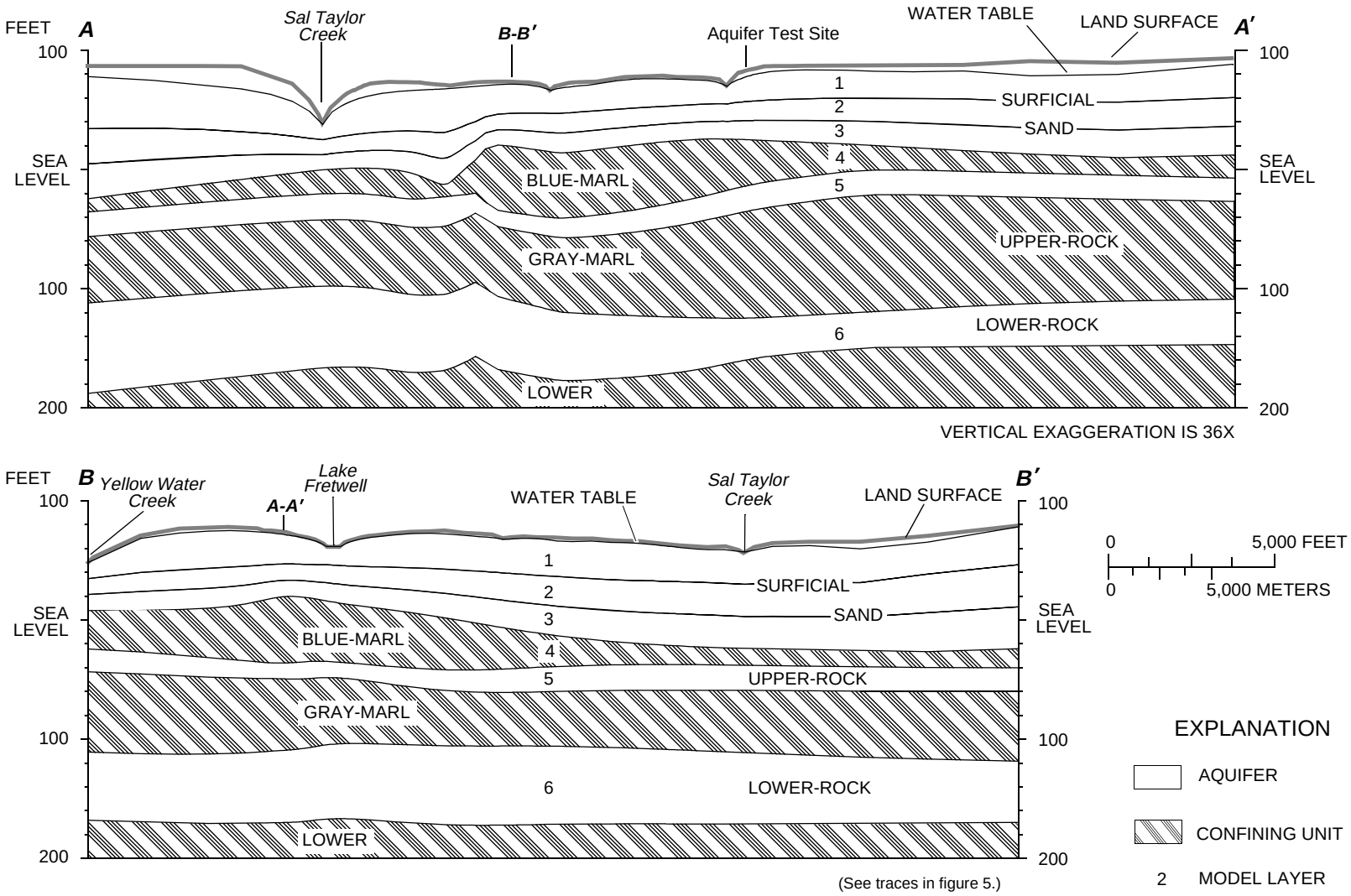

Figure 12. Generalized hydrogeologic sections A-A′ and B-B′ in the study area.

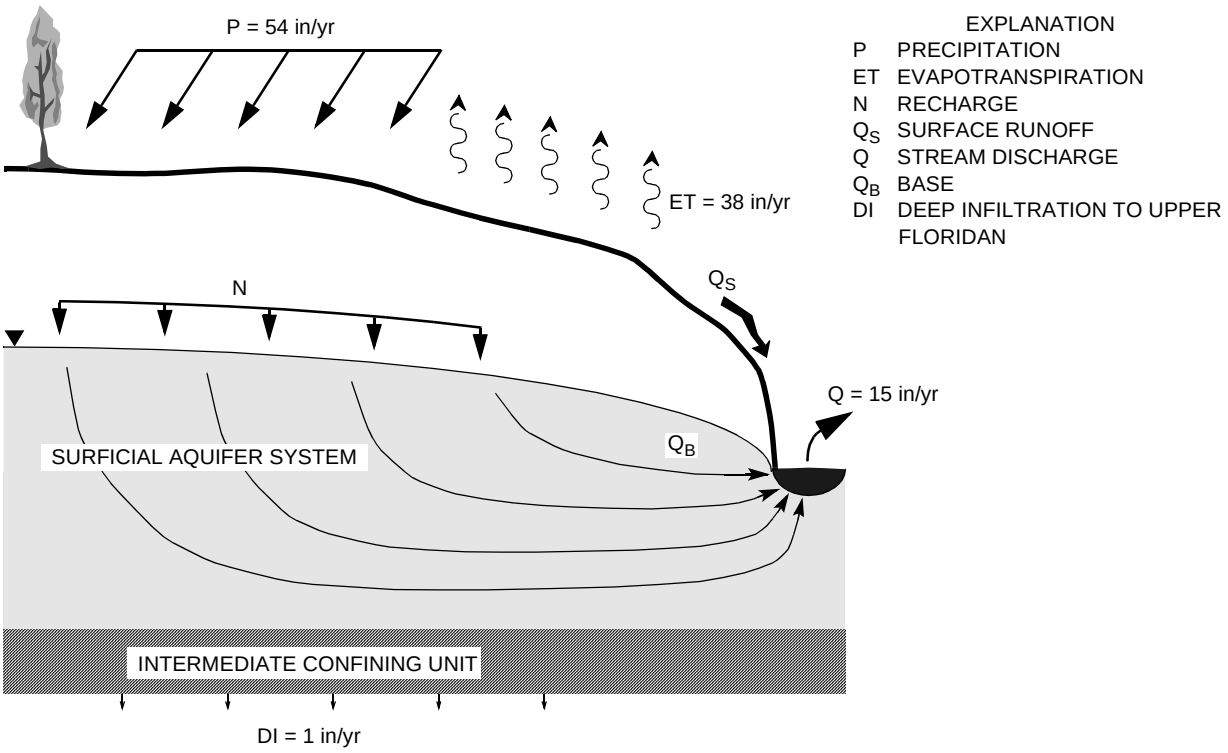

Figure 13. The water budget and its components within the study area.

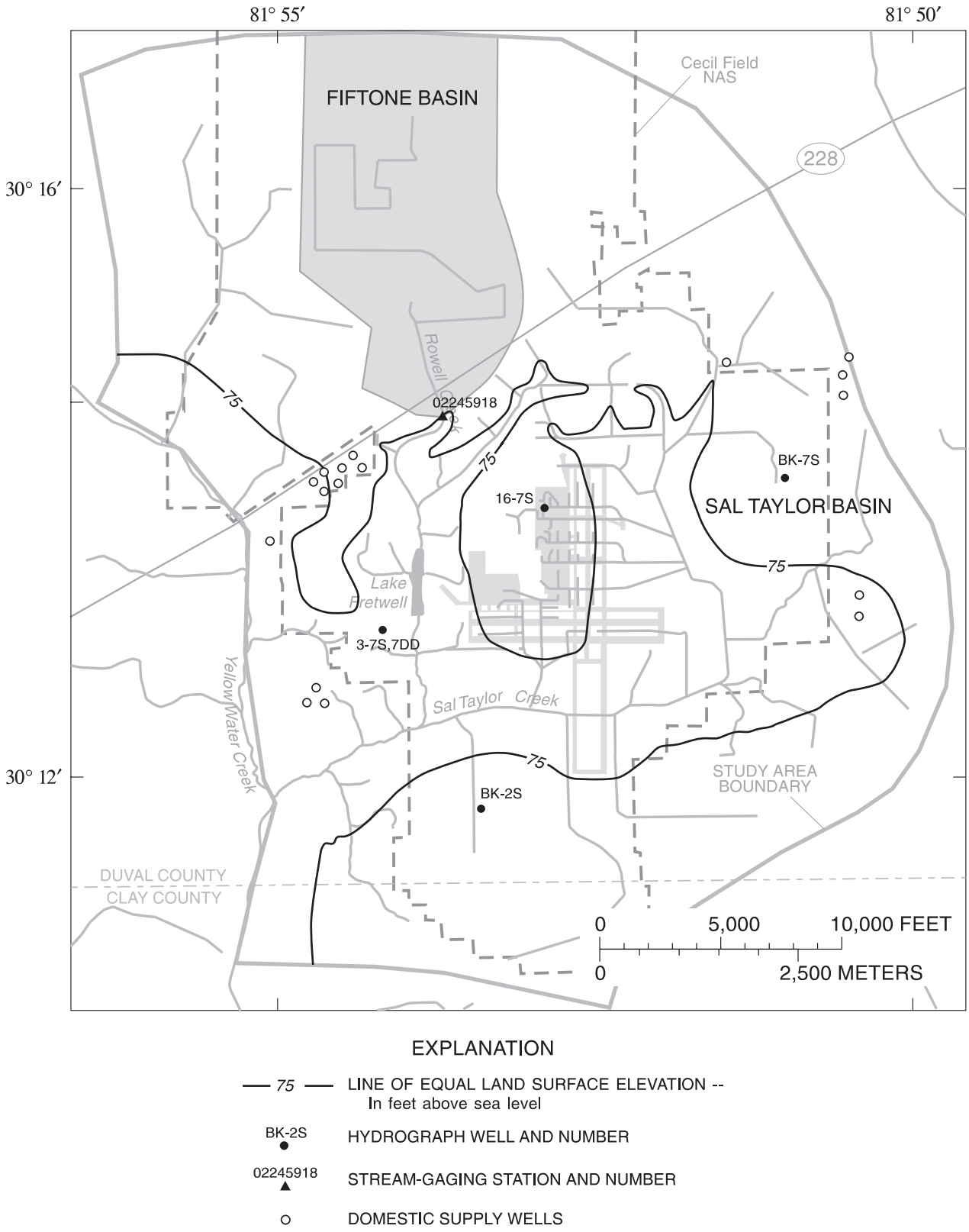

Figure 14. Locations of hydrograph and domestic supply wells, stream-gaging station Rowell Creek near Fiftone (02245918), the drainage areas of the Fiftone and Sal Taylor Basins, and the 75-foot contour of land surface elevation.

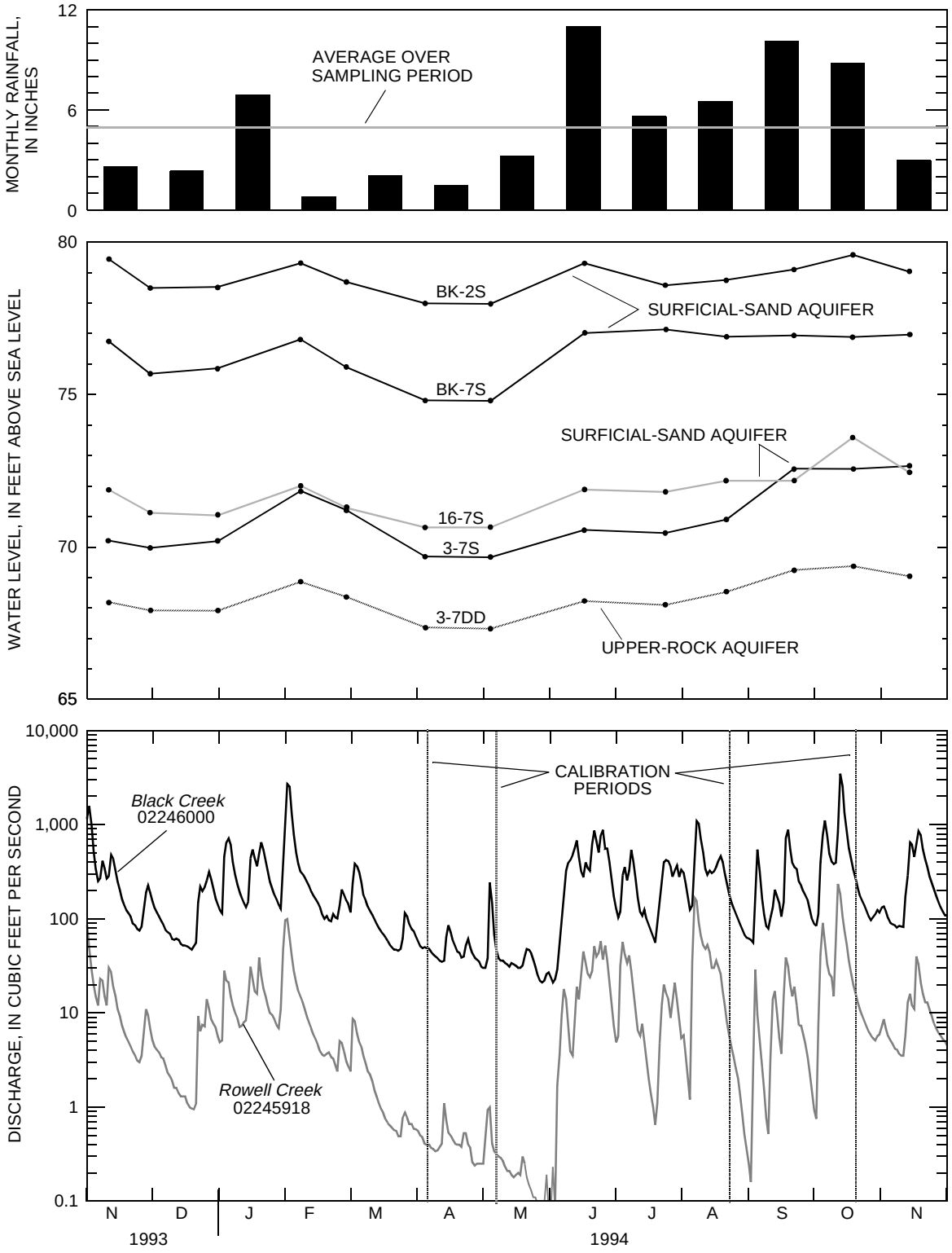

Figure 15. Monthly rainfall and ground-water levels from selected wells at Cecil Field and daily discharge at stream-gaging stations Black Creek (02246000) and Rowell Creek (02245918) from November 1993 to November 1994.

The recession-curve-displacement method (Rorabaugh, 1964; Rutledge, 1993) was used to estimate the long-term recharge rate to the Black Creek Basin (fig. 4) using daily stream discharge collected at station 02246000 during 1932-94. Although this method has some theoretical basis, the method is strongly governed by three empirical values: the recession index, κ, critical time, T_c, and time base, T^*. The recession index and critical time are inversely related to the diffusivity, *Kb*/*S*, of the contributing aquifer system (Linsley and others, 1958; Rorabaugh, 1964) and are positively correlated to one another. Estimates of κ range from 25 d/logQ to 210 d/logQ (fig. 16) at station 0224600 on the Black Creek. Large estimates of κ (210 d/logQ) assume that the short-term responses are due to surface-water impoundments and that base flow is only represented by the long-term recession. The computed recharge rates estimated with this range of κ are fairly insensitive to this parameter.

The time base is the duration of time after a peak in streamflow when overland runoff is still a component of stream discharge. A frequently cited estimate of time base is the empirical equation $T^* = A^{0.2}$ (Linsley and others, 1958), where T^* is the time base in days and A is the drainage area in square miles. For the Black Creek Basin, the time base is 3 days according to this estimate. Low slopes and impoundments such as those present in the study area tend to prolong the duration of overland runoff events. Estimates of T^* under these conditions tend to be greater than estimates based on drainage area.

Recession indices of 25, 70, and 210 d/logQ and time bases of 3, 6, and 9 days were used to estimate recharge rates. Ranges of values of the two parameters were used to assess the uncertainty associated with these parameters. Critical times (T_c) were not tested independently because T_c is a function of κ (Rutledge, 1993). Potential recharge rates to the Black Creek Basin ranged from 4 to 10 in/yr (fig. 16).

The water-budget analysis and recharge rate estimates provide a general idea of how much water passes through the surficial aquifer system, but cannot discern what fraction of flow passes through the surficial-sand or upper-rock aquifers or the quantity of deep infiltration. The direction and velocity of the movement of contaminants from specific sites are also not determined through a water-budget analysis. A ground-water flow model is needed to address these more specific questions.

SIMULATION OF GROUND-WATER FLOW AND ADVECTIVE TRANSPORT OF CONTAMINANTS IN THE SURFICIAL AQUIFER SYSTEM

A three-dimensional numerical model was used to quantitatively analyze ground-water flow and the advective transport of contaminants through the surficial aquifer system. The McDonald and Harbaugh (1988) modular finite-difference model (MODFLOW) was used to simulate flow in the surficial aquifer system and solve the governing equation:

$$-\nabla(Kb\nabla h) + q + (P - Q_S) - ET = S\frac{\partial h}{\partial t}, \qquad (2)$$

where

∇ is del, the vector differential operator;
K is hydraulic conductivity, in feet per day;
b is thickness, in feet;
h is hydraulic head, in feet;
q is a source or sink, in feet per day;
$P - Q_S$ is precipitation minus surface runoff, in feet per day;
ET is evapotranspiration, in feet per day;
S is storage coefficient in confined aquifers and the specific yield in unconfined aquifers, dimensionless; and
t is time, in days.

Description of Ground-Water Flow Model

To implement a finite-difference model, the study area was discretized into a rectangular grid of cells by row and column. The model grid covered an area greater than 36 mi^2 and was divided into 117 rows of 91 columns (fig. 17). Smaller cells were used in more stressed areas such as along creeks or drains and near observation wells to avoid over-linearization in areas of interest. Variably spaced, small cells were used near sites 5, 16, and 17, the north fuel farm, and along reaches of Sal Taylor and Rowell Creeks, where water-level data are relatively numerous and discharge is considerable. Of the 74,529 model cells, 72,534 were active cells that ranged in size from 2,500 to 13×10^6 ft^2. The largest cells were in peripheral areas of little stress or away from areas of interest.

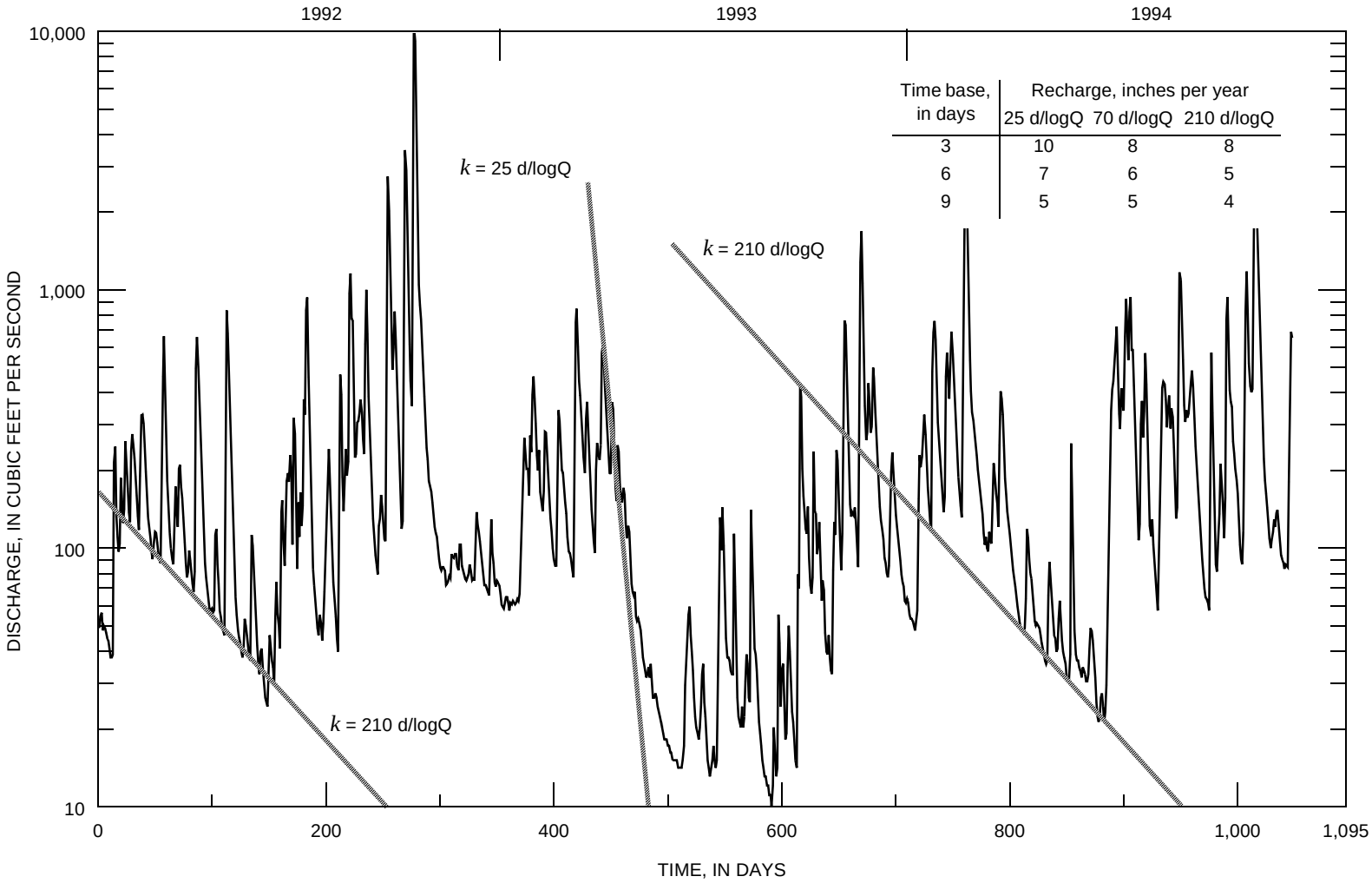

Figure 16. Discharge at stream-gaging station 02246000 on the Black Creek and selected base-flow recession curves for 1992-94.

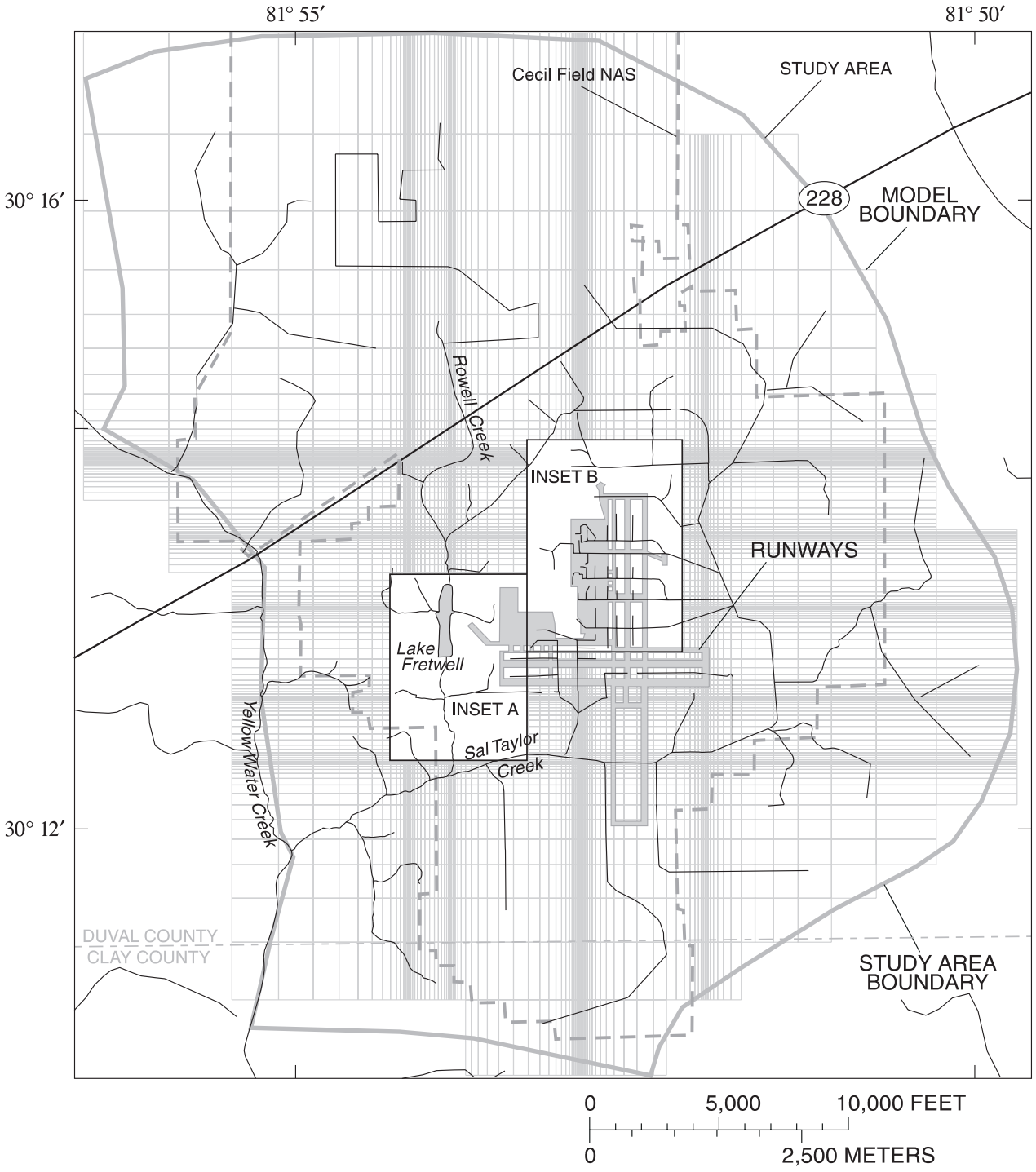

Figure 17. Model grid and extent.

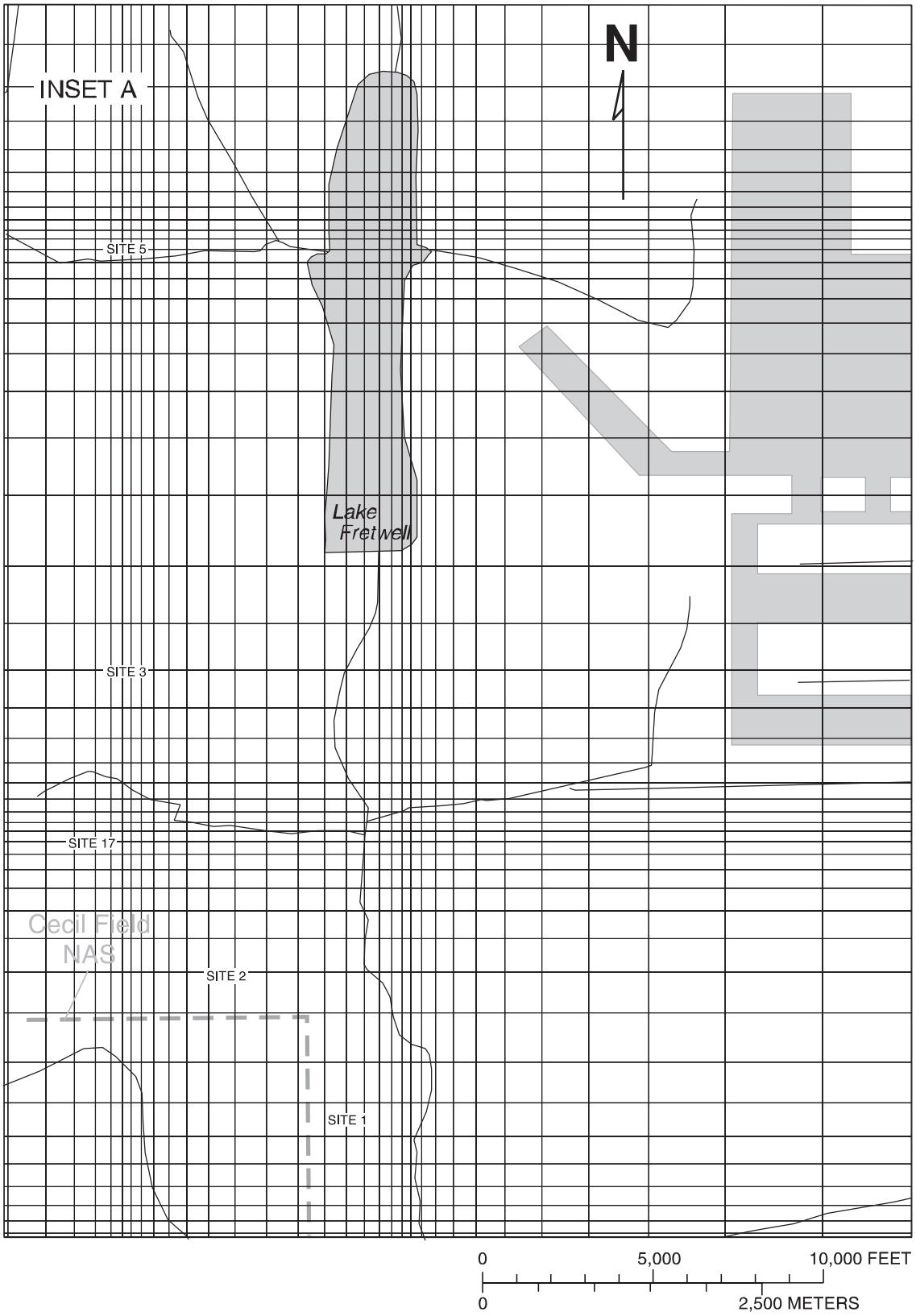

Figure 17a. Model grid and extent.

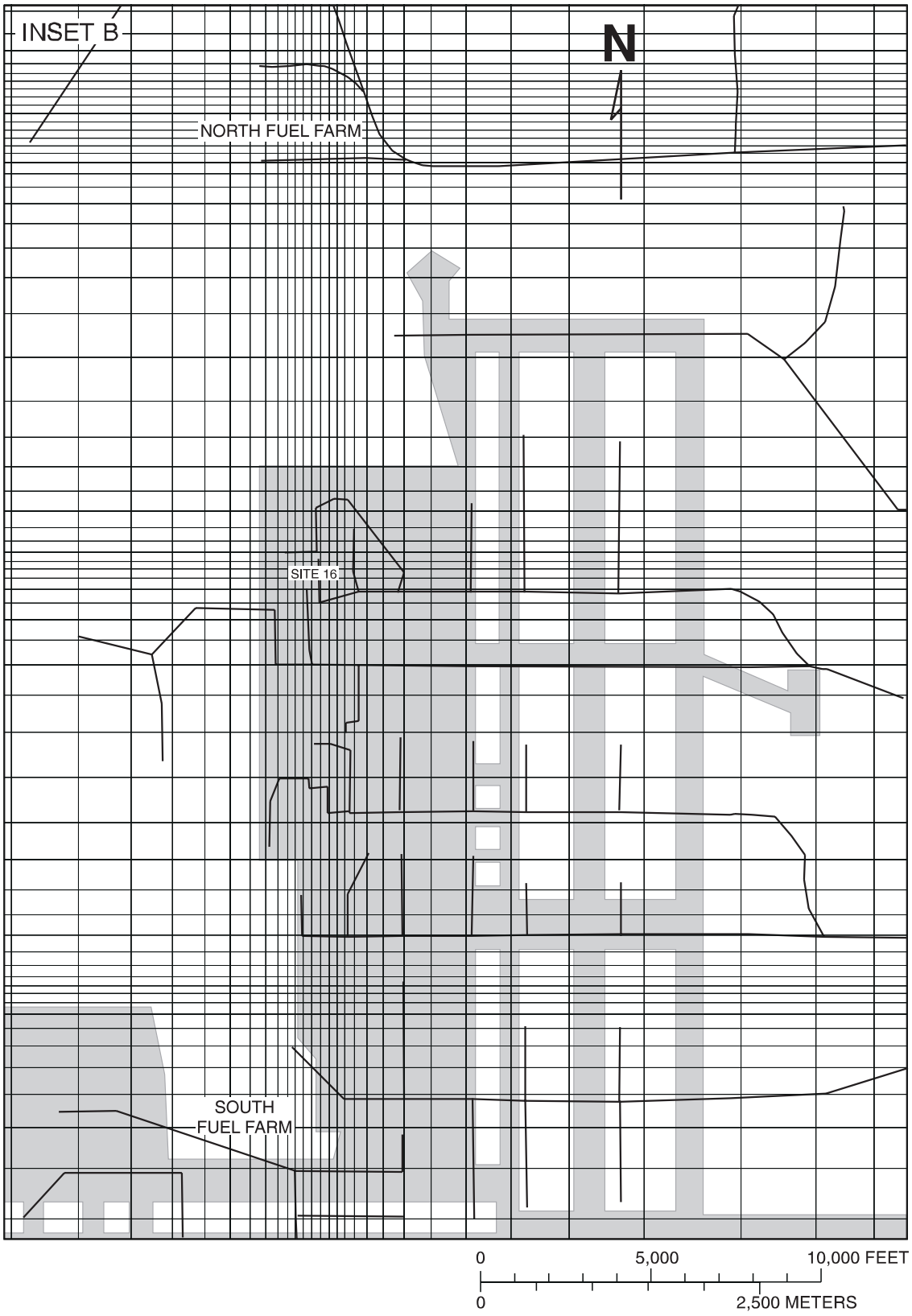

Figure 17b. Model grid and extent.

The grid was generally oriented parallel to the primary drains: Sal Taylor (east-west), Yellow Water, and Rowell Creeks (north-south) (fig. 1). No measurements of anisotropy were available and a lateral anisotropy ratio of 1:1 was used for simulation. Values of aquifer and confining-unit hydraulic properties were assigned to the center of each cell, defined as a node, by interpolation from observed point values.

The model was vertically discretized into seven layers, three of which were used to simulate the surficial-sand aquifer (fig. 12). The surficial-sand aquifer was discretized into layers 1, 2, and 3 by dividing the wetted thickness into three equal parts. Layers 4, 5, and 6 represented the blue-marl confining unit, the upper-rock aquifer, and lower-rock aquifer, respectively. Simulation of the blue-marl confining unit as an active layer (4) is atypical and is not necessary to effectively simulate flow and transport in the surficial-sand aquifer. Because contaminant movement through the blue-marl confining unit is a regulatory concern, the confining unit was simulated as an active model layer rather than as a leakance unit. Simulation of the blue-marl confining unit as an active layer allows for lateral migration within the confining unit which cannot be accounted for if it is simulated as a leakance unit. Layer 7 represented the Upper Floridan aquifer during the calibration period and was a specified-head lower boundary for the model.

Vertical impedance to flow within the surficial-sand aquifer and between the other aquifers was simulated by assigning leakance values at each cell between model layers. The leakance is the average vertical hydraulic conductivity of the aquifer or confining unit material between nodes divided by the vertical distance between corresponding nodes in adjacent model layers and is in units of feet per day per foot. Within the intermediate confining unit, the leakances represent the resistance to flow across the gray-marl and lower confining units (fig. 2).

Hydraulic Properties

Three aquifer tests were conducted near well D-4560 (fig. 1) to provide initial estimates of the hydraulic properties of the aquifers and confining units in and immediately beneath the surficial aquifer system. The lateral hydraulic conductivities of the surficial-sand, upper-rock, and lower-rock aquifers were estimated from the aquifer tests. Vertical hydraulic conductivities also were estimated for the blue-marl and gray-marl confining units as well as the surficial-sand aquifer.

An aquifer test consists of pumping water from the aquifer at a known rate and measuring the drawdowns in nearby observation wells. Hydraulic conductivities are estimated by fitting a model to the measured drawdowns. The appropriate flow model to use is dictated by the geology of the site and the configuration of observation wells. The drawdown response in a single, confined aquifer can be described quite well by the analytical Theis (1935) model because it meets the assumptions of this solution. More complicated systems, such as the one at Cecil Field NAS, require a model that can account for responses to stress in the shallowest aquifer, which is unconfined, and the hydraulic connection between lower aquifers, which are confined.

Three production wells and eight observation wells were used for the aquifer tests. Individual production wells were screened in the surficial-sand, upper-rock, and lower-rock aquifers, respectively (fig. 18). Six of the observation wells were screened within 200 ft of the production wells, with four in the surficial-sand aquifer and one each in the upper-rock and lower-rock aquifers. The remaining two observation wells were screened at the water table, 1,500 ft away and in the upper-rock aquifer, 8,500 ft away from the site, respectively. These two wells monitor background water levels for detrending water-level responses measured in the surficial-sand and upper-rock aquifers.

The surficial-sand, upper-rock, and lower-rock aquifers were pumped at rates of 5, 54, and 85 gal/min, respectively, and water levels were monitored continuously in wells screened in the aquifer being stressed and in vertically adjacent aquifers during each test. The aquifer tested was stressed for about 2 days and allowed to recover about 2 weeks before testing the next aquifer. Absolute drawdowns were estimated by measuring the water-level change in each observation well during the test. These drawdowns were then adjusted for regional trends using the water-level change measured in the background well screened in the same aquifer. A background well for the lower-rock aquifer did not exist and no trend was assumed to exist in that aquifer during any of the tests.

Hydraulic properties were estimated from the aquifer tests by fitting results computed using a variably saturated, radially symmetric, numerical model, VS2DT (Lappala and others, 1987; Healy, 1990) to the measured drawdowns. The VS2DT aquifer-test model spanned the entire shallow-aquifer system from land surface to the base of the lower-rock aquifer and was used to analyze all three tests. The entire vertical section was simulated for all test analyses to avoid prescribing boundary conditions within the section.

The VS2DT analyses were based on assumptions that the lateral and vertical hydraulic conductivity and specific storage of each aquifer or confining unit could be described by a single value. Only a

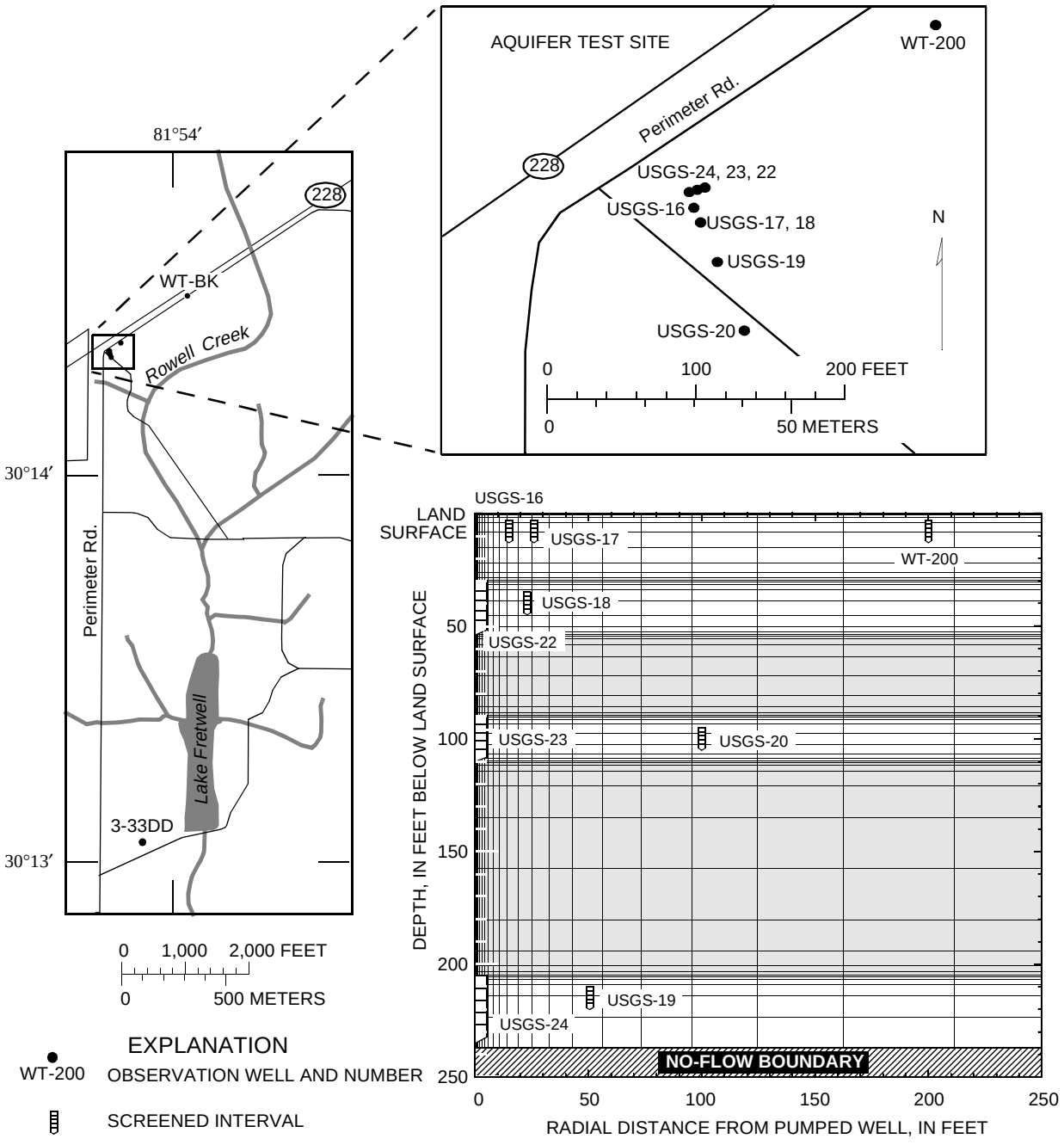

Figure 18. Location of aquifer test site at Cecil Field Naval Air Station, background observation wells, a cross-section showing well placement and model grid within 250 feet of the wells pumped for the aquifer tests, and nearby hydrologic features.

fraction of these parameters were estimated during any individual test. The results of several aquifer tests were used in succession to update unestimated parameters. Parameters were estimated iteratively until the properties used for all three aquifer tests were internally consistent (table 1).

Additional lateral hydraulic conductivity data within the surficial-sand aquifer were determined from slug tests (U.S. Department of the Navy, 1992b) at sites 1, 2, 3, 5, 16, 17, and the north and south fuel farms (fig. 17, A and B). Three wells were tested at each site except for site 3, where four wells were tested. These lateral hydraulic conductivity values represent averages over the first 10 to 15 ft of saturated, surficial-sand aquifer and range from 0.6 to 5 ft/d. The variability in lateral hydraulic conductivity at each site, as defined by dividing the largest value by the smallest value, ranged from twofold at sites 5 and 16 to fivefold at site 2 and the south fuel farm.

Table 1. Aquifer and confining unit properties determined from aquifer tests

[Values of K_{xy}, K_z, and S_s estimated from aquifer test results unless otherwise noted; all thicknesses were measured; ft/d, feet per day; ft, feet; --, not applicable]

Aquifer or confining unit	K_{xy}, ft/d	K_z, ft/d	S_s, 10^{-6}/ft	Thickness, ft	Model layer
Surficial-sand aquifer	5	0.4	40	54	1, 2, and 3
Blue-marl confining unit	0.01[a]	.01	9	36	4
Upper-rock aquifer	40	4[a]	2	20	5
Gray-marl confining unit	.002[a]	.002	5[a]	95	--
Lower-rock aquifer	20	2[a]	2	32	6

[a] Assumed $K_{xy}/K_z = 10$ for aquifers and $K_{xy}/K_z = 1$ for confining units. Estimated $S_s = 5 \times 10^{-6}$/ft by extrapolation from shallower intervals.

The initial transmissivity arrays input to the study-area flow model were calculated by multiplying the lateral hydraulic conductivity for each unit from table 1 by the corresponding thickness for that layer (figs. 6-11). One value of lateral hydraulic conductivity was assigned to the surficial-sand aquifer because the variability at each site was not significantly less than the variability for all of the sites, as determined by the slug tests.

The initial leakance arrays input to the model were calculated by dividing the vertical hydraulic conductivity from table 1 by the internode-distance between layers.

Surface-Water Features

The distribution of surface-water features controls the direction and rate of flow in the surficial aquifer system. In addition to Yellow Water, Sal Taylor, and Rowell Creeks, many smaller tributaries exist, both natural and man-made (fig. 14). Most of the stream elevation data were taken from 1:24,000 scale, U.S. Geological Survey (USGS) quadrangle maps. This information was supplemented by spot elevations obtained near sites 1, 5, 16, 17, and the north fuel farm.

Interaction between the surficial-sand aquifer and the creeks, runway drains, and Lake Fretwell was simulated by river nodes. These surface-water features were simulated as a group because they all contribute to the Black Creek Basin discharge. The flow rate in or out of the aquifer at a river node is defined by:

$$Q_B = \frac{K_{RB} L W}{M} (H_{RIVER} - H_{AQUIFER}), \qquad (3)$$

where

K_{RB} is the hydraulic conductivity of the riverbed, in feet per day;

L is the length of river reach across a cell, in feet;

W is the average width of a reach, in feet;

M is the average thickness of the riverbed, in feet;

H_{RIVER} is the average stage of the river or lake, in feet; and

$H_{AQUIFER}$ is the head in the aquifer beneath the river, in feet.

This equation only applies if $H_{AQUIFER}$ is greater than the assigned elevation of the river or lake bottom.

Uniform K_{RB}, W, and M values of 0.05 ft/d, 10 ft, and 1 ft, respectively, were assumed for all creeks throughout the study area. Initial values were selected so that riverbed conductance could control discharge from the model cells. All river reaches shown in figure 17 were represented in the model and the length, L, of river reach equalled the amount of reach bounded by the cell. A total of 2,007 river nodes was assigned to layer 1. The river bottom elevation for all creeks was set equal to the river stage to ensure all simulated reaches would be either gaining or inactive.

Different conductances and river bottom elevations were used to simulate Lake Fretwell, because the areal extent of the lake in contact with the surficial-sand aquifer was greater than the areal extent of the river bottoms. In addition, portions of the lake lose water to the surficial-sand aquifer. The simulated lake was defined by the model nodes that fell within the shaded outline shown

in figure 17, inset A. For each lake cell, the area in contact with the surficial-sand aquifer, LW, was set to the surface area of the cell and the river bottom was set far below the lake stage so the lake could be gaining or losing. A uniform hydraulic conductivity value was used for all of the riverbed and lake bottom conductances and was estimated by model calibration.

A variable hydraulic conductivity was also used to simulate the runway drains, which are pipes buried beneath the runways. Cracks in the drain walls and joints between pipe sections probably are the primary conduits of flow and controlled seepage into the drains. An independent hydraulic conductivity could not easily be estimated for the drain lines and the final estimates were based on model calibration.

North of SR 228 and along the eastern edge of the study area, perennial swampy areas exist where the water table ranges from less than 1 ft below land surface to land surface. During intense rainfall, the water table approaches land surface over a larger area that is approximated by the 75-ft land surface elevation contour (fig. 14). The area where the land surface elevation was greater than 75 ft was simulated as drains with high conductances and outlet heads set at land surface. If the water table rises to land surface, the drains behave as specified heads, otherwise they have no effect. Conceptually, the drain nodes simulated the effects of relatively high evapotranspiration and ground-water discharge in these areas.

Boundary Conditions

Proper representation of model boundary conditions is one of the most important aspects in the simulation of an aquifer system. Model boundaries are assigned to represent the actual hydrologic boundaries as accurately as possible. If model boundaries are necessarily highly generalized, they are placed far enough away from the influence of hydrologic stresses in the model area to minimize their effects on simulation results.

The upper boundary, layer 1, is the water table and is represented in MODFLOW as a free surface except where it rises to land surface. A spatially uniform recharge rate was applied to this boundary in all simulations. This did not result in a spatially uniform flux across the water table due to rejection of water in areas where the water table is near or at land surface. The lower model boundary, layer 7, is a sink for the lower-rock aquifer. Specified heads were used to define the lower boundary and represent typical Upper Floridan water levels throughout the study area (fig. 4). Seasonal changes were not considered because they are typically small (2 to 4 ft) relative to the difference in water levels between the upper-rock and lower-rock aquifers and the Upper Floridan aquifer (20 to 25 ft, fig. 19).

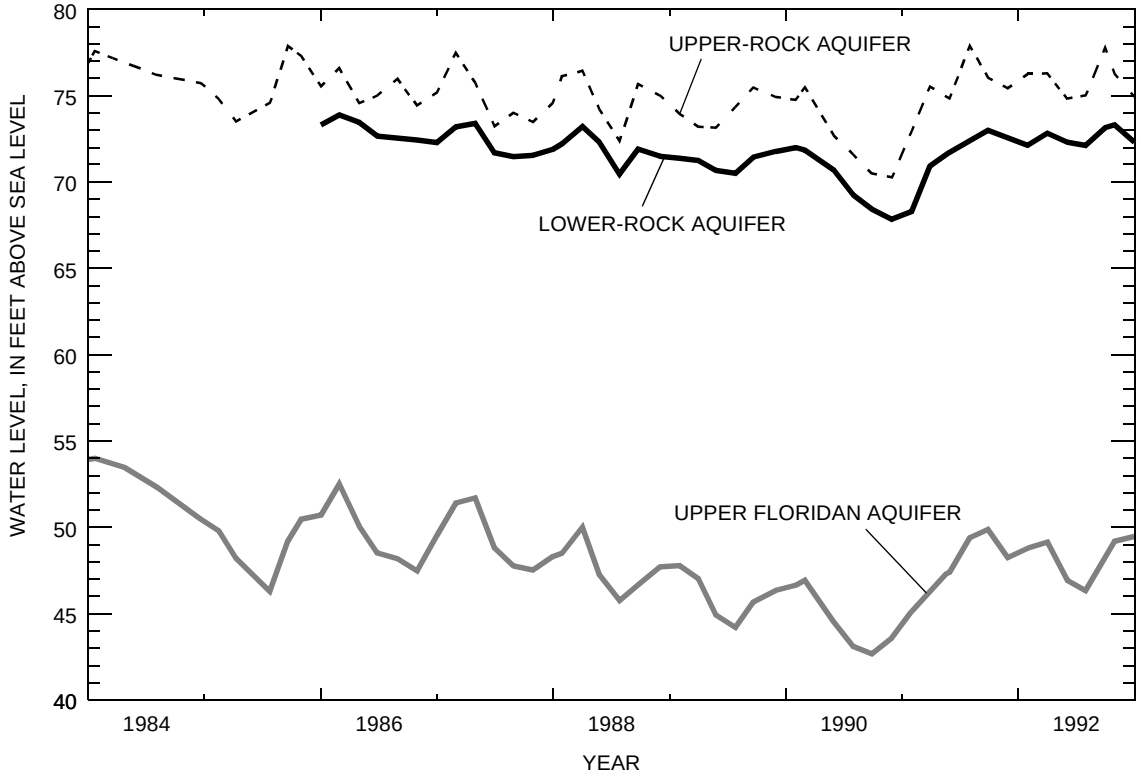

Figure 19. Long-term hydrographs from wells DS-238, 226, and 227 located near well D-4560.

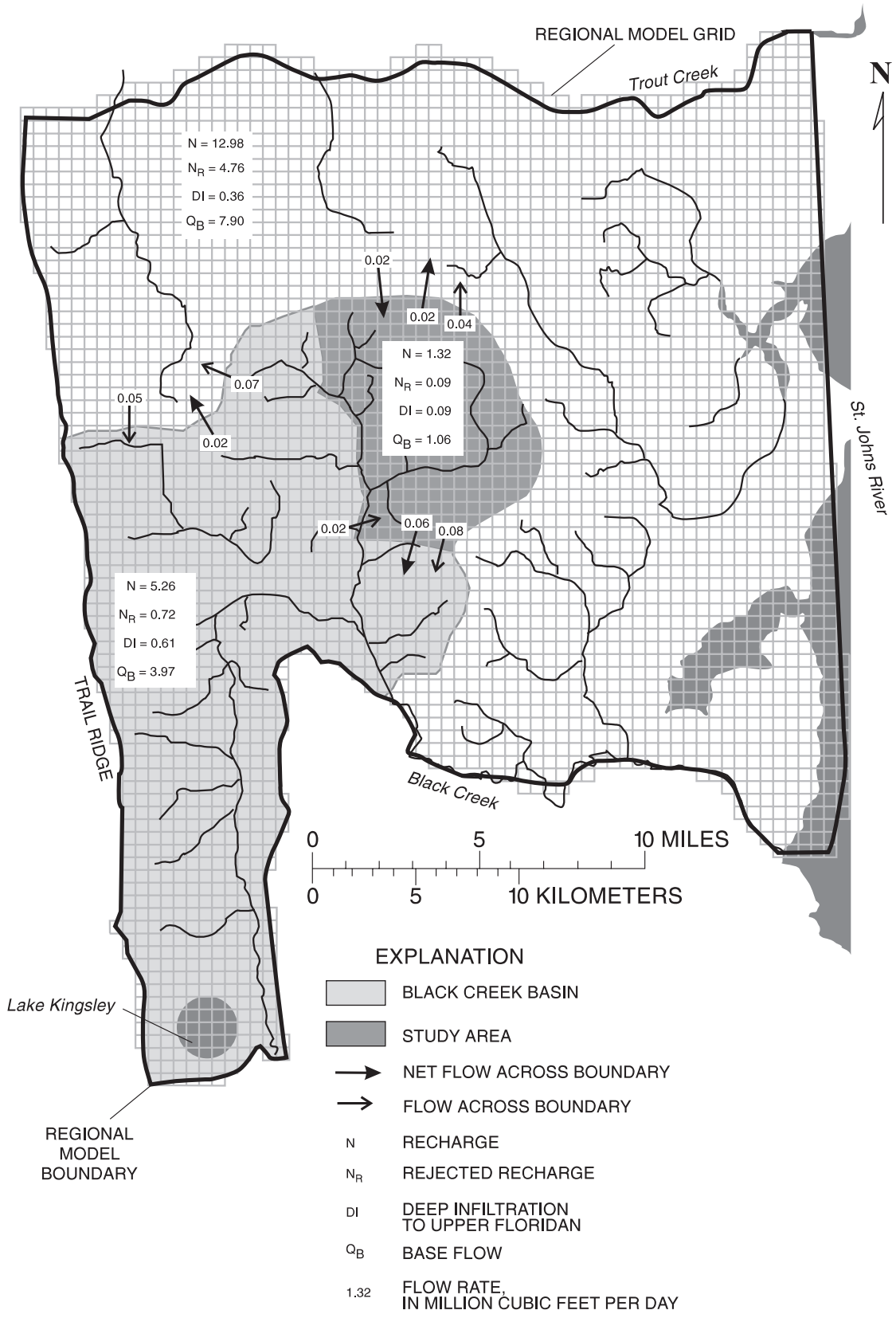

Figure 20. Grid, boundaries, and simulated volumetric budget of the regional model used to test the lateral boundary conditions for the study area.

All the lateral model boundaries in each layer are assumed to be ground-water divides that coincide with surface-water features. This assumption prescribes that areas contributing recharge to the surficial-sand, upper-rock, and lower-rock aquifers are defined predominantly by surface-water divides, not the Upper Floridan aquifer. The northern and eastern edges of the study area coincide with the boundaries of the Black Creek Basin (fig. 4). This divide constitutes a no-flow boundary because water flows downward and perpendicularly away from the boundary. The southern boundary and the western boundary north of Yellow Water Creek follow ridges from the edges of the basin to the Yellow Water Creek (fig. 17). These divides constitute no-flow boundaries because water flows parallel to but not across them. The southern segment of the western boundary lies along the Yellow Water Creek where water moves upward from deeper to shallower aquifers and is discharged to river nodes.

A simplified, regional-scale model was constructed initially to investigate the validity of assigning no-flow boundary conditions to the lateral boundaries of the study area (fig. 17). Laterally, the regional model covered the area between Trail Ridge and the St. Johns River from west to east and between Trout Creek and Black Creek from north to south (fig. 20). The regional model was divided into uniform, square cells that were 2,000 ft on a side in 83 rows of 65 columns and was vertically discretized into four layers. Layers 1, 2, and 3 represented the surficial-sand, upper-rock, and lower-rock aquifers, respectively. Layer 4 represented the Upper Floridan aquifer and was the specified-head lower boundary for the regional model. The base of the surficial-sand aquifer was set at 10 ft below sea level; uniform hydraulic conductivity and thickness values were used, except for the thickness of the surficial-sand aquifer, which varied due to the water table (table 2). Lateral hydraulic conductivities assigned to the regional model layers were those determined by aquifer test, except for layer 1, which according to slug-test results may be biased high when representing regional conditions. Rivers, lakes, and swampy areas were simulated as previously described. The upper and lower boundaries of the regional model were defined in a manner similar to that used for the study area model. No-flow conditions were assigned to lateral boundaries for layers 1, 2, and 3. Only one steady-state solution using a recharge rate of 6 in/yr was considered.

The lateral boundaries of the study area are entirely internal to the regional model. Accordingly, if the assignment of no-flow boundaries to the study-area model is valid, then the regional model should simulate no-flow between the study area and the immediately adjacent areas. A volumetric budget from the regional model indicates that only 6 percent of the water entering the study area leaves laterally. The largest lateral flow was 0.05×10^{6} ft^3/d (4 percent of the total flow) across the southern boundary in the upper-rock aquifer. Given the small magnitude of this error, the no-flow boundaries assigned to the study-area model are considered reasonable. Part of the apparent lateral flow is a byproduct of the finite-difference approximation of the study area where the flows across a boundary are similar to or greater than the net flow across a boundary. The simulated potentiometric surfaces of the surficial-sand, upper-rock, and lower-rock aquifers also suggest that little or no lateral flow would be expected across the study area boundaries (fig. 21).

Table 2. Hydraulic properties of the regional model

[All hydraulic characteristic values were based directly on aquifer-test results unless otherwise noted; ft/d, feet per day; ft, feet; 1/d, per day]

Aquifer (layer)	Hydraulic conductivity, ft/d	Thickness, ft	Vertical leakance, 1/d
Surficial-sand (1)	3[a]	Variable	3×10^{-4}
Upper-rock (2)	40	20[b]	2×10^{-5}
Lower-rock (3)	20	50[b]	5×10^{-6} [c]

[a] The average hydraulic conductivity is closer to 3 ft/d instead of 5 ft/d when slug test results are considered.
[b] Represents an average thickness over Cecil Field Naval Air Station.
[c] Value obtained from Krause and Randolph (1989).

Simulation Approach

Within the study area, the long-term water levels in and ground-water discharge from the surficial-sand aquifer change very little. Therefore, most of the questions currently raised by site assessments and remediation plans can be addressed with a steady-state ground-water flow model based on a modification of equation 2:

$$\nabla(K\nabla h) + q + \bar{N} = 0, \qquad (4)$$

where

$\bar{N}$ is the long-term recharge rate, in feet per day.

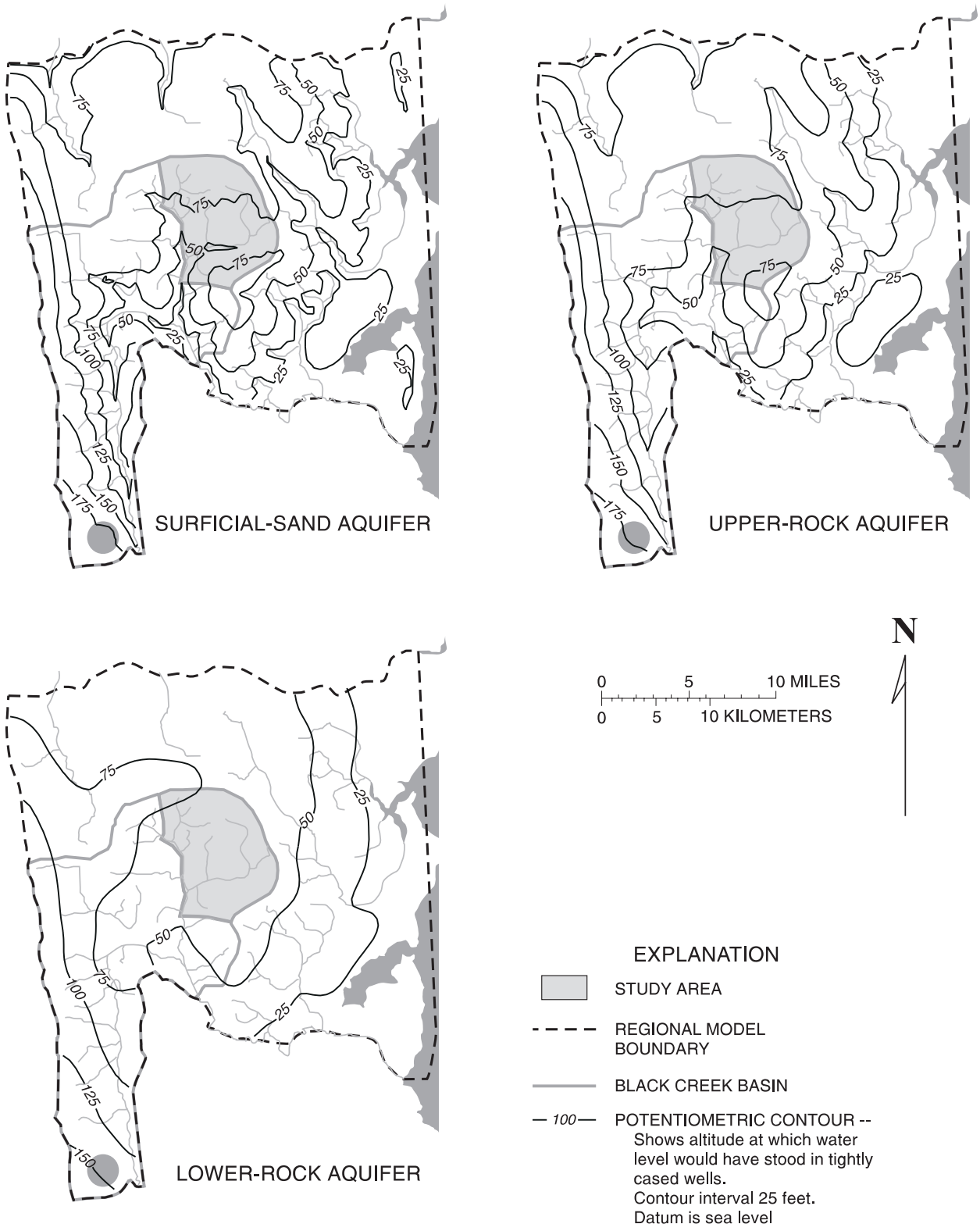

Figure 21. Simulated potentiometric surface of the surficial-sand, upper-rock, and lower-rock aquifers in the regional model area.

The water-level and base-flow data used for model calibration were obtained from several synoptic surveys conducted over approximately a year-long period. Given the infrequent sampling over a short period, long-term trends in water levels are difficult to assess. However, available data indicate that during any given year, water levels will fluctuate seasonally about 3 ft, and the surficial-sand aquifer infrequently approaches, at best, a quasi-steady state condition. Model calibration strategies are complicated by attempting to fit discontinuous, synoptic data to the transient equation 2. Such efforts require estimating the specific yield and storage coefficients, estimating the temporal distribution of ground-water recharge and evapotranspiration during the calibration period, estimating the initial head distribution, and establishing the hydraulic characteristics to develop the model.

Alternatively, the synoptic surveys can be treated as independent "snapshots" of the ground-water system taken at various times. The data from these surveys can be fitted to the simpler steady-state equation:

$$\nabla(K\nabla h) + q + N' = 0, \qquad (5)$$

where

N' is the effective recharge rate during a given survey, in feet per day, or

$$N' = (P - Q_o) - ET - S_y\frac{\partial h}{\partial t}.$$

The effective recharge rate estimated for each synoptic-survey period serves as a dummy variable and is not an estimate of the long-term recharge rate.

Several assumptions are necessarily made to apply this approach.

- The change in head with respect to time, $\frac{\partial h}{\partial t}$, at any given location can be treated as a constant during each synoptic survey.
- Survey periods are short enough to assume that all measurements are made at the same instant. Most of the water-level surveys at Cecil Field were performed over 2-day periods.
- The spatial distribution of effective recharge, N', is unknown. This leads to assumptions of a spatially uniform field of N', because the true distribution is usually not known. The problems associated with spatial variability are not unique to this approach, because the variables $(P - Q_o)$, ET, and S_y required by the transient solution can also be spatially variable.
- No water is contributed to the ground-water system from compressibility-based storage, and, thus, $S\frac{\partial h}{\partial t} = 0$. The reasonableness of this assumption is derived from the fact that specific yield, S_y, is usually three orders of magnitude greater than compressibility-based storage.

The restrictiveness of these assumptions was tested with a hypothetical, two-dimensional, cross-sectional, MODFLOW model. The cross-sectional model was constructed to be similar to a transect that extends perpendicularly from Rowell Creek to a ground-water divide 3,000 ft away and generally parallel to ground-water flow. The cross-sectional model was constructed with two layers and used the hydraulic properties and dimensions shown in figure 22. A variably spaced grid covered the 3,000 ft in 40 columns, beginning with a 3-ft-wide column and multiplying successive columns by 1.13. Both lateral boundaries and the base of the confined aquifer at 30 ft below sea level were no-flow boundaries. The upper boundary was a specified recharge rate applied to a free surface. A 100-day period was simulated in six stress periods with the recharge and evapotranspiration rates listed in table 3. The creek was simulated as a specified-head boundary using the water levels shown in figure 23 over the 100-day simulation period. A steady-state solution with a long-term recharge rate, N, of 6 in/yr and a creek elevation of 45 ft above sea level served as the initial condition.

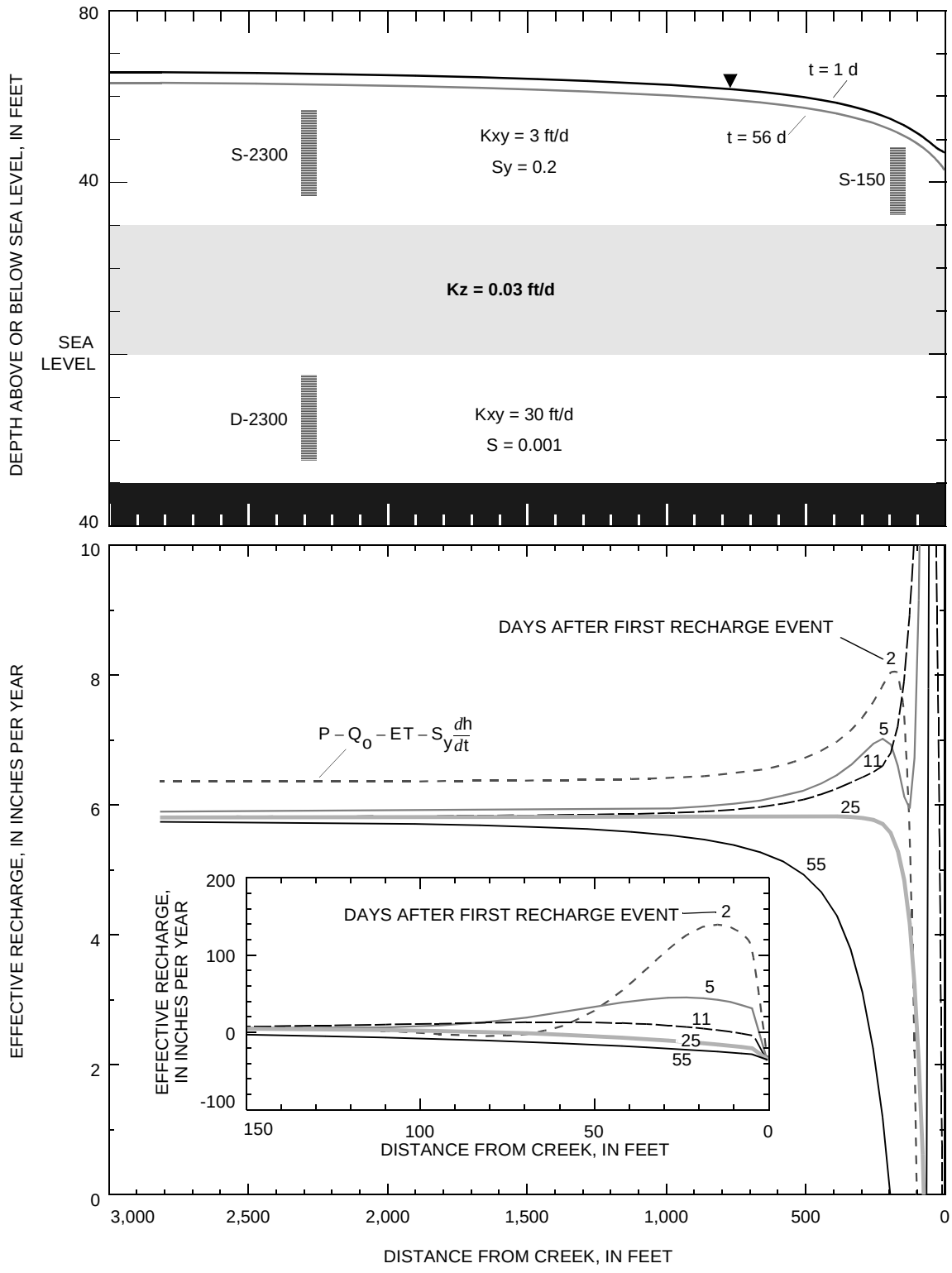

Figure 22. Hypothetical cross section that shows the expected effective recharge distribution for an aquifer system similar to the surficial-sand aquifer system.

Table 3. Stress period durations, recharge rates, and evapotranspiration rates used in the two-dimensional, cross-sectional model for testing applicability of effective recharge rates

Boundary condition	Stress period					
	1	2	3	4	5	6
End of period, day	1	56	57	63	64	100
Period length, days	1	55	1	6	1	36
P - Q_o, inches per day	3	0	5	0	3	0
Evapotranspiration, inches per day	0	0.1	0	0.1	0	0.1

The results of the cross-sectional model demonstrate that the assumptions necessary to apply synoptic-survey data to model calibration will probably be met when using effective-recharge. The simulated change in head with respect to time, $\frac{\partial h}{\partial t}$, in both aquifers approached a constant value a few days after each recharge event (fig. 23), and water levels at distances of 150 ft or more from the creek changed less than 0.1 ft during any 2-day period. The spatial distribution of effective recharge ($N' = (P - Q_o) - ET - S_y\frac{\partial h}{\partial t}$) is fairly uniform over about 80 percent of the recharge area (fig. 22) and departs most from the assumed uniform distribution either immediately after a recharge event or during the later periods of a ground-water recession. The net effective recharge rate does not depart greatly from the long-term average of 6 in/yr except during and immediately after large recharge events (fig. 23). Some water is contributed to the ground-water system from compressibility-based storage, but the amounts are small relative to the quantities released by specific yield. This is shown directly and by the small difference between N' and base flow, Q_B (fig. 23).

Although the effective recharge rates, N', estimated for each synoptic-survey period are not estimates of the long-term recharge rate, estimates obtained during extreme conditions apparently can serve to bracket the long-term recharge rate.

Model Calibration

Calibration is the attempt to reduce the difference between model results and measured data by adjusting model input. Calibration is generally accomplished by adjusting input values of hydraulic conductivity and recharge until an acceptable calibration criterion is achieved. The differences between simulated and measured ground-water levels and stream discharges are generally the bases for demonstrating the "goodness" or improvement of the calibration. Simulated water levels and discharges from a calibrated, deterministic ground-water model usually depart from measured water levels and discharges, even after a diligent calibration effort. The discrepancy between model results and measurements (model error) usually is caused by simplification of the conceptual model, grid scale, and the difficulty in obtaining sufficient measurements to account for all of the spatial variation in hydraulic properties throughout the model area.

Calibration improvement was determined by decreases in sum-of-squares error (SS) which is defined by:

$$SS = \sum_{k=1}^{nwl} (\hat{h}_k - h_k)^2 + \sum_{l=1}^{nq} ((\hat{q}_l - q_l)w_l)^2, \qquad (6)$$

where

$\hat{h}_k$ is a simulated water level, in feet;
h_k is a measured water level, in feet;
nwl is the number of water-level comparisons;
$\hat{q}_l$ is a simulated discharge, in cubic feet per day;
q_l is a measured discharge, in cubic feet per day;
w_l is a weight which is the standard deviation of all measured water levels divided by the standard deviation of all measured flow rates (Watson and others, 1980); and
nq is the number of flow-rate comparisons.

Although the sum-of-squares error serves as the objective function, root-mean-square (RMS) error is reported instead because RMS error is more directly comparable to actual values and serves as a composite of the average and the standard deviation of a set. Root-mean-square error is related to the sum-of-squares error by:

$$RMS = \sqrt{\frac{SS}{nwl + \sum_{l=1}^{nq} w_l}}. \qquad (7)$$

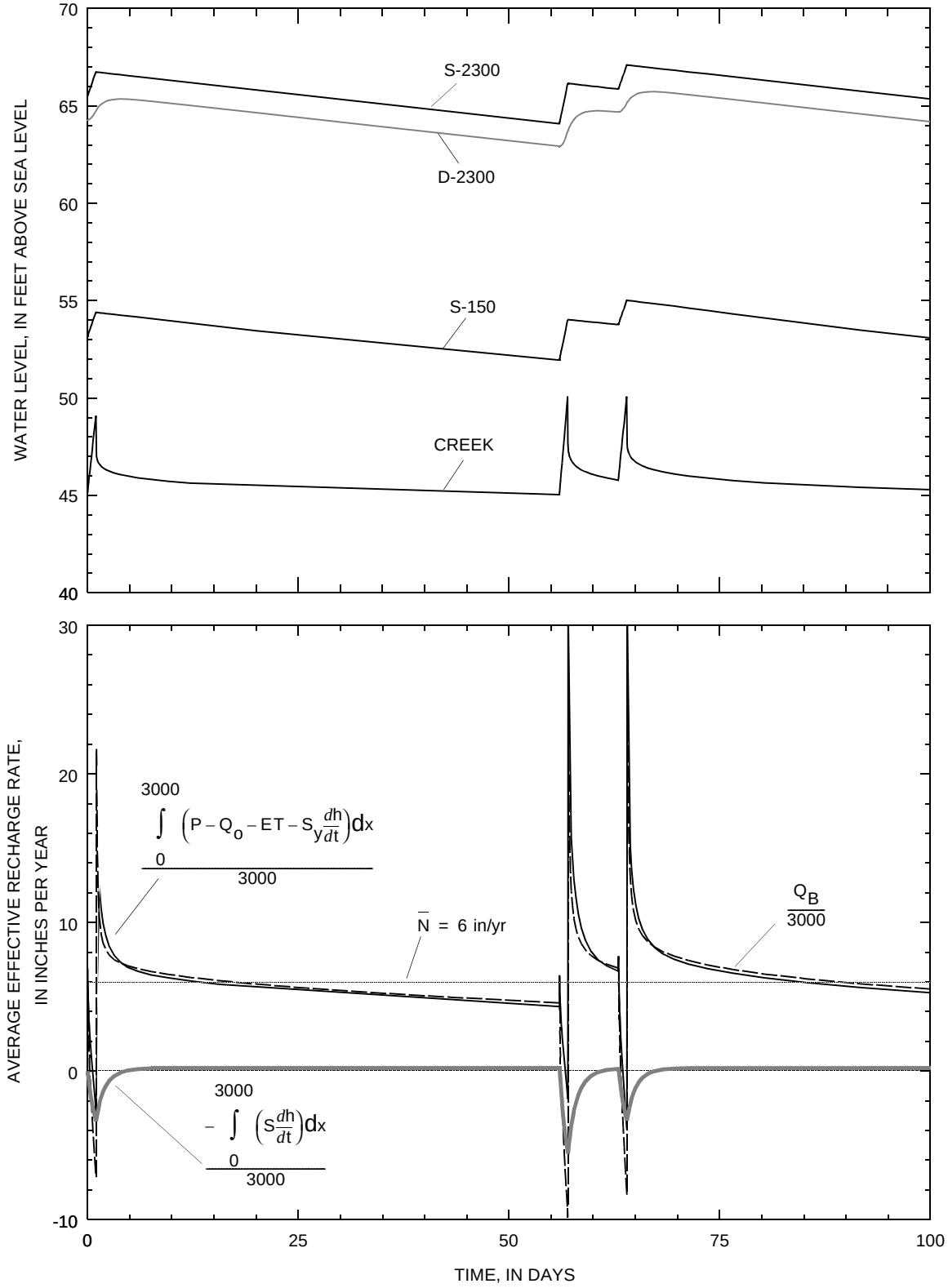

Figure 23. Hypothetical time series that shows the expected water-level changes and average effective recharge rates for an aquifer system similar to the surficial-sand aquifer system.

Water-Level and Discharge Measurements

As measured water levels rarely coincide with the center of a cell, simulated water levels were interpolated laterally to points of measurement from the centers of surrounding cells. Simulated water levels were interpolated because they were assumed to be part of a continuous distribution. Vertical interpolation was not considered because of the discontinuity and associated refraction of potential fields from an aquifer across a confining unit.

The model was calibrated to 697 water-level and 4 discharge measurements. The water levels were obtained from 212 wells during 4 synoptic surveys that spanned from April 6 to October 19, 1994 (fig. 15). Eight discharge measurements from Rowell Creek and Black Creek were available for the four surveys, but only discharge measurements from the first two surveys were used for calibration. The discharge measurements from the later surveys were both made within a week of a large rainfall event and stream discharge appeared to contain a significant component of surface runoff (fig. 15).

Because the study area only covered 20 percent ($36\ mi^2/177\ mi^2$) of the Black Creek Basin, simulated ground-water discharge was multiplied by about five for comparison to the actual discharge measurements. This approach is based on the assumption that base flow was contributed uniformly across the basin. The base-flow results simulated by the regional model indicate that the entire study area contributes 21 percent ($12\ ft^3/s$)/($58\ ft^3/s$) of the base flow (fig. 20), which suggests that, regionally, base-flow discharges are contributed uniformly. In addition, the response of the Fiftone subbasin ($2\ mi^2$) (fig. 14) and the Black Creek Basin (fig. 15) to rainfall events and the recession to base flow is very similar.

Parameter Estimation

Model calibration is facilitated by a parameter estimation program (Halford, 1992). The parameter estimation process is initialized by using the model to establish the initial differences between simulated and measured water levels and discharges. These differences, or residuals, are then minimized by the parameter estimation program. To implement parameter estimation, the sensitivity coefficients, the derivatives of simulated water level or discharge change with respect to parameter change, are calculated by the influence coefficient method (Yeh, 1986) using the initial model results. Each parameter is changed a small amount and MODFLOW is used to compute new water levels and discharges for each perturbed parameter. The current arrays of sensitivity coefficients and residuals are used by a quasi-Newton procedure (Gill and others, 1981, p. 137) to compute the parameter changes that should improve the model. The model is updated to reflect the latest parameter estimates and a new set of residuals is calculated. The entire process of changing a parameter in the model, calculating new residuals, and computing a new value for the parameter is continued iteratively until model error or model-error change is reduced to a specified level or until a specified number of iterations are made (Halford, 1992).

Logs of the parameters, *log*(x), are used because the estimated hydraulic conductivities, x, are usually log-normally distributed (Domenico and Schwartz, 1990). Log-parameters also are better behaved from a numerical perspective, because estimates are restricted to positive values and are scaled to some degree. Log-recharge rates are also used, thus ensuring that all estimated values of *N*' are positive. Consequently, all sensitivities, covariances, and correlation coefficients are based on $\frac{\partial}{\partial \log x}\hat{h}$ and $\frac{\partial}{\partial \log x}\hat{q}$, not $\frac{\partial}{\partial x}\hat{h}$ and $\frac{\partial}{\partial x}\hat{q}$.

Another benefit of this type of parameter estimation is the covariance matrix computed for the estimated parameters. This matrix is ranked by the magnitude of the main diagonal, because it is a rough indicator of the relative sensitivity of the model to a parameter. Specifically, the main diagonal is $C_{i,i} = \sum_{k=1}^{nwl} \left(\frac{\partial \hat{h}_k}{\partial \log x_i}\right)^2 + \sum_{l=1}^{nq} \left(\frac{\partial \hat{q}_l}{\partial \log x_i}\right)^2$. The off-diagonal components, $C_{i,j}$, describe the degree of interdependence between parameters, but evaluation is difficult without some sort of normalization (Gill and others, 1981).

Normalization is achieved by computing correlation coefficients (Hill, 1992), $\rho_{i,j} = \frac{C_{i,j}}{\sqrt{C_{i,i}C_{j,j}}}$, similar to r computed for a linear regression. If $\rho_{i,j}$ is ± 1, then x_i is a dependent variable of x_j. Alternatively, if $\rho_{i,j}$ is 0, then x_i is an independent variable of x_j. Correlation coefficients greater than 0.95 usually indicate a pair of parameters are highly correlated and cannot be estimated independently (Hill, 1992).

Twelve parameters (table 4) were used as global multipliers that changed the value of either hydraulic conductivity or recharge by a fixed amount throughout the study area. The only exception is the hydraulic conductivity of the drains which were adjusted beneath the runways and flight-support areas only. The initial values of hydraulic conductivity came from the aquifer test results; lower confining unit vertical hydraulic conductivities were taken from Krause and Randolph (1989). An initial recharge rate of 6 in/yr was used for all four synoptic-survey periods.

The minimum, maximum, average, and RMS errors of the calibrated model were -3.79, 4.36, 0.13, and 1.40 ft, respectively. A more detailed listing of the error statistics by layer and synoptic-survey period is provided in table 5. The greater number of water-level measurements available during synoptic-survey periods 3 and 4 did not overly bias model calibration toward those periods (table 5). The water-level residuals did not exhibit any apparent trend across the study area during any of the synoptic-survey periods (figs. 24-29). Simulated potentiometric surfaces and water-level residuals are only shown for synoptic-survey period 3 because the distribution of residuals is similar in all periods.

Table 4. Initial and final values of parameters estimated to calibrate the model

[ft/d, feet per day; in/yr, inches per year]

Estimated parameter	Initial	Final
K_{xy} of surficial-sand aquifer, ft/d	5	2.8
K_z of surficial-sand aquifer, ft/d	.4	.048
K_z of blue-marl confining unit, ft/d	.01	.0096
K_{xy} of upper-rock aquifer, ft/d	40	180
K_z of gray-marl confining unit, ft/d	.002	.0027
K_z of lower confining unit, ft/d	.002	.0012
K_{RB} of riverbeds, ft/d	.05	.7
K of drains beneath runways, ft/d	.005	.035
N′ during survey period 1, in/yr	6	4.6
N′ during survey period 2, in/yr	6	4.6
N′ during survey period 3, in/yr	6	6.0
N′ during survey period 4, in/yr	6	7.5

Table 5. Water-level error statistics from calibrated Cecil Field Naval Air Station model by layer and synoptic-survey period

[in/yr, inches per year; minimum, maximum, average, and RMS in feet; n, number of samples; --, no observation]

Layer	SYNOPTIC-SURVEY PERIOD																			
	(1) April 6, 1994 N′ = 4.6 in/yr					(2) May 7, 1994 N′ = 4.6 in/yr					(3) August 22, 1994 N′ = 6.0 in/yr					(4) October 19, 1994 N′ = 7.5 in/yr				
	Minimum	Maximum	Average	RMS	n	Minimum	Maximum	Average	RMS	n	Minimum	Maximum	Average	RMS	n	Minimum	Maximum	Average	RMS	n
1	-2.49	4.34	0.37	1.41	93	-2.44	4.36	0.43	1.42	93	-3.67	3.79	-0.01	1.40	109	-3.55	4.08	0.01	1.52	112
2	-1.62	3.71	.57	1.49	26	-1.54	3.76	.61	1.50	26	-2.83	3.33	.08	1.16	29	-3.31	2.53	.03	1.23	29
3	-3.74	1.64	-.34	1.59	25	-3.79	1.67	-.31	1.59	25	-3.06	1.71	-.07	1.10	39	-3.77	1.86	.01	1.37	36
4	-3.34	1.99	-.13	1.64	6	-3.35	2.03	-.10	1.81	5	-2.84	2.16	.03	1.33	8	-3.63	2.05	.00	1.53	8
5	-.40	.73	.24	.54	5	-.32	.69	.25	.52	5	-1.66	.62	-.22	.75	8	-1.79	.59	-.38	.87	7
6	--	--	--	--	--	--	--	--	--	--	-.37	.06	-.15	.26	2	.17	.17	.17	.17	1
All	-3.74	4.34	.26	1.45	155	-3.79	4.36	.32	1.46	154	-3.67	3.79	-.02	1.28	195	-3.77	4.08	.00	1.43	193
																Composite water level statistics for all periods				
																-3.79	4.36	.13	1.40	697

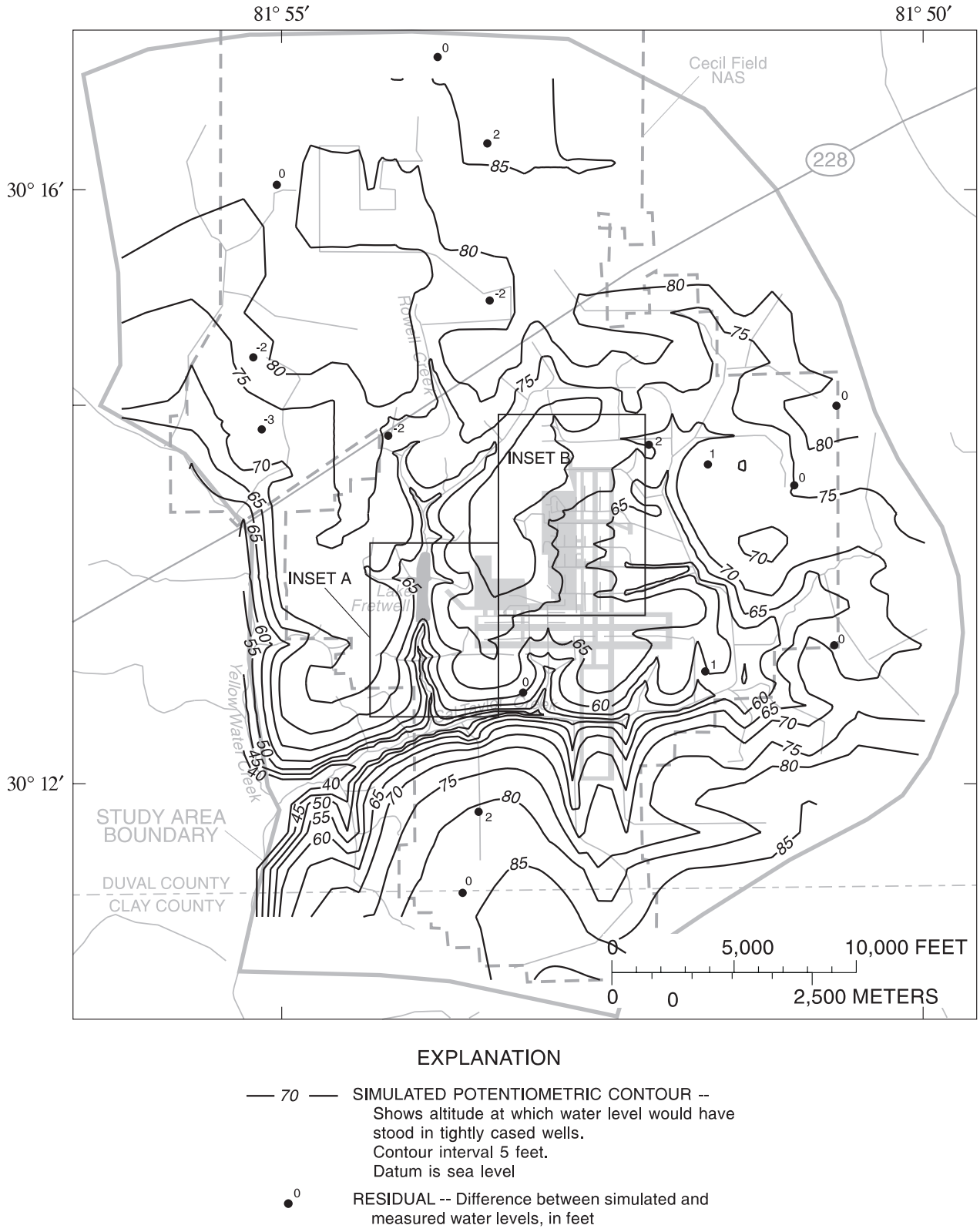

Figure 24. Simulated potentiometric surface of the top third of the surficial-sand aquifer (layer 1) on August 22, 1994.

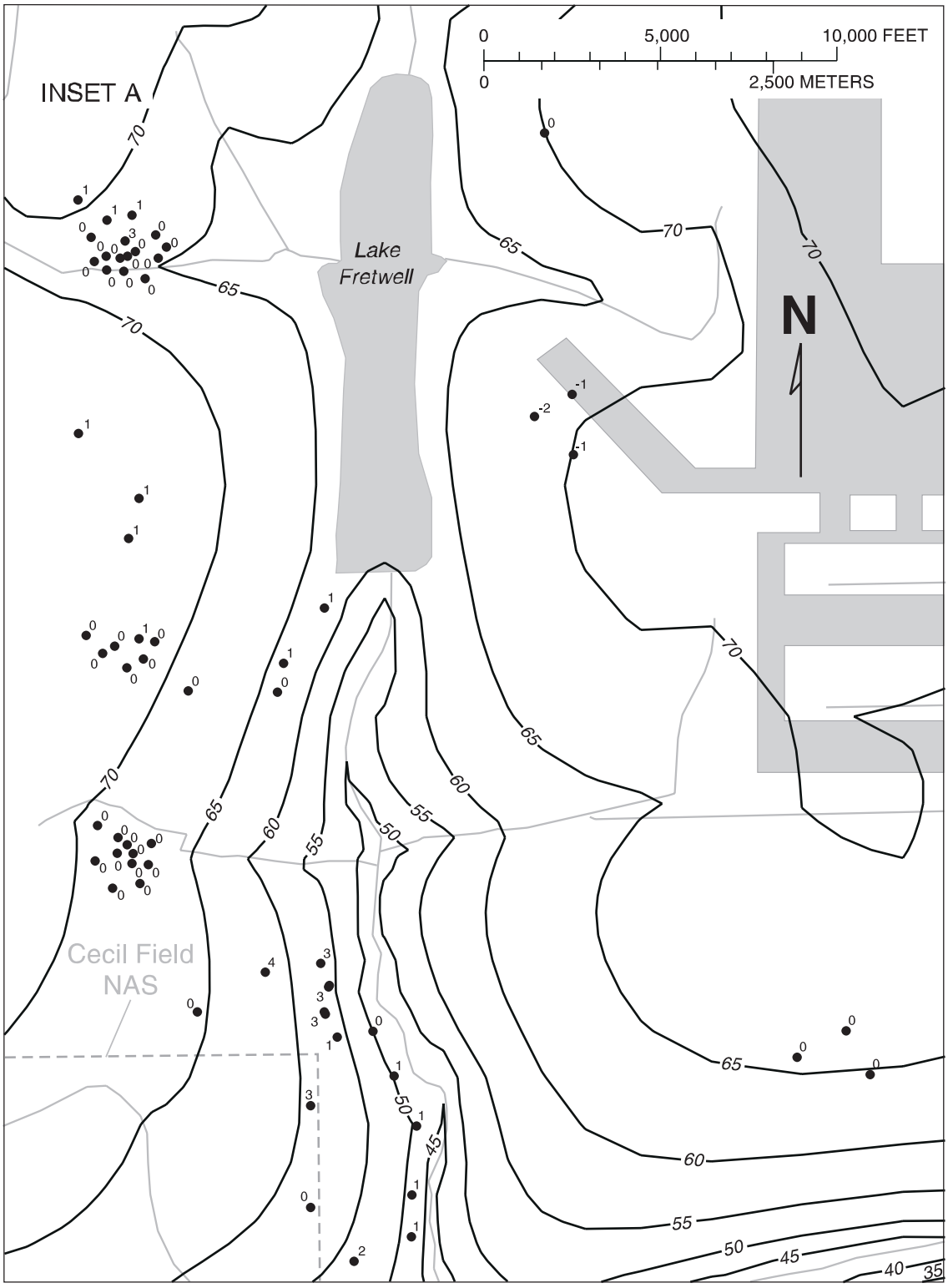

Figure 24a. Simulated potentiometric surface of the top third of the surficial-sand aquifer (layer 1) on August 22, 1994, inset A.

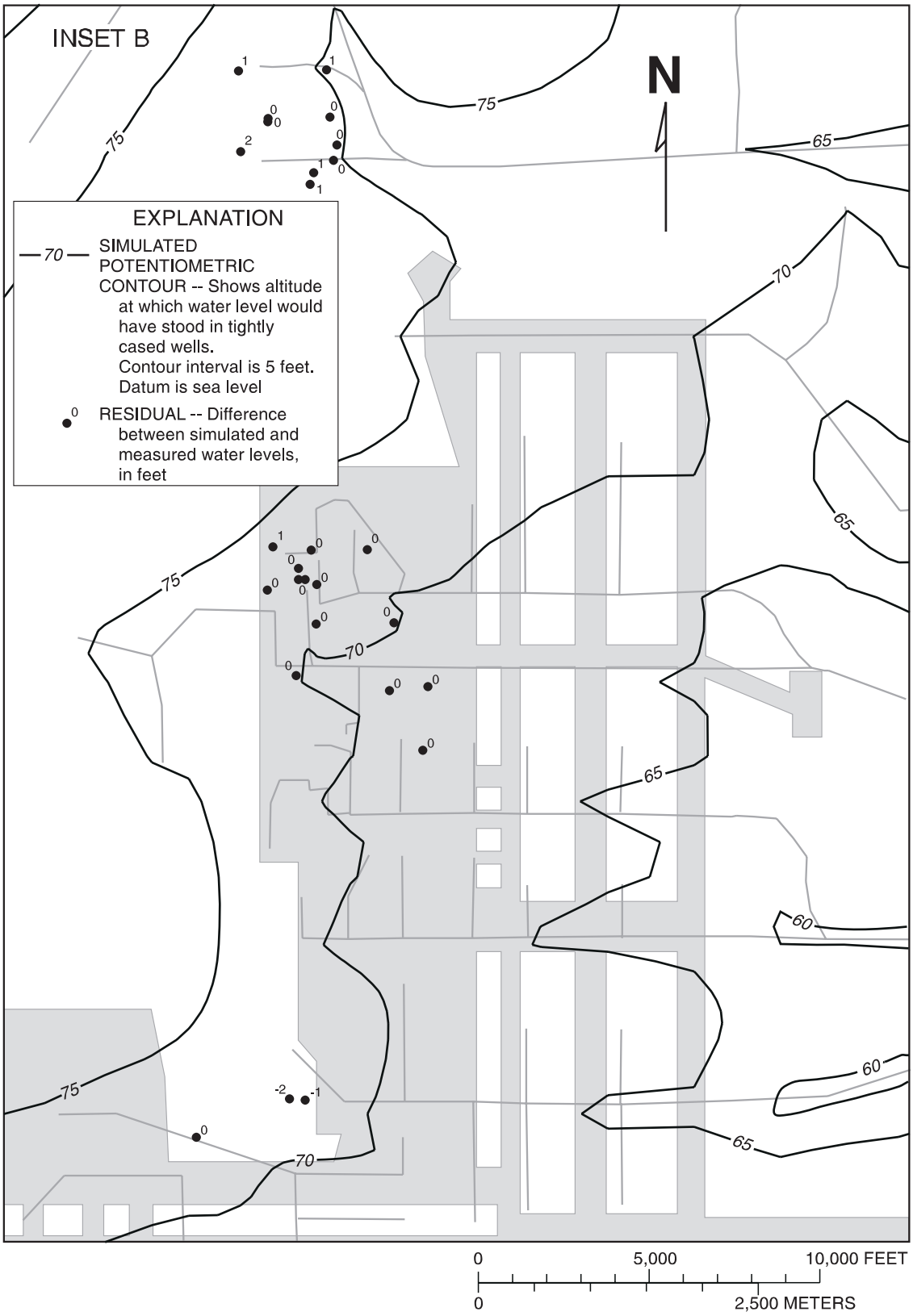

Figure 24b. Simulated potentiometric surface of the top third of the surficial-sand aquifer (layer 1) on August 22, 1994, inset B.

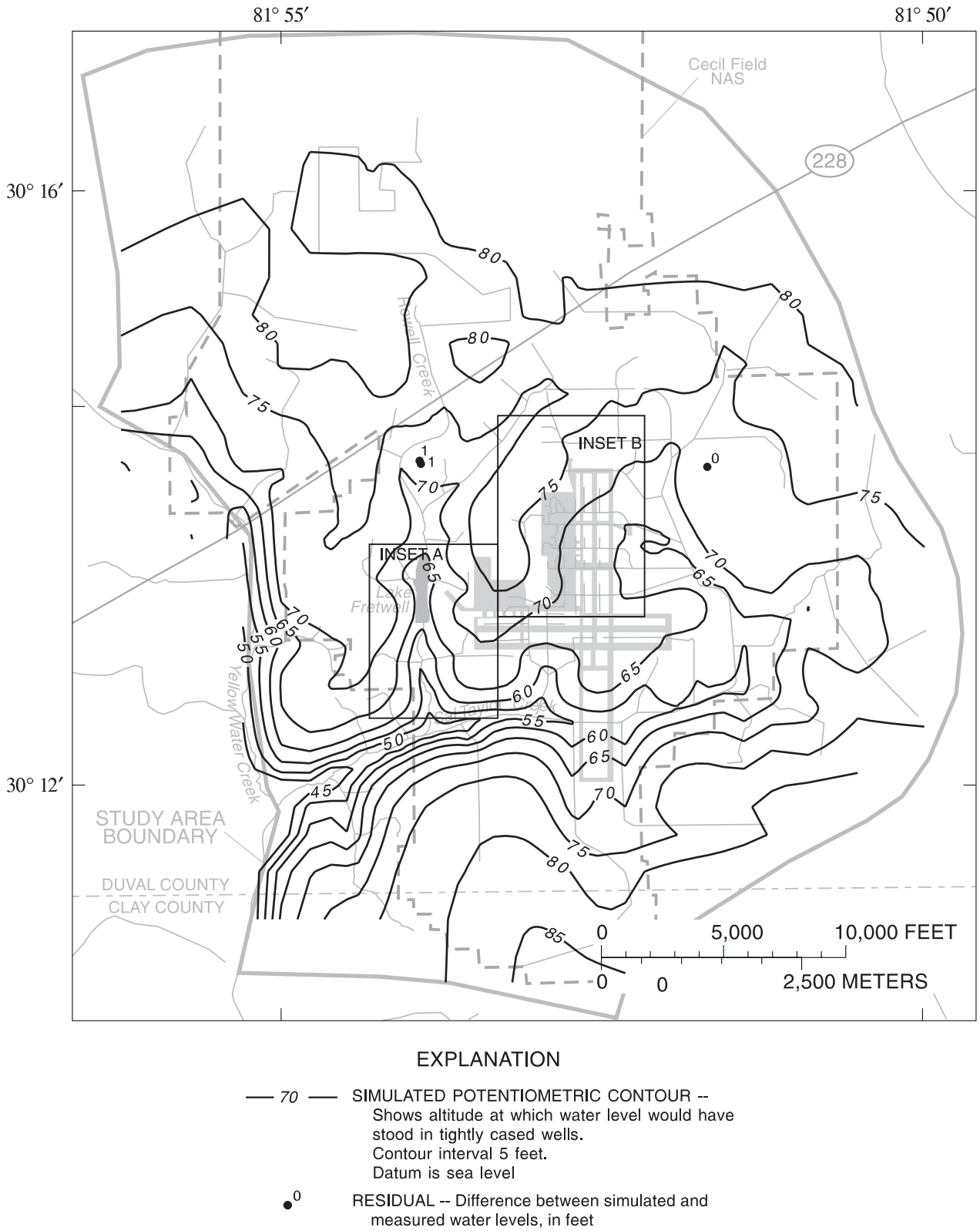

Figure 25. Simulated potentiometric surface of the middle third of the surficial-sand aquifer (layer 2) on August 22, 1994.

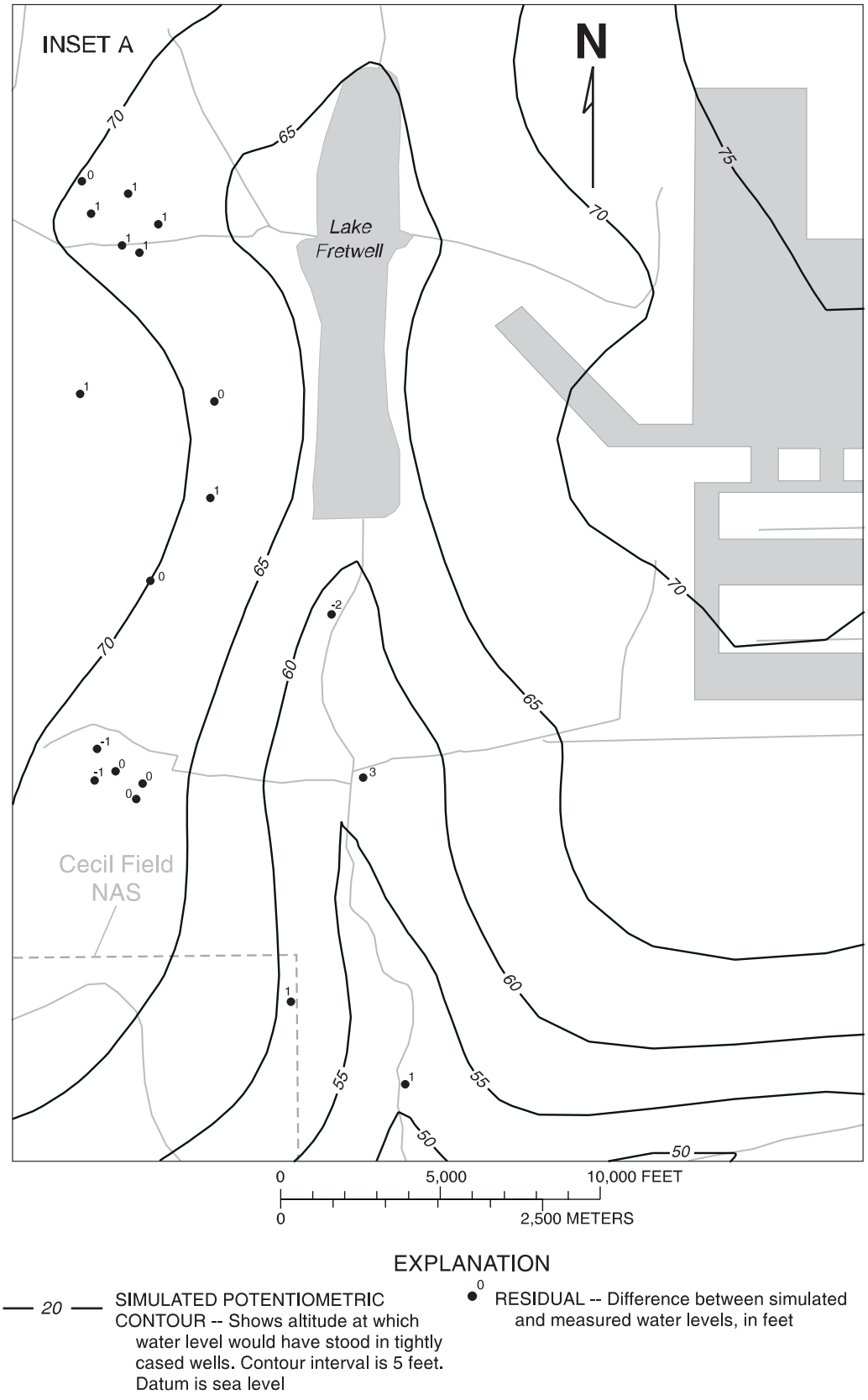

Figure 25a. Simulated potentiometric surface of the middle third of the surficial-sand aquifer (layer 2) on August 22, 1994, inset A.

Figure 25b. Simulated potentiometric surface of the middle third of the surficial-sand aquifer (layer 2) on August 22, 1994, inset B.

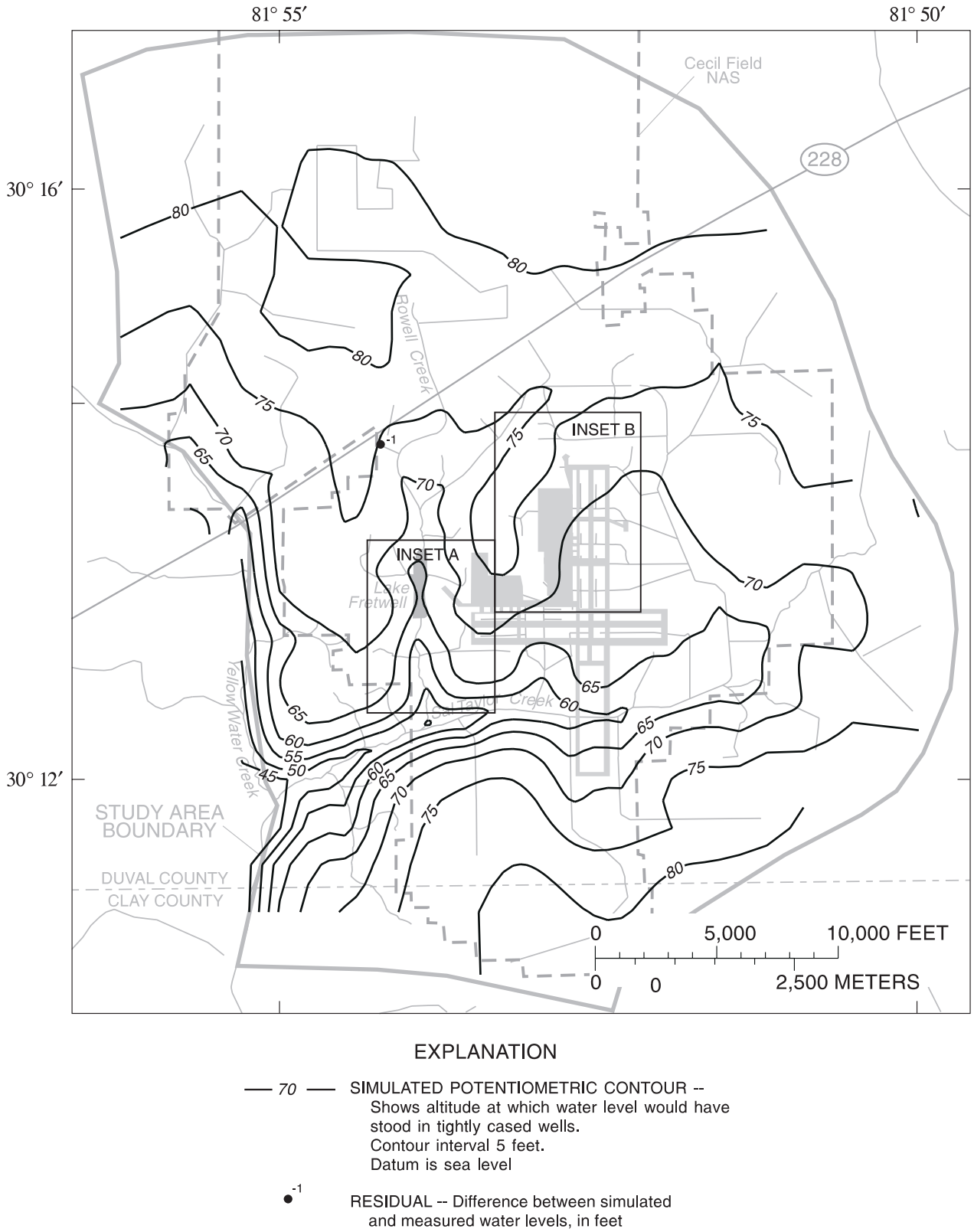

Figure 26. Simulated potentiometric surface of the bottom third of the surficial-sand aquifer (layer 3) on August 22, 1994.

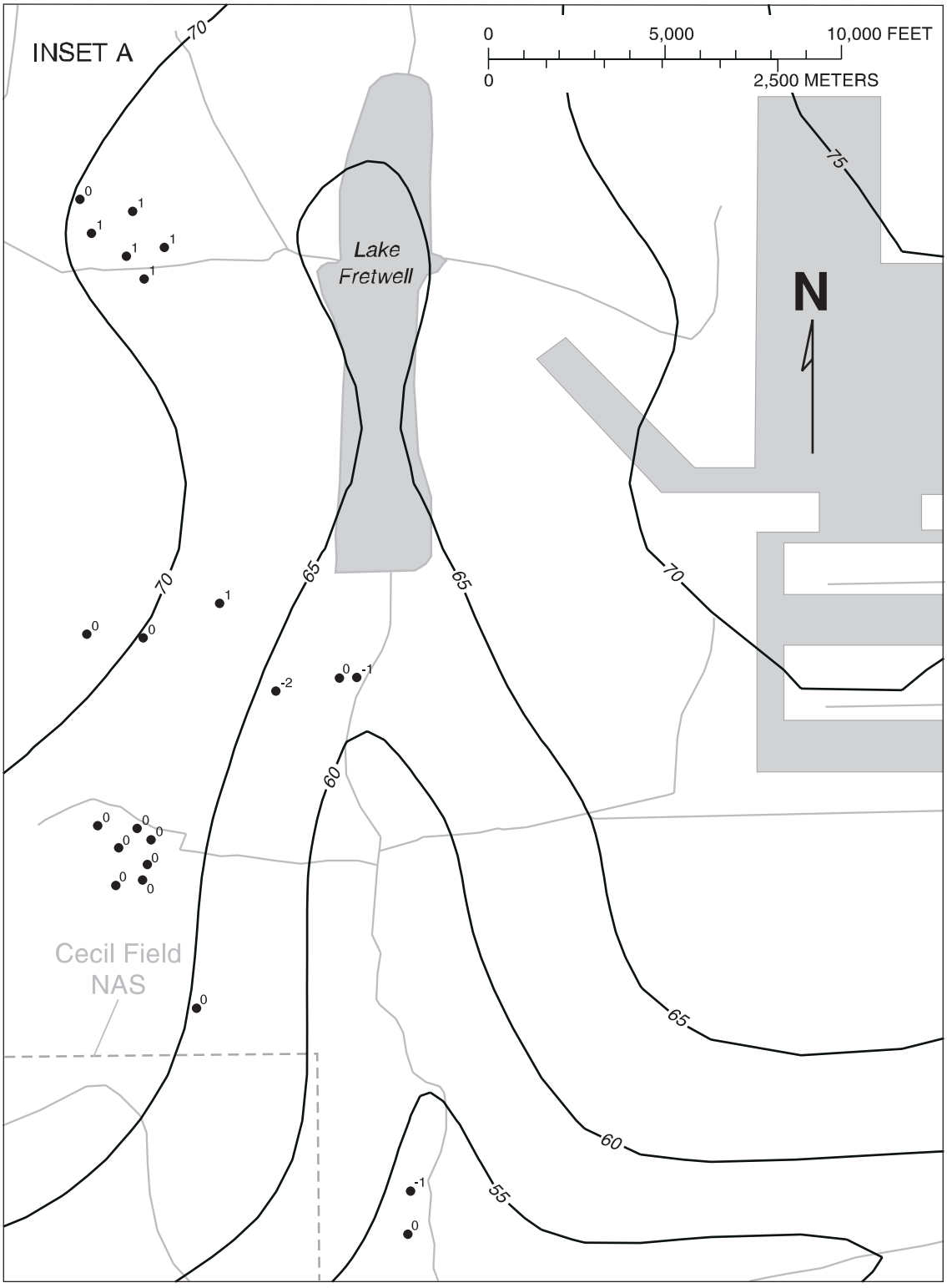

Figure 26a. Simulated potentiometric surface of the bottom third of the surficial-sand aquifer (layer 3) on August 22, 1994, inset A.

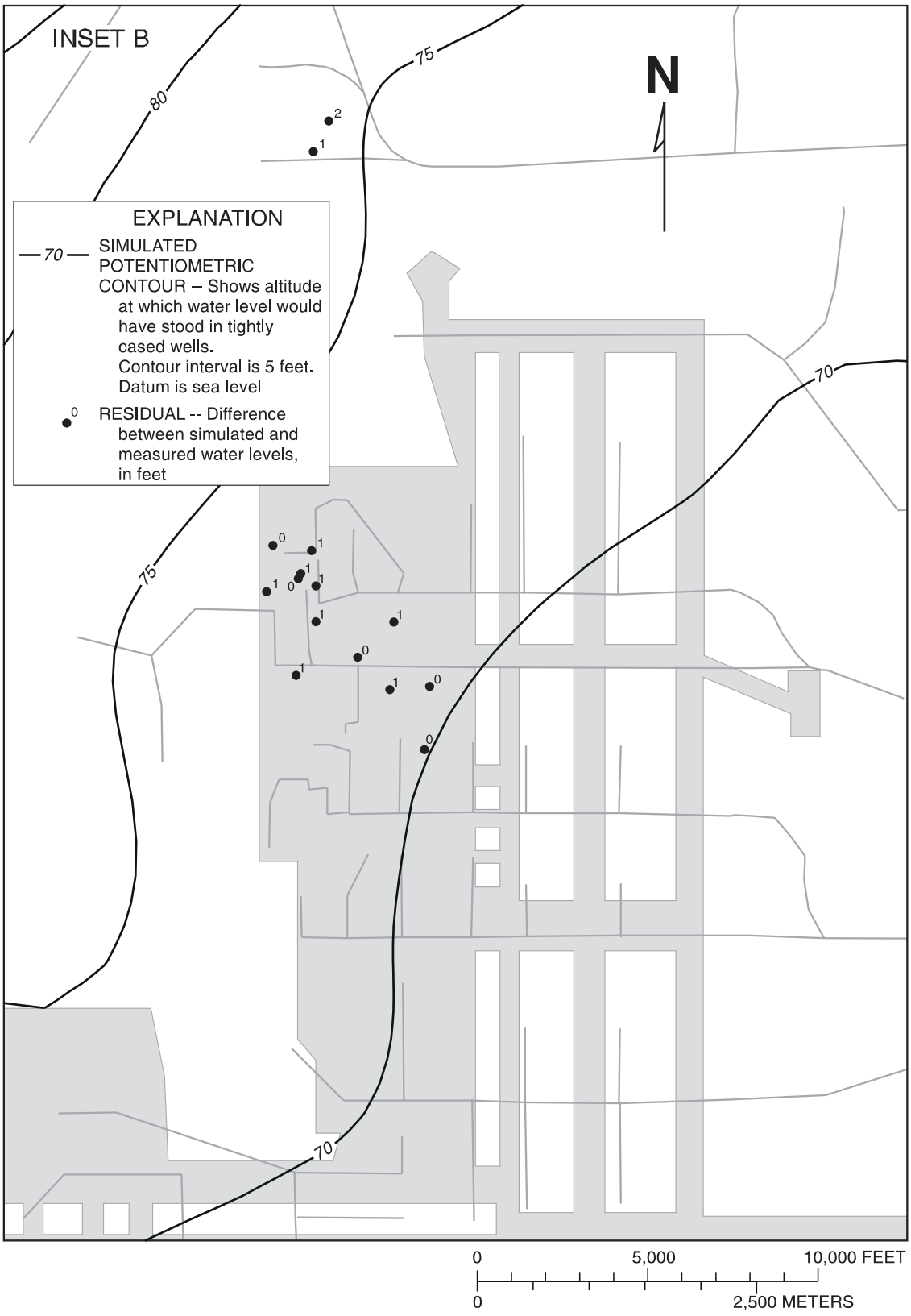

Figure 26b. Simulated potentiometric surface of the bottom third of the surficial-sand aquifer (layer 3) on August 22, 1994, inset B.

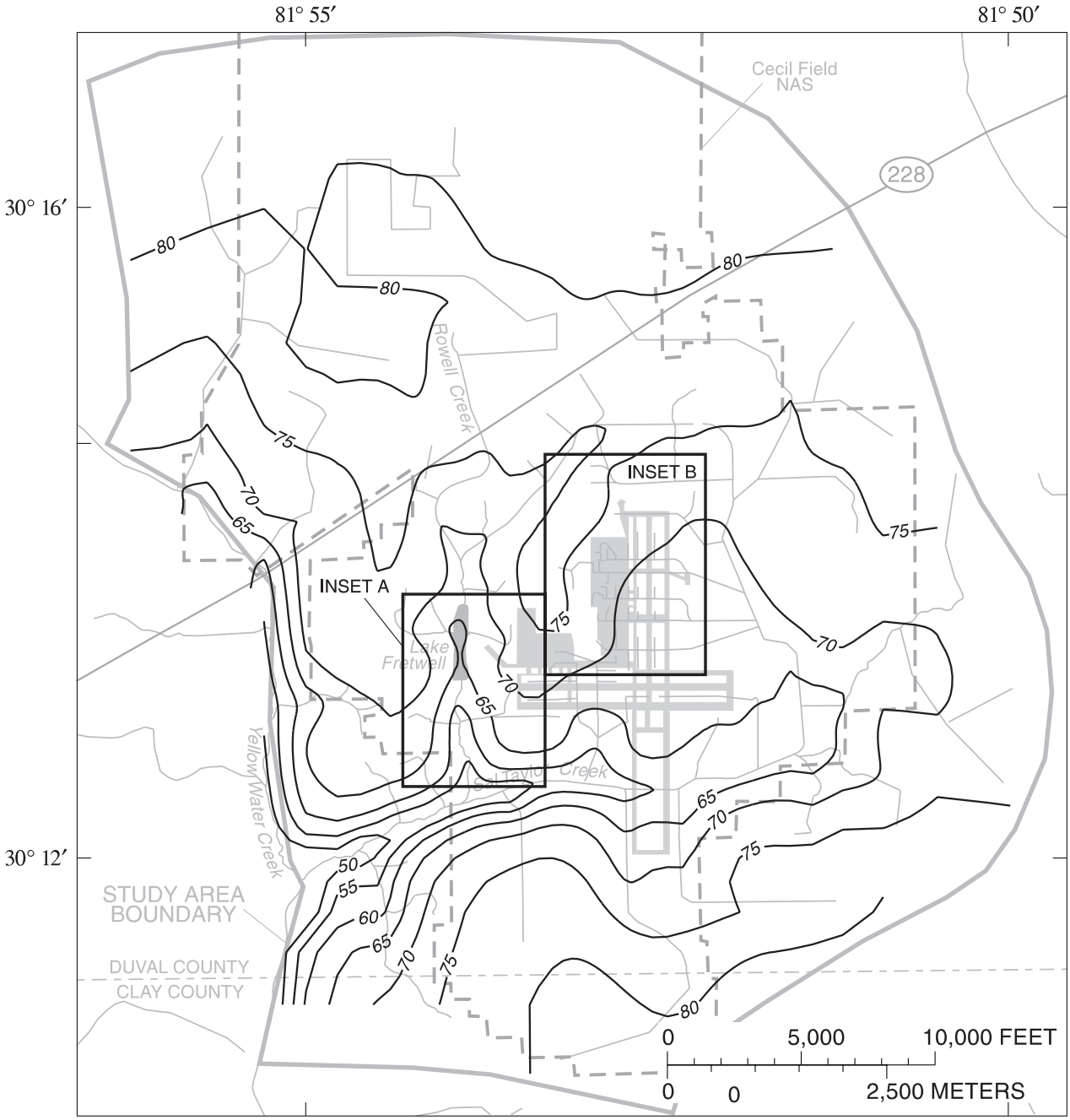

Figure 27. Simulated potentiometric surface of the blue-marl confining unit (layer 4) on August 22, 1994.

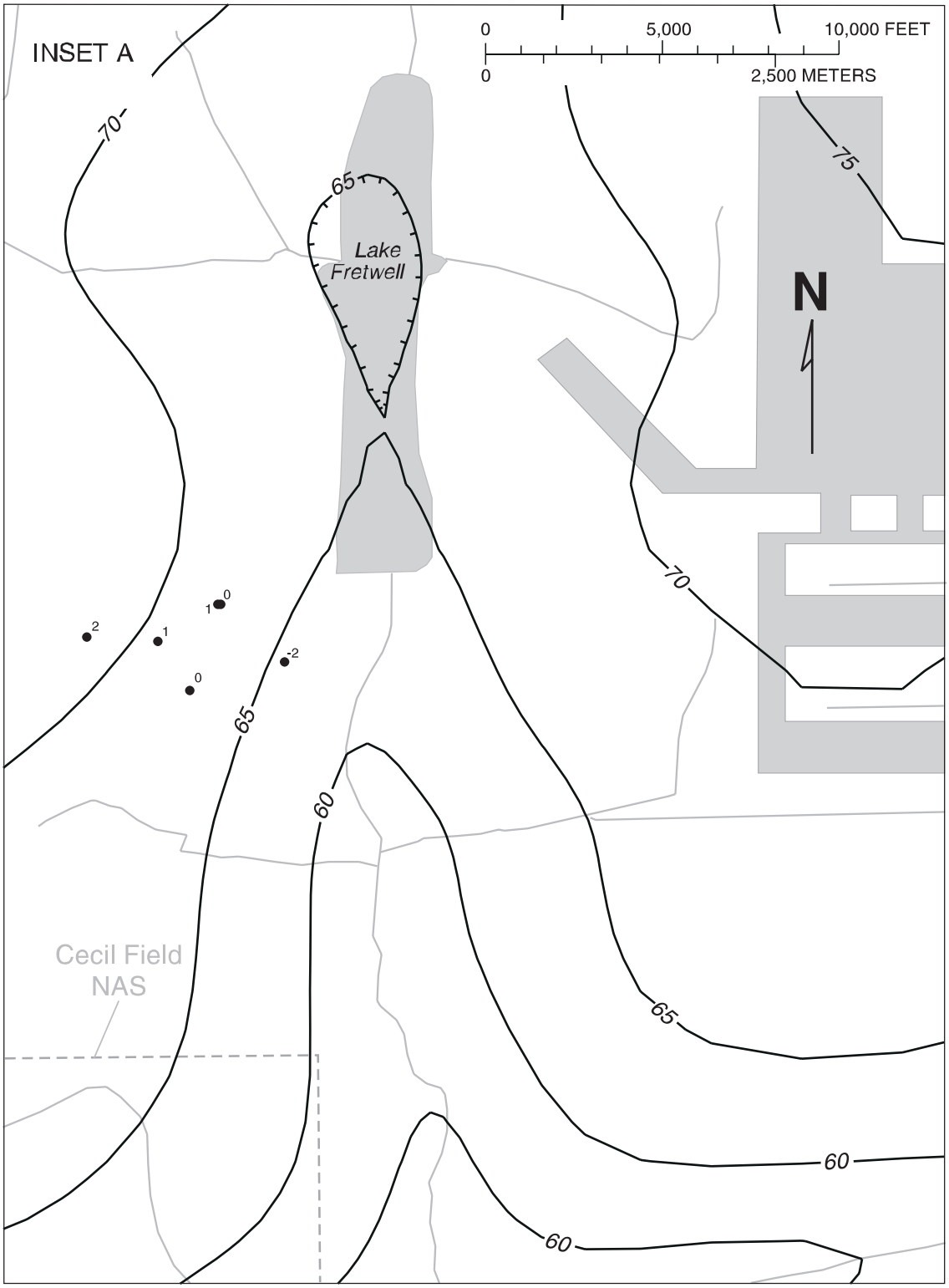

Figure 27a. Simulated potentiometric surface of the blue-marl confining unit (layer 4) on August 22, 1994, inset A.

Figure 27b. Simulated potentiometric surface of the blue-marl confining unit (layer 4) on August 22, 1994, inset A.

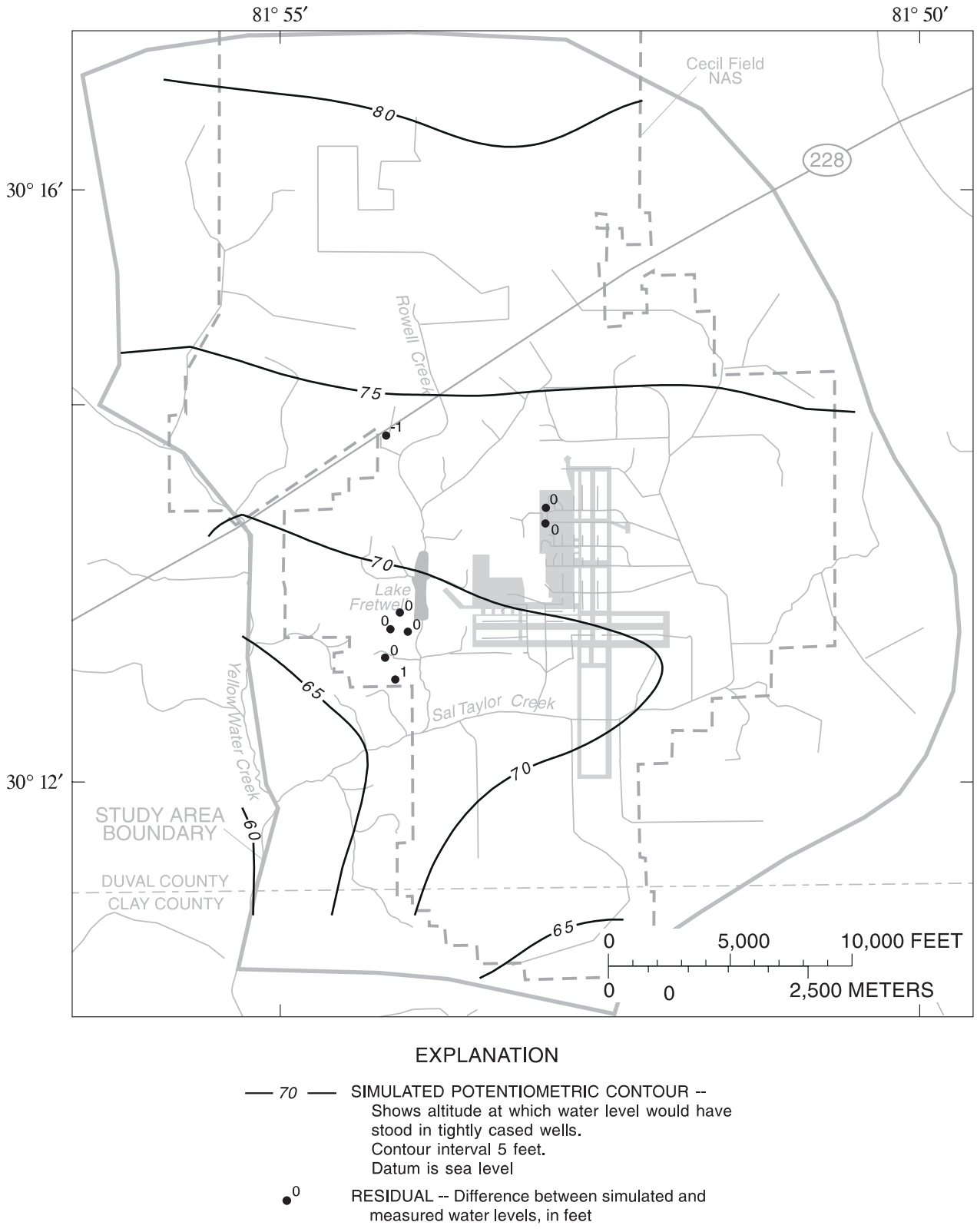

Figure 28. Simulated potentiometric surface of the upper-rock aquifer (layer 5) on August 22, 1994.

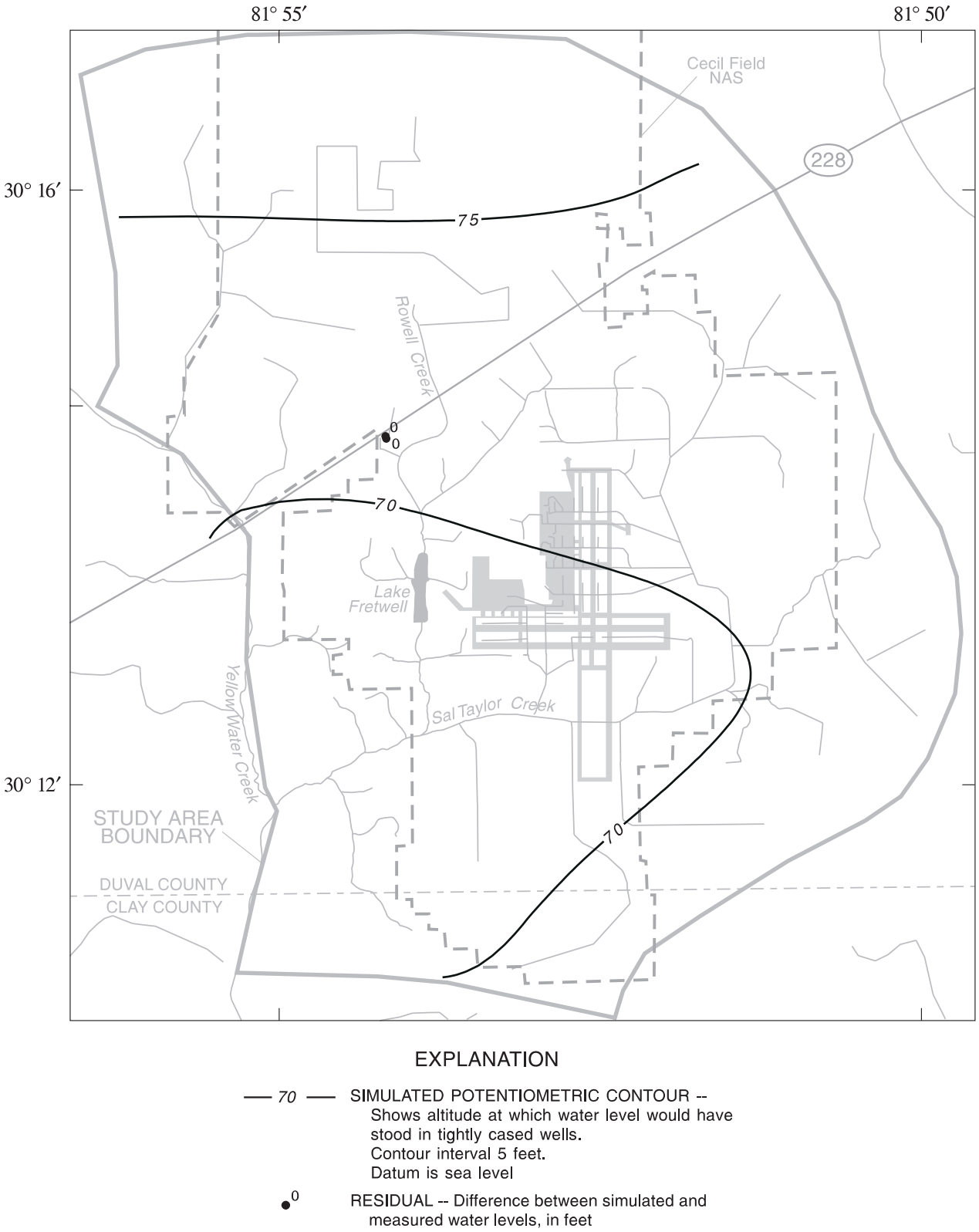

Figure 29. Simulated potentiometric surface of the lower-rock aquifer (layer 6) on August 22, 1994.

Simulated water levels for all four synoptic-survey periods approximate the measured levels well over the range of approximately 40 ft observed in the study area (fig. 30). The measured water levels that were compared range from 48 to 85 ft or 67 percent of the range of water levels in the surficial-aquifer system. The histogram of water level residuals (fig. 30) shows that 57 percent of the simulated water levels were within 1 ft and 85 percent were within 2 ft of measured water levels.

Although the model can simulate the ground-water flow system beneath Cecil Field NAS fairly well, there are a few areas where the model is deficient. The simulated water table north of SR 228, along the western edge of the study area, is 2 to 3 ft less than the measured water table, probably because the drains that specify land surface are assigned at too low a level (see residuals of -3 and -2 ft in fig. 24). The simulated water table south of Lake Fretwell, on the west bank of Rowell Creek, is 3 to 4 ft above the measured water table because an unmapped drain probably exists (see residuals of 3 and 4 ft in fig. 24, inset A). The lack of vertical interpolation when calculating heads for comparison to measured values is another source of error (see residual of 3 ft along Rowell Creek in fig. 25, inset A). This is only significant in the surficial-sand aquifer near the creeks where both simulated and measured water levels show head differences of about 10 ft between the top and bottom of the surficial-sand aquifer.

The simulated discharges for the Black Creek Basin compare favorably with measured values obtained during synoptic-survey periods 1 and 2 (table 6). The simulated discharge measurements from the later periods could not be directly compared to measured rates because surface runoff is not simulated. However, the measured water levels for these periods were reasonably well simulated by calibrating to an effective-recharge rate (figs. 24-29) and simulated ground-water discharge to the Black Creek Basin was less than half the measured values.

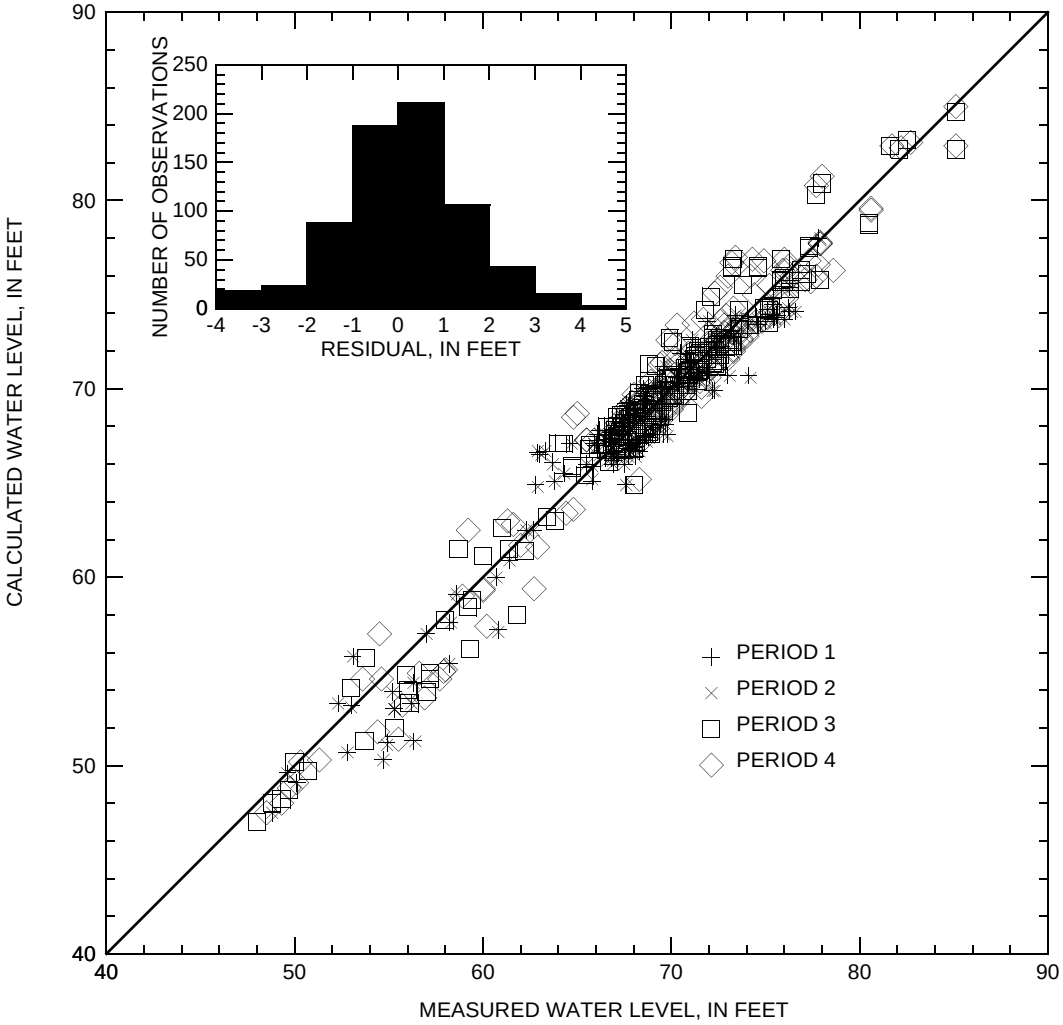

Figure 30. Comparison of simulated to measured water levels and histogram showing residual distribution for the calibrated model.

Most of the estimated parameters are not highly correlated to one another (table 7). The only exception is the strong inverse correlation, -0.97, between the vertical hydraulic conductivity of the gray-marl and lower confining units. The average vertical hydraulic conductivity of the gray-marl and lower confining units must be about 0.0015 ft/d or less to simulate the measured water levels in the surficial aquifer system.

Table 6. Simulated and measured discharges from Rowell and Black Creeks during the four synoptic-survey periods

[Discharge in cubic feet per second; $\hat{q}$, simulated; q, measured]

Date	Synoptic-survey period	Discharge			
		Rowell Creek		Black Creek	
		$\hat{q}$	q	$\hat{q}$ [a]	q
April 6, 1994	1	0.5	0.4	51	48
May 7, 1994	2	.5	.3	50	47
August 22, 1994[b]	3	.6	6	62	180
October 19, 1994[b]	4	.7	12	73	270

[a] Simulated discharge was multiplied by 177 mi^2/36 mi^2 for comparison to measured discharge.

[b] Discharges during periods 3 and 4 were not considered as part of the calibration criteria.

The high degree of correlation between the two parameters is due to a sparsity of water-level measurements in the lower-rock aquifer which does not allow for differentiating between the confining effects of the gray-marl and the lower confining units. The second highest degree of correlation of 0.82 is between the lateral hydraulic conductivity of the surficial-sand aquifer and the riverbed conductance.

Sensitivity Analysis

Each estimated parameter was varied, independently, from 0.2 to 5 times their calibrated value to determine how these parameters affected simulation results. This range was greater than the uncertainties associated with the parameters, but provided a more complete perspective on parameter sensitivity. Model sensitivity was described in terms of RMS error using only water-level measurements. The sensitivity of the model to changing one parameter while all others are held at their calibrated values is shown in figure 31. Model error was determined to be most

Table 7. Correlation coefficients between parameters from the calibrated model

[--, not applicable]

Estimated parameters	Correlation coefficients, $\rho_{i,j}$											
K_{xy} surficial-sand aquifer	1.00	--	--	--	--	--	--	--	--	--	--	--
N′ during period 1	-.27	1.00	--	--	--	--	--	--	--	--	--	--
N′ during period 2	-.26	.00	1.00	--	--	--	--	--	--	--	--	--
N′ during period 3	-.47	.00	.00	1.00	--	--	--	--	--	--	--	--
N′ during period 4	-.42	.00	.00	.00	1.00	--	--	--	--	--	--	--
K_z surficial-sand aquifer	.67	-.16	-.16	-.31	-.26	1.00	--	--	--	--	--	--
K_z blue-marl confining unit	.44	-.12	-.09	-.13	-.05	.27	1.00	--	--	--	--	--
K_z lower confining unit	.30	-.16	-.15	-.33	-.18	.14	.15	1.00	--	--	--	--
K_{xy} upper-rock aquifer	-.64	.40	.34	.34	.25	-.54	-.56	-.33	1.00	--	--	--
K runway drains	.22	-.07	-.07	-.25	-.38	.18	.12	.12	-.15	1.00	--	--
K_z gray-marl confining unit	-.20	.03	.03	.26	.12	-.07	-.09	-.97	.18	-.05	1.00	--
K_{RB} riverbeds	.82	-.12	-.11	-.47	-.44	.70	.32	.45	-.62	.17	-.37	1.00
$\rho_{i,j} = \frac{C_{i,j}}{\sqrt{C_{i,i}C_{j,j}}}$	K_{xy} surficial-sand aquifer	N′ during period 1	N′ during period 2	N′ during period 3	N′ during period 4	K_z surficial-sand aquifer	K_z blue-marl confining unit	K_z lower confining unit	K_{xy} upper-rock aquifer	K runway drains	K_z gray-marl confining unit	K_{RB} riverbeds
Main diagonal, $C_{i,i}$	31,000	15,000	14,000	4,300	4,000	3,500	3,300	3,000	2,500	1,900	1,700	400

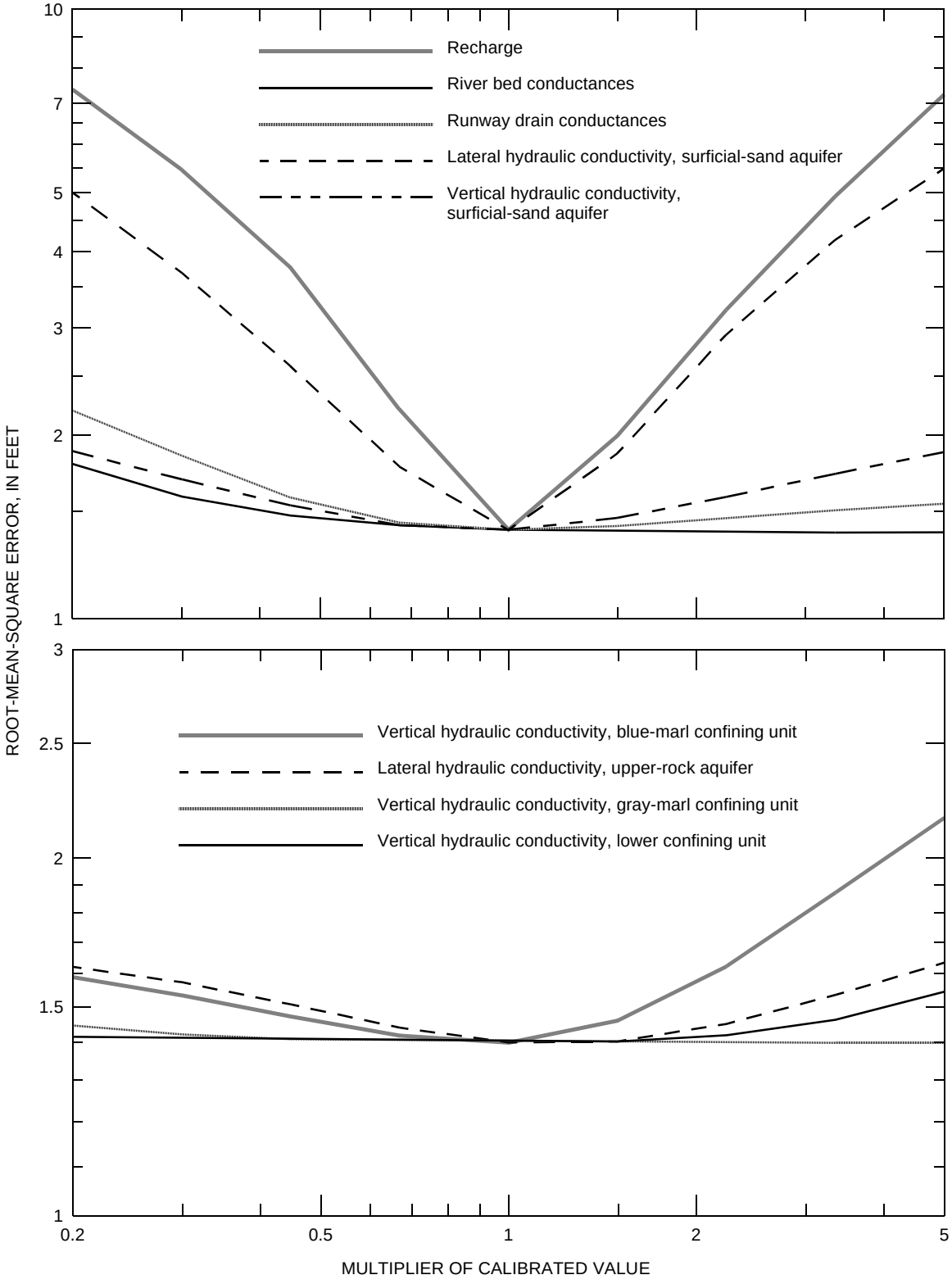

Figure 31. Model sensitivity to independent changes in model calibration parameters.

sensitive to changes in recharge and the lateral hydraulic conductivity of the surficial-sand aquifer. The model displays an intermediate degree of sensitivity to changes in the vertical hydraulic conductivity of the surficial-sand aquifer, the vertical hydraulic conductivity of the blue-marl confining unit, and the runway drain conductances (fig. 31). Generally, the model is less sensitive to changes in the hydraulic properties of the deeper aquifers and confining units (fig. 31) due to fewer observations at depth and less circulation through the deeper aquifers.

The model sensitivity to riverbed conductance was asymmetrical, with model error increasing for values less than the calibrated value and remaining constant for values greater than the calibrated value (fig. 31). Any large value of riverbed conductance would have sufficed; it did not need to be estimated, given the lack of model sensitivity to increasing riverbed conductance and the degree of correlation with the lateral hydraulic conductivity of the surficial-sand aquifer. This result indicates that stream and lake interaction was controlled by the hydraulic conductivity of the surficial-sand aquifer instead of the riverbed conductance.

A post-calibration sensitivity analysis of the model boundaries was not performed, because the results of the regional model simulations serve as a sensitivity analysis of the no-flow lateral boundaries of the study-area model. The original test of the no-flow boundaries is still valid because the hydraulic properties and boundaries used in the regional model are similar to those used in the calibrated study-area model.

Simulation of Ground-Water Flow

The analysis of ground-water flow and potential movement of contaminants within the surficial aquifer system was addressed using the calibrated model driven by the long-term, average recharge rate. This rate was assumed to be 6 in/yr because it is bracketed by the effective-recharge rates of 4.6 and 7.5 in/yr estimated for dry and wet conditions, respectively. The results of the cross-sectional model also suggest that the long-term rate should fall between the two extremes (fig. 23).

The water-table configuration is strongly influenced by almost all of the drainage features, even the smallest of drains (fig. 24). The simulated lateral flow direction near the top of the surficial-sand aquifer is usually perpendicular to the nearest drainage feature. The simulated potentiometric surface at the bottom of the surficial-sand aquifer is only influenced by the larger surface drainage features (fig. 26). In the deeper upper-rock and lower-rock aquifers, only the deeply incised lower reach of Sal Taylor Creek and Yellow Water Creek influence the simulated potentiometric surfaces of these aquifers (figs. 28 and 29). Simulated lateral flow in the upper-rock and lower-rock aquifers generally is from the northern and eastern edges of the study area towards Yellow Water Creek in the southwestern part of the study area.

The simulated volumetric flow budget for the surficial aquifer system and the intermediate confining unit is schematically shown in figure 32. The arrows indicate the flow across the boundaries between layers. Only 4.6 of the 6 in/yr of applied recharge is available to circulate through the ground-water system because 1.4 in/yr is rejected to additional evapotranspiration and runoff (fig. 32). The rates of recharge rejection are not spatially uniform; most recharge is rejected north of SR 228 and east of the runways in the Sal Taylor Creek Basin at rates of 3 in/yr or more (fig. 33). These are areas where the water table is perennially near or at land surface.

Most of the simulated ground-water flow (78 percent after discounting the 1.4 in/yr of rejected recharge) circulates solely within the surficial-sand aquifer (fig. 32), which indicates that most of the contaminant migration can be expected to be through the surficial-sand aquifer. The remaining 1.0 in/yr (22 percent) passes to the upper-rock aquifer with 0.2 in/yr (4 percent of the 4.6 in/yr of total circulation) continuing downward to the lower-rock aquifer. Most of the 0.8 in/yr of flow that discharges from the upper-rock aquifer to the surficial-sand aquifer does so along Yellow Water, Rowell, and Sal Taylor Creeks (fig. 34). Simulated deep infiltration from the study area to the Upper Floridan aquifer amounts to 0.2 in/yr. The higher rates of deep infiltration occur along the eastern half of the study area (fig. 35).

Simulation of Movement of Contaminants

The advective movement of conservative contaminants from selected sites to discharge points was simulated using a particle-tracking routine, MODPATH (Pollock, 1989). For this analysis, the dissolved contaminant was assumed not to appreciably alter the density of the ground water. A column of three particles that extended from 10 to 40 ft below the water table was used to approximate the initial position of contaminants at selected sites. For half of the sites, the different initial depths below the water table did not affect the particle paths (fig. 36, sites 1, 2, 3, or 8). However, at sites 5, 7, 13, 16, and the fuel farms, the particle paths diverged more with depth because the nearest drain or creek was not a major point of discharge, and the deeper flow paths were captured by a more remote surface-water outlet at a lower stage.

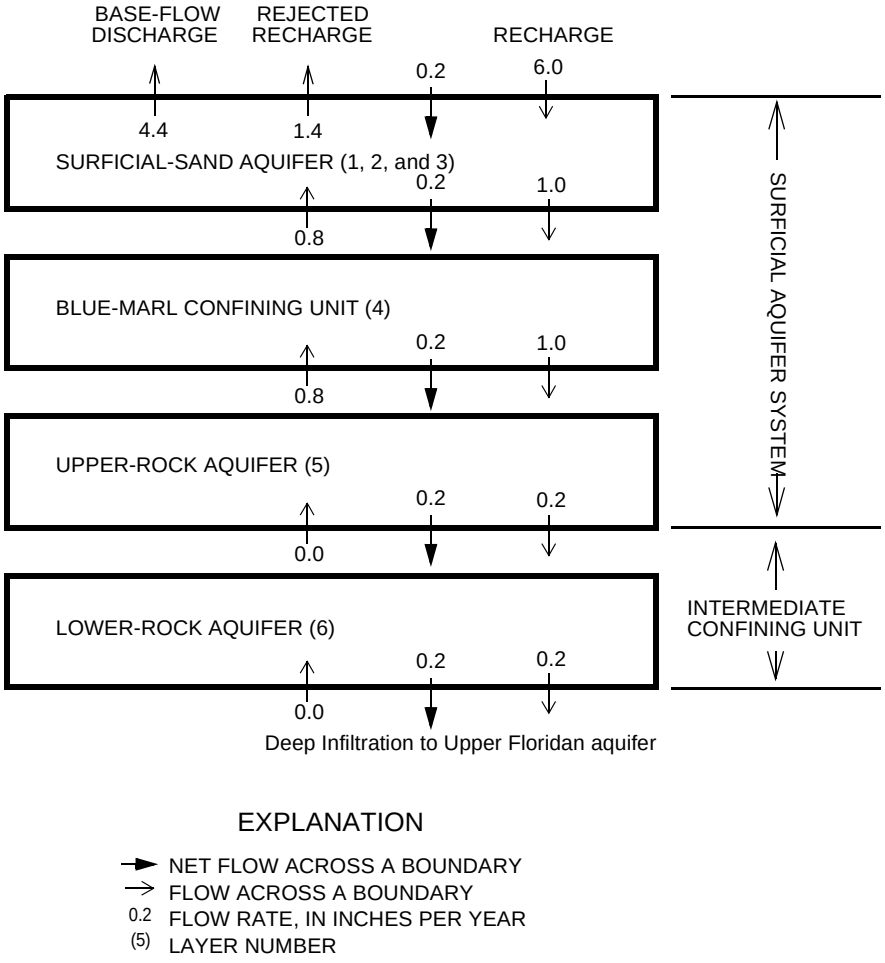

Figure 32. Simulated volumetric flow budget using a recharge rate of 6 inches per year.

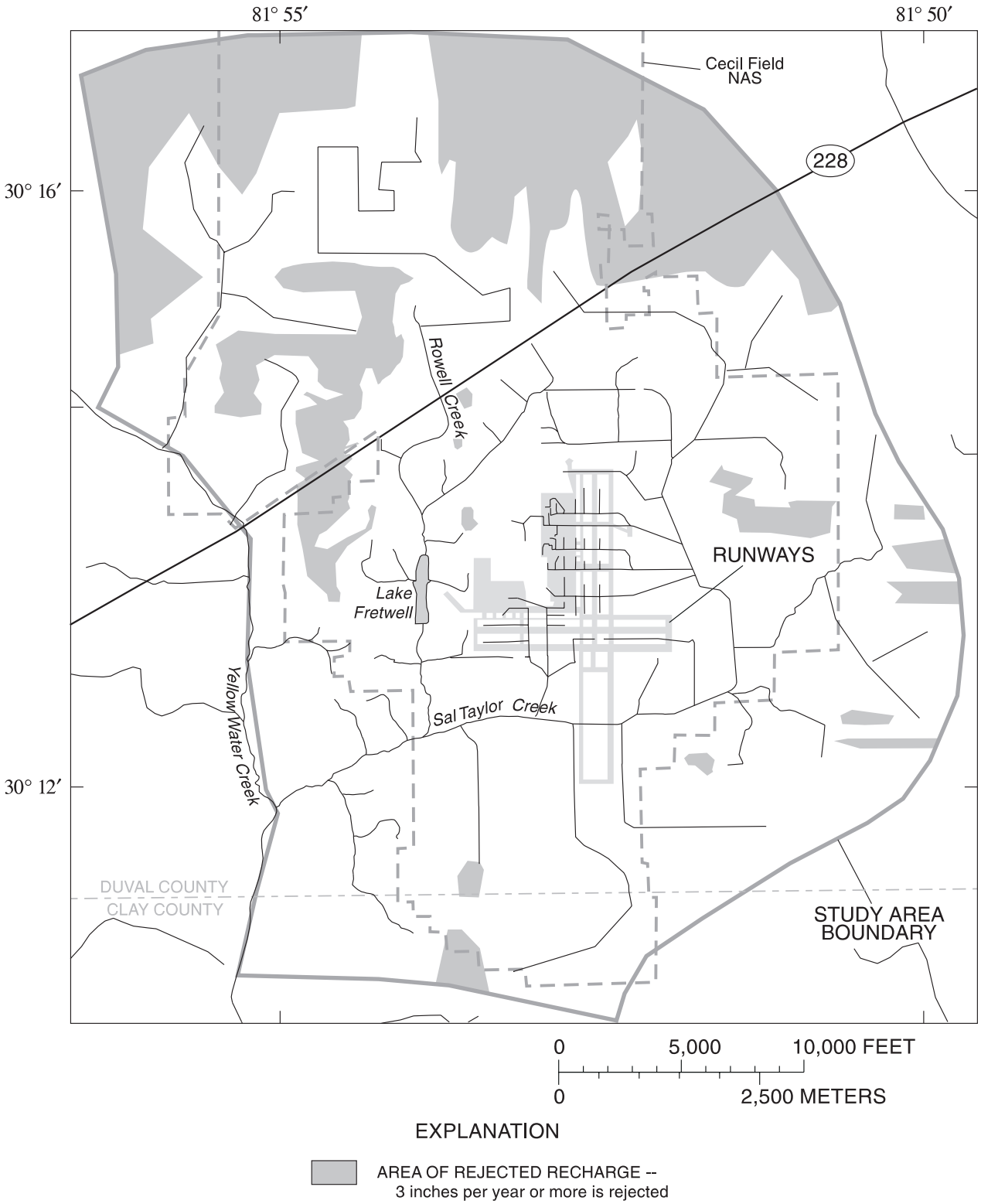

Figure 33. Locations of simulated rejected recharge in the study area.

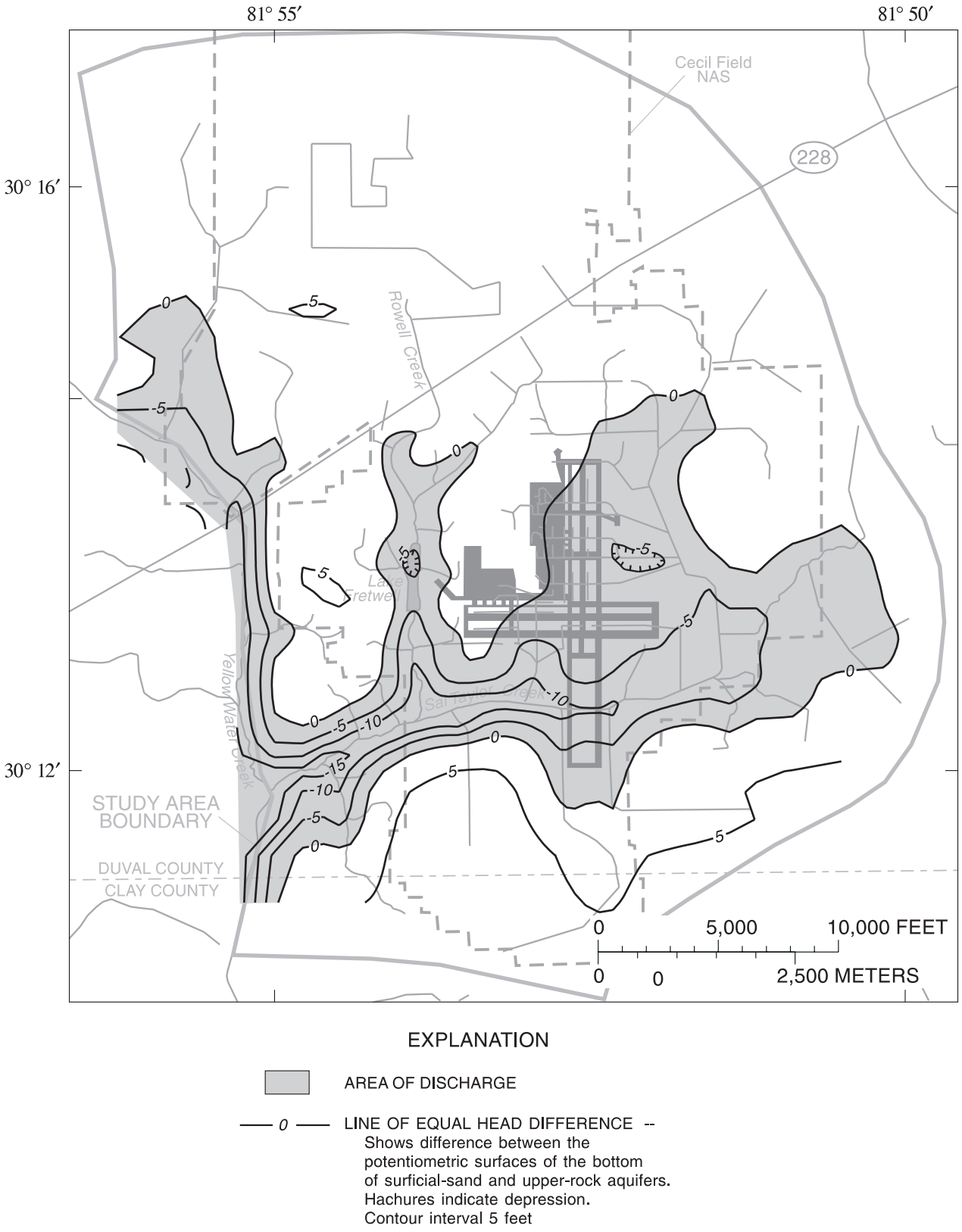

Figure 34. Average simulated head difference between the bottom of the surficial-sand aquifer (layer 3) and upper-rock aquifer (layer 5) potentiometric surfaces.

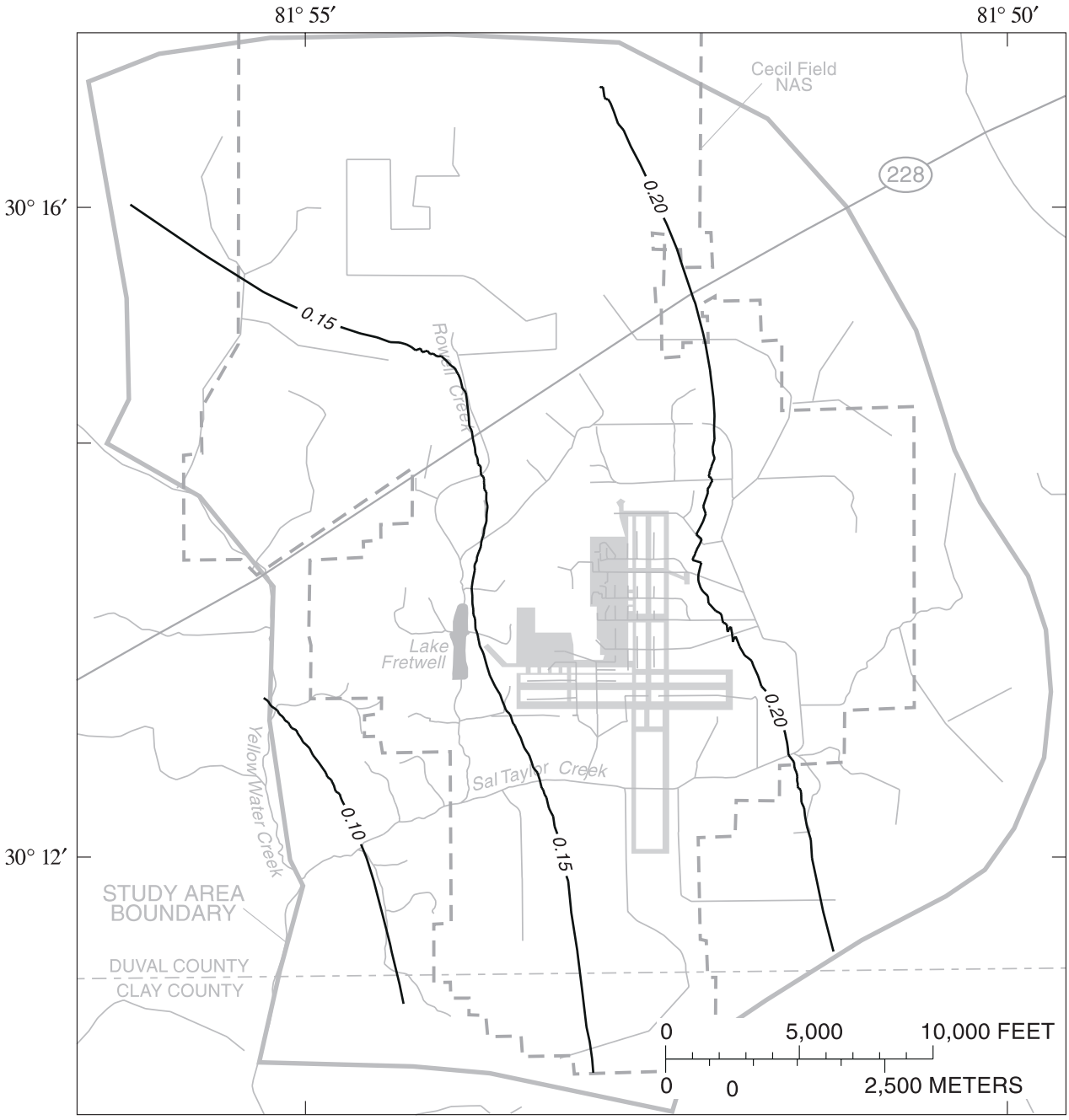

EXPLANATION

—— 0.10 —— LINE OF EQUAL DEEP INFILTRATION -- Interval 0.05 inch per year

Figure 35. Simulated deep infiltration to the Upper Floridan aquifer (layer 7) from the lower-rock aquifer (layer 6) using a recharge rate of 6 inches per year.

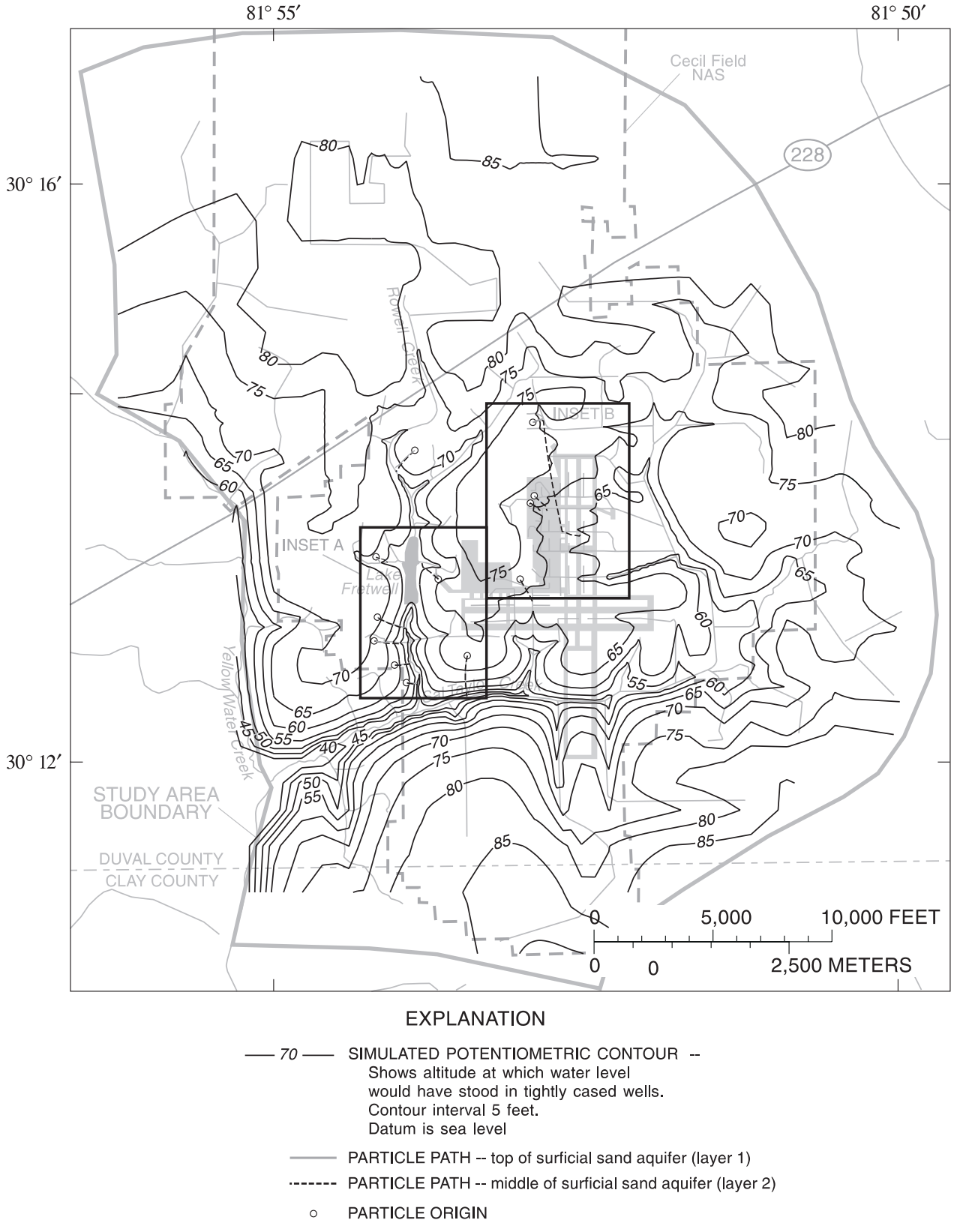

Figure 36. Simulated flow paths from selected sites to their respective discharge points using a recharge rate of 6 inches per year.

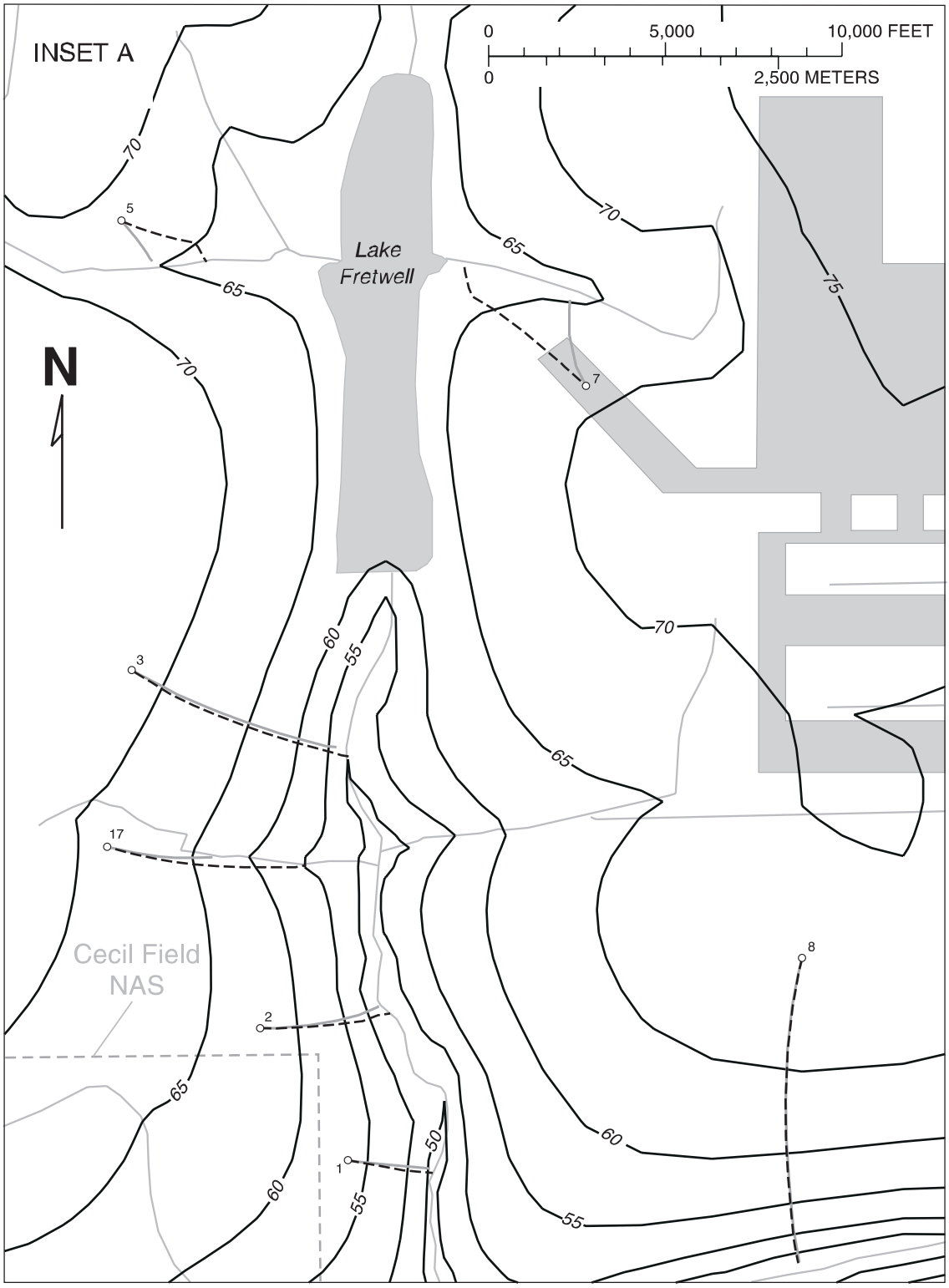

Figure 36a. Simulated flow paths from selected sites to their respective discharge points using a recharge rate of 6 inches per year, inset A

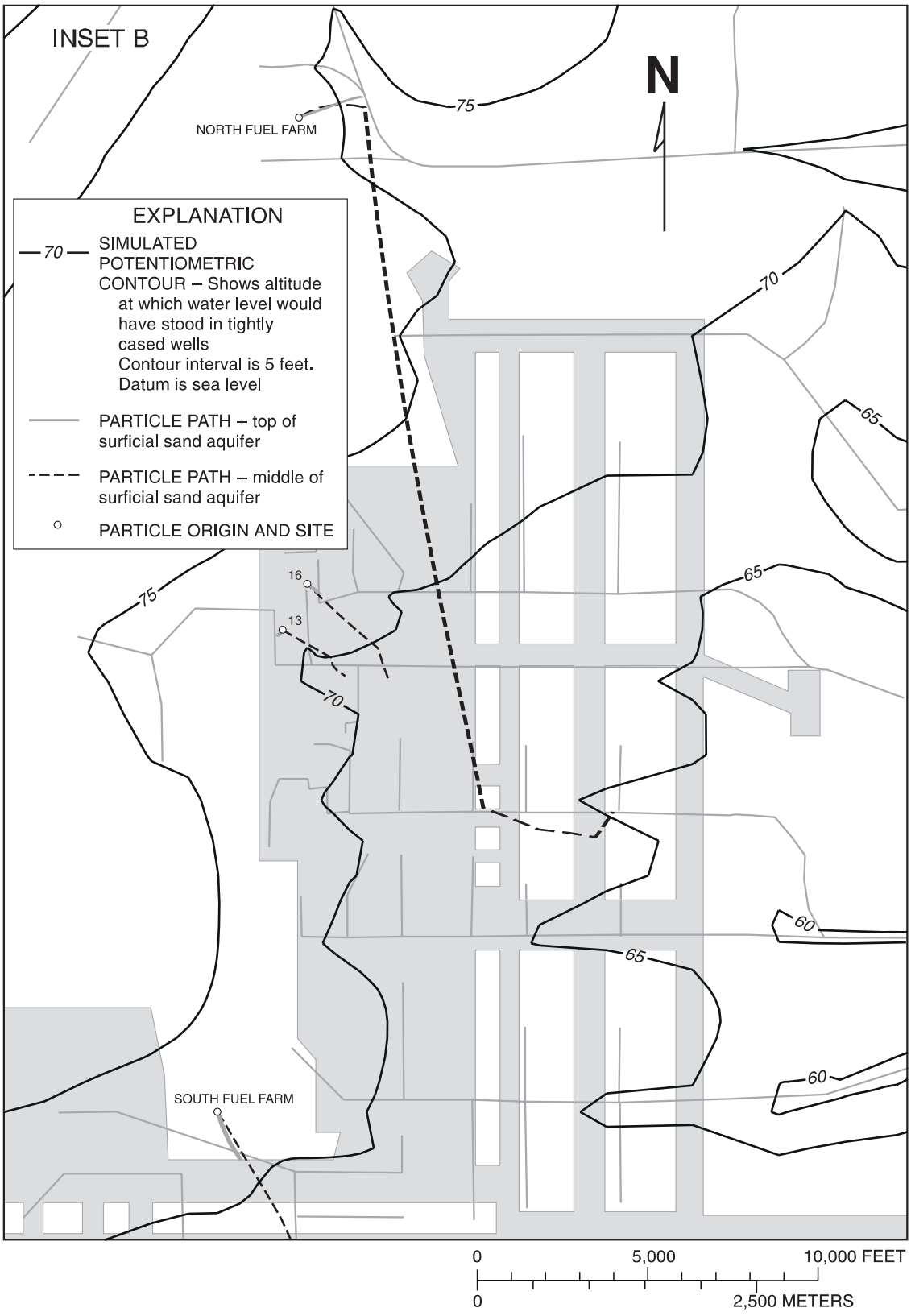

Figure 36b. Simulated deep infiltration to the Upper Floridan aquifer (layer 7) from the lower-rock aquifer (layer 6) using a recharge rate of 6 inches per year, inset B.

Most of the particles traveled 1,500 ft or less before being discharged from the ground-water system. For an assumed effective porosity of 20 percent, typical traveltimes are 40 years or less. If the effective porosity ranges from 10 to 30 percent, traveltimes will range from half as long to 1.5 times longer than those computed with an effective porosity of 20 percent. Traveltimes for particles released 10 ft below the water table were shorter compared to those released 40 ft below the water table for any given site (table 8). The pathline with the shortest traveltime (2 years) originated at site 16; the pathline with the longest traveltime (300 years) originated at the north fuel farm (table 8 and fig. 36).

Table 8. Approximate traveltimes of particle movement from selected sites to their respective discharge points

Site identifier	Approximate traveltime, in years, for particles released below the water table[a]	
	10 feet	40 feet
1	4	5
2	8	11
3	20	30
5	5	20
7	11	40
8	40	40
11	50	70
13	4	40
16	2	50
17	12	30
North Fuel Farm	20	300
South Fuel Farm	5	60

[a] Traveltimes are based on an effective porosity of 20 percent throughout the study area. Associated particle paths are displayed in figure 36.

The ground-water flow patterns around many of the sites of contamination are similar to the flow pattern around site 3 and can be illustrated by examining site 3 in detail. Site 3 is located about 1,200 ft west of Rowell Creek and just south of Lake Fretwell (fig. 37). The model simulates the flow field at site 3 reasonably well, but not perfectly, as shown by the discrepancy between the simulated particle paths and the measured TCE plume (U.S. Department of the Navy, 1995). Ground-water flow from site 3 is toward the east-southeast and has a downward component (fig. 37). As ground water flows away from site 3, the lateral direction changes little, but the vertical gradients reverse and are upward about 500 ft away from Rowell Creek. All flow from around site 3 converges on Rowell Creek and is discharged (fig. 37).

The effects of the flow field on plume development and contaminant transport were shown by tracing a panel of 112 particles from site 3 and examining their positions 5, 10, 15, and 20 years after release (fig. 37). The initial positions of the particles were defined by a panel with a 120-ft-long trace along the land surface and a vertical extent of about 45 ft (see 0 yr in fig. 37). The difference in velocity between the shallowest and deepest particles became noticeable after 10 years of travel and pronounced after 20 years when the distance between the leading and trailing edges of the panel was about 300 ft (fig. 37). The velocity difference between the shallowest and deepest particles is due to addition of recharge to the flow system. This difference becomes more exaggerated within 500 ft of Rowell Creek because the upward gradients force the water added by recharge in this area to circulate near the surface.

Ground-water flow from the north fuel farm is atypical compared to the other sites of contamination. At most of the other sites, the flow field is fairly uniform. Particles released 100 to 200 ft perpendicular to the paths shown in figure 36 will have paths that roughly parallel those shown initially at these sites. The flow field near the north fuel farm is divergent because it is just east of a ground-water divide (fig. 36), and because small displacements of the particle release location, either laterally or vertically, can greatly alter the particle path and terminus.

The effects of the divergent flow field can be illustrated best by tracing eight particles from the north fuel farm and examining their paths in plan and section (fig. 38). Particles that were started about 15 ft below the water table all moved downward initially but reversed direction and were captured by nearby creeks. The pathlines and traveltimes for these particles were relatively short and ranged from 15 to 34 years. The particles that were started about 40 ft below the water table all moved downward across the blue-marl confining unit and into the upper-rock aquifer (fig. 38). After entering the upper-rock aquifer, these particles traveled about 2,000 to 4,000 ft south of the north fuel farm before emerging from the upper-rock aquifer into the surficial-sand aquifer (fig. 38).

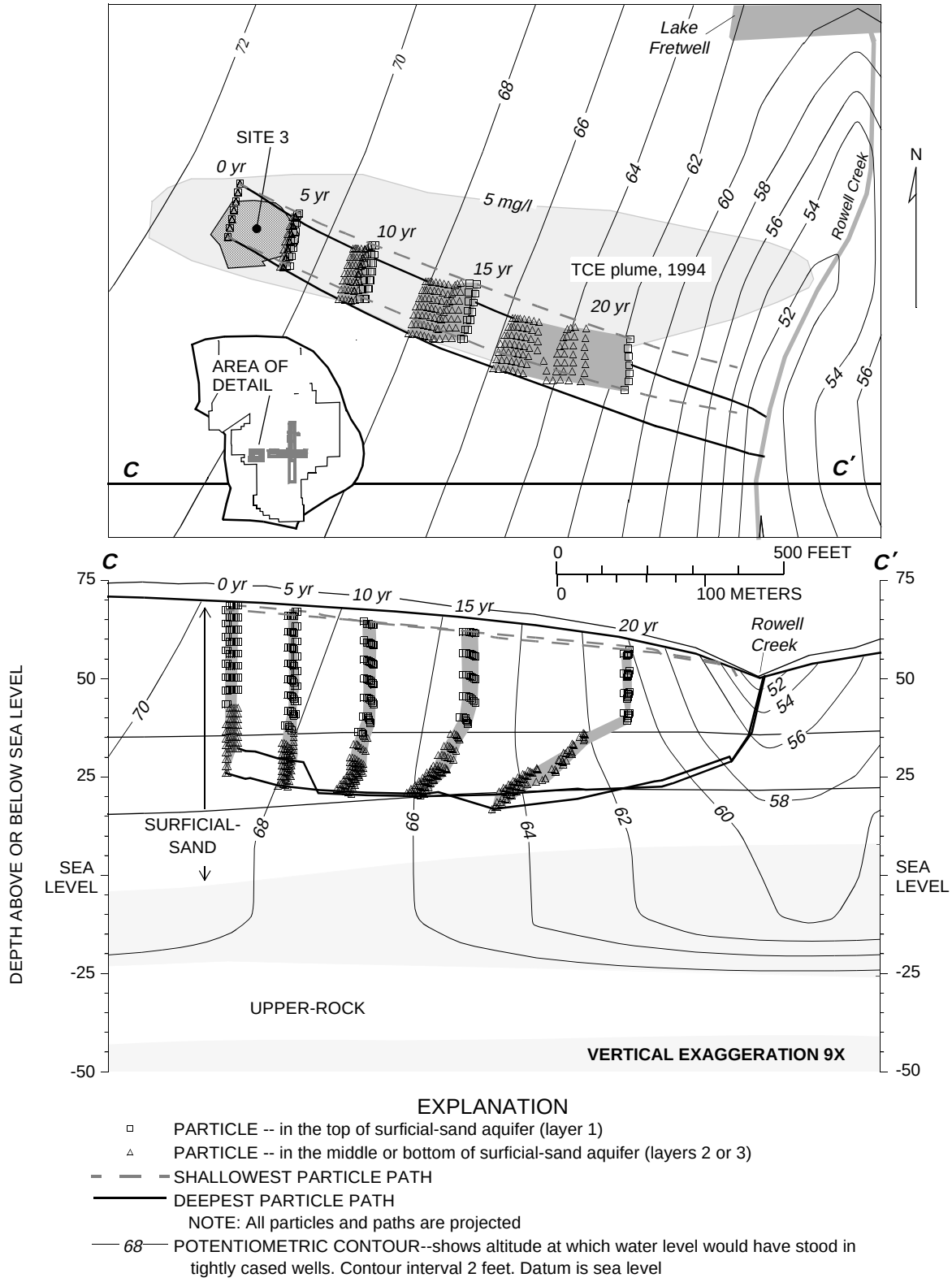

Figure 37. Simulated flow paths, particles, traveltimes, and potentiometric contours near site 3, using a recharge rate of 6 inches per year.

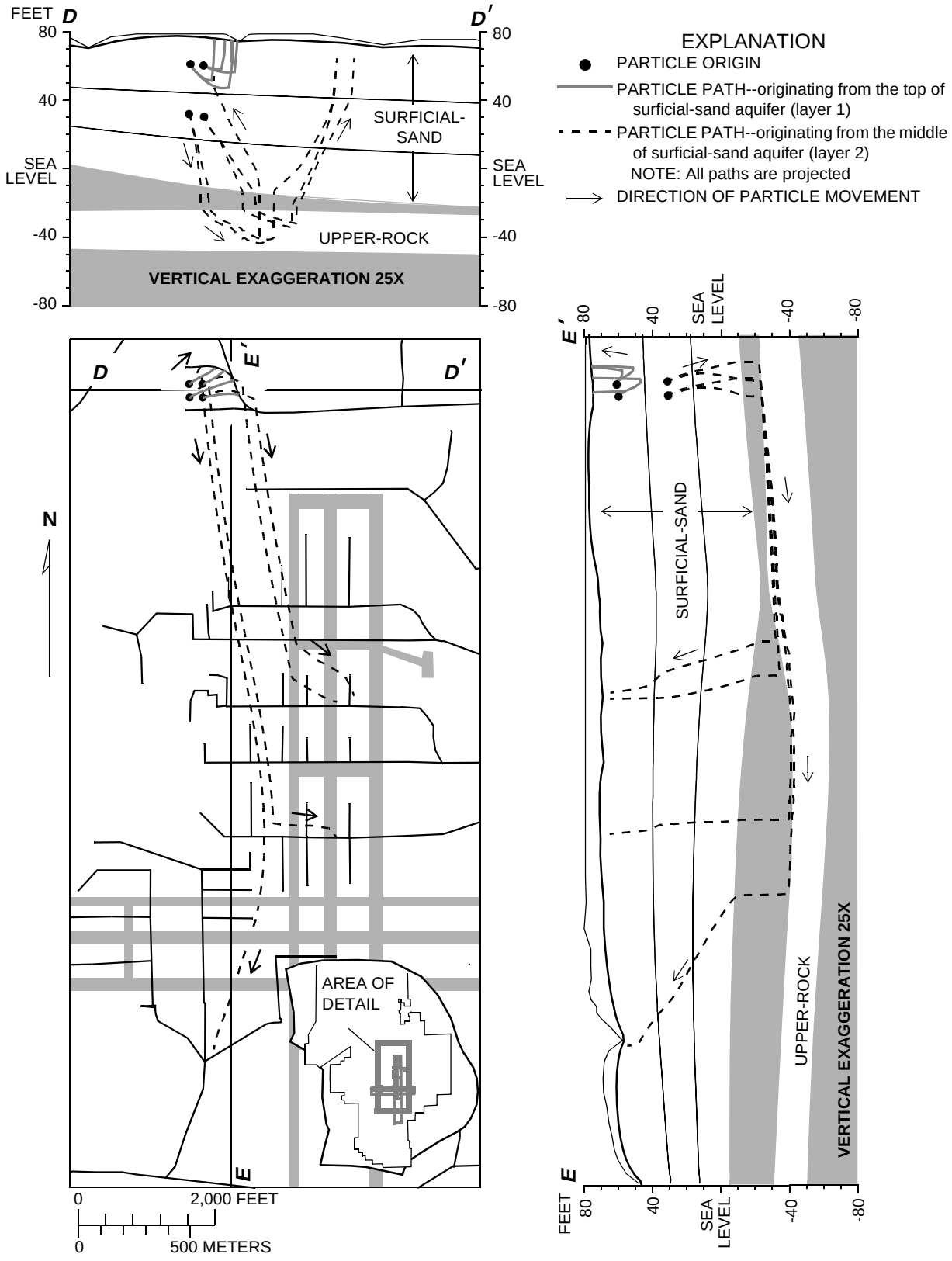

Figure 38. Simulated flow paths from the north fuel farm to their respective discharge points, using a recharge rate of 6 inches per year.

The sharp bends and sudden changes in particle direction, seen in plan view (fig. 38), are clearly the effects of movement between the surficial-sand and upper-rock aquifers when seen in section (fig. 38). Traveltimes for the particles that were started about 40 ft below the water table ranged from 340 to 480 years.

The domestic supply wells near the base do not substantially influence ground-water flow through the surficial aquifer system but concern exists about where the water originates, what path it takes, and how long it takes to travel from land surface to a well. The effects of the wells were simulated by assuming that they were screened in the upper-rock aquifer and were pumped at a rate of 750 gal/d. The cluster of wells along SR 228 had the greatest effect on the potentiometric surface of the upper-rock aquifer and created a drawdown of about 0.06 ft in the vicinity of the wells (fig. 39).

The contributing areas and traveltimes to the domestic supply wells were determined by seeding the perimeter of each well with 800 particles and backtracking upgradient to the water table. The contributing areas are not very extensive (fig. 39). The shortest traveltimes for particles to reach wells were for those along the western side of the base and ranged from 70 to 80 years. The shortest traveltimes for particles to reach wells along the eastern edge of the base ranged from 90 to 200 years.

Model Limitations

The study-area model addresses questions about the advective movement of contaminants through the surficial aquifer system beneath Cecil Field NAS fairly well, but it cannot mimic the true system exactly. The study-area model, or any other model, is limited by simplification of the conceptual model, discretization effects, difficulty in obtaining sufficient measurements to account for all of the spatial variation in hydraulic properties throughout the model area, and limitations in the vertical accuracy of land surface representations.

The conceptual model has been simplified by assuming most of the current questions raised by site assessments and remediation plans can be addressed with a steady-state ground-water flow model. However, available data indicate that during any given year, water levels will fluctuate seasonally about 3 ft, and the surficial-sand aquifer infrequently approaches, at best, a quasi-steady state condition. A steady-state model is adequate to estimate the advective movement of contaminants over a few years or more, but might not be adequate to estimate the advective movement of contaminants over less than a few years.

Lateral discretization of the study area into a rectangular grid of cells and vertical discretization into layers forced an averaging of hydraulic properties. Each cell represents a homogeneous block or some volumetric average of the aquifer medium. Discretization errors occurred in even the smallest model cells, which were 50 ft on a side and about 15 ft thick, because the surficial-sand aquifer contains clay lenses that are about 1 ft thick interbedded in silty-sand. Due to the averaging of the hydraulic properties, the model cannot simulate the dispersive effects of aquifer heterogeneity.

The model of a heterogeneous aquifer system was simplified further by describing the hydraulic conductivities of the aquifers and confining units as global multipliers that changed the values by a fixed amount throughout the study area. The lack of sufficient measurements to account for all of the spatial variation in hydraulic properties throughout the model area necessitated this gross simplification. Simplifying the model to this degree does not invalidate it, but does mean model results should only be interpreted at scales larger than the representative elemental volume of hydraulic conductivity.

Vertical accuracy of land surface representations was limited by the source material used. Locations and elevations of streams were obtained from 1:24,000 USGS quadrangle maps of the area. Elevations of drains that defined land surface elevations greater than 75 ft were obtained from the Jacksonville 1:250,000, 1-degree, Digital Elevation Model (DEM). Both land surface representations have a limited vertical accuracy. Elevations from the quadrangle sheets are assumed to be within ±5 ft, half of the contour interval. The DEM reports elevations to the nearest 3.3 ft but was based on the source sheets for 1:250,000 USGS maps which were published with a 25-ft contour interval.

Because the land surface models are not perfect and do not always adequately represent the topography, a few areas of anomalously high discharge occur through the surface drains. Most of these areas are located close to SR 228, along the western edge of Cecil Field NAS. Although the flux from these cells is high, the excess discharge from any one cell is less than 1 gal/min and the total excess discharge is no more than 4 percent of the total budget.

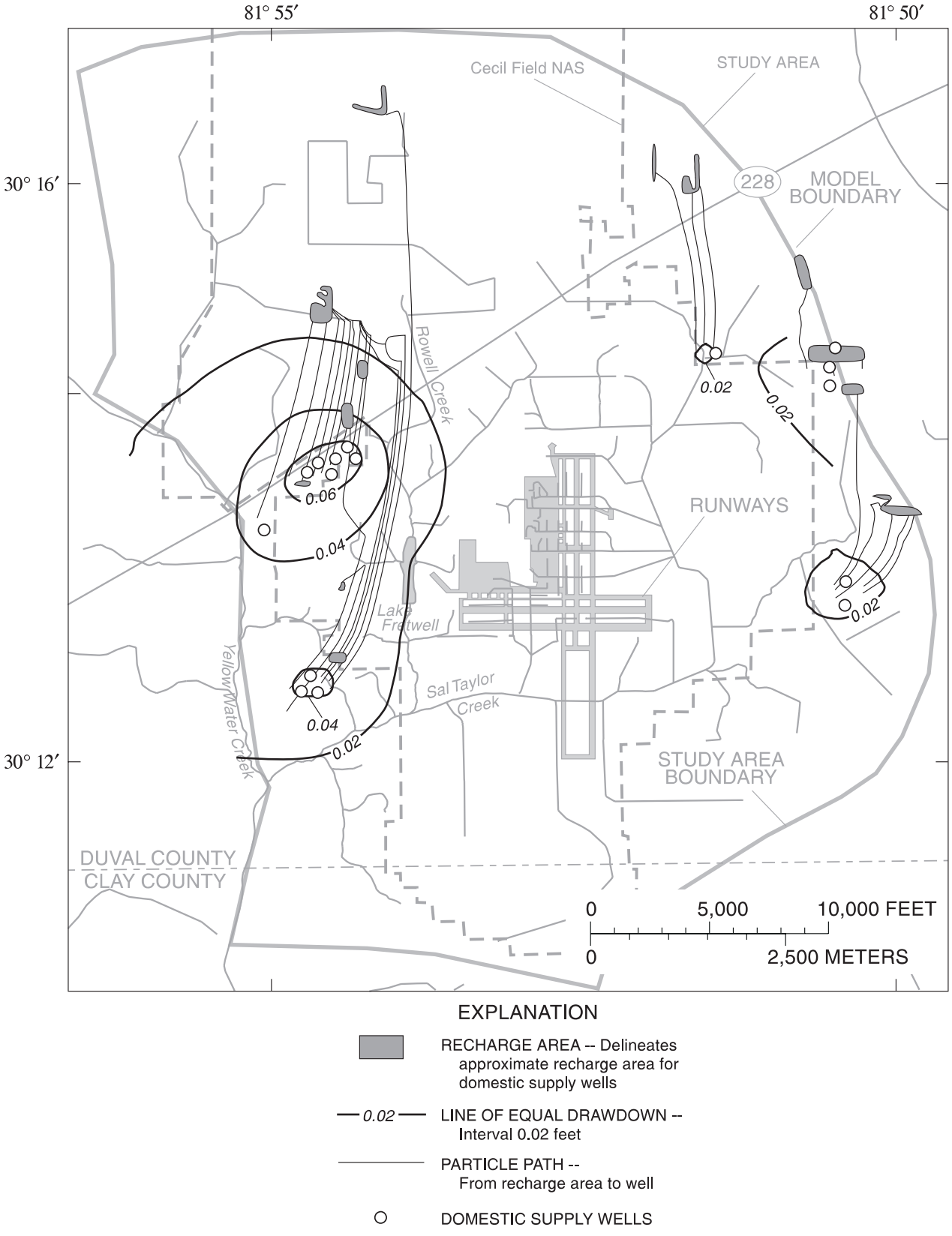

Figure 39. Simulated contributing areas for domestic supply wells screened in the upper-rock aquifer (layer 5) and drawdowns associated with producing 750 gallons per day per well.

SUMMARY

As part of the Installation Restoration Program, Cecil Field NAS in Jacksonville, Florida, is considering remedial-action alternatives to control the movement of contaminants from sites that could discharge contaminants to the surface. This requires an understanding of how the ground-water flow system responds to current conditions and any future stresses or alterations imposed on the system. Numerical simulation provides the most tractable way of achieving this level of understanding.

The geologic units in the study area consist of sediments of Holocene to Miocene age that extend from land surface to the base of the Hawthorn Group. Previous investigators have defined this sequence as two regional hydrogeologic units: the surficial aquifer system and the intermediate confining unit. This report further subdivided the sequence into six local hydrogeologic units because this study was primarily concerned with ground-water movement near the surface. The surficial aquifer system was subdivided into three hydrogeologic units: the surficial-sand aquifer, the blue-marl confining unit, and the upper-rock aquifer. The intermediate confining unit was also subdivided into three hydrogeologic units: the gray-marl confining unit, the lower-rock aquifer, and the lower confining unit. The hydrogeologic structure within the study area was defined by depth and thickness data from gamma-ray and geologists' logs.

The recession-curve-displacement method was used to estimate the long-term recharge rate in the study area using discharge measurements at Black Creek near Middleburg (0224600) from 1932 to 1994. Estimates of recession index and time-base values at station 0224600 ranged from 25 to 210 d/logQ and from 3 to 9 days, respectively. Potential recharge rates to the study area ranged from 4 to 10 in/yr, using the given ranges of recession index and time-base values.

Ground-water flow through the surficial aquifer system was simulated with a seven-layer, finite-difference model that extended vertically from the water table to the top of the Upper Floridan aquifer. Initial estimates of the hydraulic properties of the aquifers and confining units came from a series of aquifer tests conducted on the base. The distribution of surface-water features controls the directions and rates of flow in the surficial aquifer system. All the lateral model boundaries in each layer are assumed to be ground-water divides that coincide with surface-water features.

The effective-recharge approach was used to calibrate a series of independent steady-state models to the available data which consisted of "snapshot" images of a transient system. This approach assumes recharge, evapotranspiration, and the water released from specific yield can be approximated by one term, the effective-recharge rate. To apply this approach, necessity and practicality force the assumptions that the change in head with respect to time is constant during each survey, that survey periods are short, that the spatial distribution of effective recharge is spatially uniform, and that no water is contributed to the ground-water system from compressibility-based storage. These assumptions were tested with a transient, cross-sectional model which demonstrated that the needed assumptions will probably be met.

The model was calibrated to 697 water-level and four discharge measurements. The water levels were obtained from 212 wells during four synoptic surveys that spanned from April 6 to October 19, 1994. Eight discharge measurements from Rowell and Black Creeks were available for the four survey periods, but only discharge measurements that represented base-flow conditions were used. Model calibration was facilitated by a parameter estimation program that estimated the log-hydraulic conductivities. Ten parameters were used as global multipliers that changed the value of either hydraulic conductivity or effective recharge by a fixed amount.

The minimum, maximum, average, and root-mean-square errors of the calibrated model were -3.79, 4.36, 0.13, and 1.40 ft, respectively, and they did not exhibit any apparent trend across the study area. The simulated flow rates for the Black Creek Basin compared favorably with measured values. Most of the estimated parameters are not highly correlated to one another. Model error was determined to be the most sensitive to changes in recharge and to the lateral hydraulic conductivity of the surficial-sand aquifer.

The ground-water flow system and potential contaminant movement within the study area is driven by an estimated long-term recharge rate of 6 in/yr. Most of the ground-water flow, 78 percent after discounting the 1.4 in/yr of rejected recharge, circulates within the surficial-sand aquifer, which indicates most of the contaminant movement can be expected to move through the surficial-sand aquifer alone. Deep infiltration from the study area to the Upper Floridan aquifer is about 0.2 in/yr, with higher rates of infiltration along the eastern half of the study area.

The advective movement of conservative contaminants from selected sites to discharge points was simulated, using a particle-tracking routine, MODPATH. For this analysis it was assumed that the dissolved contaminant does not appreciably alter the density of the ground water. A column of three particles that extended from 10 to 40 ft below the water table was used to approximate the initial position of contaminants at each site. Most of the particles traveled 1,500 ft or less before being discharged from the ground-water system. If an effective porosity of 20 percent is assumed, typical traveltimes are 40 years or less. Particles released 10 ft below the water table have shorter traveltimes than those released 40 ft below the water table for any given site. The pathline with the shortest traveltime (2 years) originated at site 16, and the pathline with the longest traveltime (300 years) originated at the north fuel farm.

The recharge areas and traveltimes to the domestic supply wells were determined by seeding the perimeter of each well with 800 particles and backtracking upgradient to the water table. The recharge areas of the domestic supply wells are not very extensive. The shortest traveltimes for particles to reach the domestic supply wells ranged from 70 to 200 years, if an effective porosity of 20 percent is assumed.

REFERENCES

Causey, L.V., and Phelps, G.G., 1978, Availability and quality of water from shallow aquifers in Duval County, Florida: U.S. Geological Survey Water-Resources Investigations Report 78-92, 36 p.

Domenico, P.A., and Schwartz, F.W., 1990, Physical and chemical hydrogeology: New York, John Wiley and Sons, Inc., 824 p.

Farnsworth, R.K., Thompson, E.S., and Peck, E.L., 1982, Evaporation atlas for the contiguous 48 United States: National Oceanographic and Atmospheric Administration Technical Report, NWS-33, 26 p.

Gill, T.E., Murray, W., and Wright, M.H., 1981, Practical optimization: Orlando, Fla., Academic Press Inc., 401 p.

Halford, K.J., 1992, Incorporating reservoir characteristics for automatic history matching: Baton Rouge, La., Louisiana State University, Ph.D. dissertation, 150 p.

Halford, K.J., Murray, L.C., Jr., Spechler, R.M., Phelps, G.G., and Bradner, L.A., 1993, Potentiometric surface of the Upper Floridan aquifer in the St. Johns River Water Management District and vicinity, May 1993: U.S. Geological Survey Open-File Report 93-451, 1 sheet.

Healy, R.W., 1990, Simulation of solute transport in variably saturated porous media with supplemental information on modifications to the U.S. Geological Survey's computer program VS2D: U.S. Geological Survey Water-Resources Investigations Report 90-4025, 125 p.

Hill, M.C., 1992, A computer program (MODFLOWP) for estimating parameters of a transient, three-dimensional, ground-water flow model using non-linear regression: U.S. Geological Survey Open-File Report 91-484, 358 p.

Krause, R.E., and Randolph, R.B., 1989, Hydrology of the Floridan aquifer system in southeast Georgia and adjacent parts of Florida and South Carolina: U.S. Geological Survey Professional Paper 1403-D, 65 p.

Lappala, E.G., Healy, R.W., and Weeks, E.P., 1987, Documentation of computer program VS2D to solve the equations of fluid flow in variably saturated porous media: U.S. Geological Survey Water-Resources Investigations Report 83-4009, 184 p.

Leve, G.W., 1966, Ground water in Duval and Nassau Counties, Florida: Florida Geological Survey Report of Investigations no. 43, 91 p.

Linsley, R.K., Kohler, M.A., and Paulhus, J.L.H., 1958, Hydrology for engineers: New York, McGraw-Hill, 508 p.

McDonald, M.G., and Harbaugh, A.W., 1988, A modular three-dimensional finite-difference ground-water flow model: U.S. Geological Survey Techniques of Water-Resources Investigations, book 6, chap. A1, 576 p.

Meyboom, P., 1961, Estimating ground-water recharge from stream hydrographs: Journal of Geophysical Research, v. 66, no. 4, p. 1203-1214.

Owenby, J.R., and Ezell, D.S., 1992, Monthly station normals of temperature, precipitation, and heating and cooling degree days 1961-90--Florida: National Oceanographic and Atmospheric Administration Climatography of the United States, no. 81, 26 p.

Pollock, D.W., 1989, Documentation of computer programs to compute and display pathlines using results from the U.S. Geological Survey modular three-dimensional finite-difference ground-water flow model: U.S. Geological Survey Open-File Report 89-381, 188 p.

Rorabaugh, M.I., 1964, Estimating changes in bank storage and ground-water contribution to streamflow: International Association of Scientific Hydrology, Publication 63, p. 432-441.

Rutledge, A.T., 1993, Computer programs for describing the recession of ground-water discharge and for estimating mean ground-water recharge and discharge from streamflow records: U.S. Geological Survey Water-Resources Investigations Report 93-4121, 45 p.

Spechler, R.M., 1994, Saltwater intrusion and quality of water in the Floridan aquifer system, northeastern Florida: U.S. Geological Survey Water-Resources Investigations Report 92-4174, 76 p.

Stem, L.T., Dollar, H.D., Howell, D.A., Lewis, D.L., Wettstein, C.A., and Yamataki, Howard, 1978, Soil survey of city of Jacksonville, Duval County, Florida: U.S. Department of Agriculture, Soil Conservation Service, 113 p.

Theis, C.V., 1935, The relation between the lowering of the piezometric surface and the rate and duration of discharge of a well using ground-water storage: Transactions of the American Geophysical Union, v. 16, p. 519-524.

U.S. Department of the Navy, Southern Division Naval Facilities Engineering Command, 1992a, Naval Air Station, Cecil Field, Jacksonville, Florida, remedial investigation/feasibility study workplan, operable units 3, 4, 5, and 6: SouthDiv Contract N62467-89-D-0317, January 1992, 288 p.

U.S. Department of the Navy, Southern Division Naval Facilities Engineering Command, 1992b, Naval Air Station, Cecil Field, Jacksonville, Florida, technical memorandum for supplemental sampling at operable units 1, 2, and 7: SouthDiv Contract N62467-89-D-0317, September 1992, 242 p.

U.S. Department of the Navy, Southern Division Naval Facilities Engineering Command, 1995, Naval Air Station, Cecil Field, Jacksonville, Florida, remedial investigation at operable unit 8: SouthDiv Contract N62467-89-D-0317, September 1995, 367 p.

U.S. Environmental Protection Agency, 1988, Ambient water quality criteria: Office of Water, Regulations, and Standards Division, EPA-440/5-86-008, 256 p.

Watson, A.T., Seinfeld, J.H., Gavalas, G.R., and Woo, P.T., 1980, History matching in two-phase petroleum reservoirs: Society of Petroleum Engineers Journal, p. 521-532.

Yeh, W.W.-G., 1986, Review of parameter identification procedures in groundwater hydrology: Water Resources Research, v. 22, no. 2, p. 95-108.